The BCL6 transcriptional corepressor (BCOR) is required for multiple aspects of murine embryonic development.

A DISSERTATION
SUBMITTED TO THE FACULTY OF THE GRADUATE SCHOOL
OF THE UNIVERSITY OF MINNESOTA
BY

Michelle Yvonne Hamline

IN PARTIAL FULFILLMENT OF THE REQUIREMENTS
FOR THE DEGREE OF
DOCTOR OF PHILOSOPHY

Dr. Vivian June Bardwell

May 2011

Acknowledgements

I would first like to thank my advisor, Dr. Vivian Bardwell, for her patience, encouragement, and mentoring throughout my development as a scientist. I would also like to thank past and current members of the Bardwell laboratory Dr. Micah Gearhart, Dr. Mark Murphy, Dr. Joseph Wamstad, Connie Corcoran, and Kinner Patel for their support, technical assistance, and scientific input in experimental design. Next, thanks to Dr. David Zarkower and his laboratory members, particularly Dr. Clinton Matson and Anthony Krentz, for their assistance in experimental design and execution. In addition, I would like to thank Dr. Anna Petryk and members of her laboratory, Dr. Paul Sharpe and his laboratory members, and Dr. Yasuhiko Kawakami for reagents and technical assistance. Finally, I would like to thank my committee, Dr. Kristin Hogquist, Dr. Michel Sanders, Dr. Naoko Shima, and Dr. Howard Towle, for their guidance and critical input.

Dedication

This dissertation is dedicated to my parents, Mr. and Mrs. Randall and Jae Hamline. You have been there for me from the very beginning, through every success and failure, believing in me every step of the way. Thank you for your unending love, encouragement, and support. This dissertation would not have been possible without you.

Abstract.

The BCL6 transcriptional corepressor (BCOR) is mutated in the human multisystemic developmental disorder Oculofaciocardiodental syndrome (OFCD). The aim of this thesis is to understand the repressive function of BCOR in embryonic development. To accomplish this, BCOR was first tandem affinity purified from human embryonic kidney cells and found to interact with chromatin modifying proteins and several transcription factors, suggesting a molecular mechanism by which BCOR effects repression. In addition, conditional overexpression and null *Bcor* alleles were created in mice to elucidate the *in vivo* role of BCOR. The conditional overexpression allele revealed tight control of *Bcor* transcript levels in B cells and a requirement for proper control of *Bcor* expression for embryonic viability. The conditional null allele revealed that *Bcor* is required in neural crest cells for craniofacial development, in hindlimb precursors for proper limb formation, and in cardiovascular progenitors for cardiovascular development and function. These findings provide important insights into the function of BCOR in embryonic development and will facilitate the future diagnosis and treatment of developmental disorders such as OFCD.

Table of Contents.

Table of Contents, continued.

List of Tables.

List of Figures.

Chapter 5…….. Page.

Chapter 1:

Introduction.

Transcription is regulated by a complex network of activating and repressing proteins.

While the basic genetic information contained within every cell of an individual's body is virtually identical, complex networks of transcriptional regulation control which pieces of this genetic information are used in any particular cell at any given time point. This is achieved through the differential recruitment of various proteins and signature markings that appropriately activate or repress gene transcription. Such spatial and temporal control of gene usage is important, not only for the proper proliferation and differentiation of an organism's varied tissues in development, but also for the prevention of cancer and maintenance of those tissues in adulthood.

This complex regulation relies largely on the modification of chromatin, which is composed of highly ordered arrays of nucleosomes arranged like "beads on a string" of deoxyribonucleic acid (DNA). Each nucleosome, in turn, is composed of 146 base pairs of DNA wrapped around a histone core octamer of H2A, H2B, H3, and H4 subunits. To control access of the transcriptional, chromatin modifying, and remodeling machinery to their associated DNA strands, histones can be post-translationally modified through acetylation, phosphorylation, methylation, ubiquitylation, sumoylation, and ribosylation [reviewed in (Campos & Reinberg, 2009)]. Such modifications can have a variety of epigenetic (or inherited chromatin changes) and non-epigenetic functions. For example, post-translational modification of histones may either facilitate or disrupt interactions between various proteins and DNA sequences by altering the charge of a residue. Alternatively, histone modifications may provide docking sites for proteins at specific DNA sequences. In general, these modifications collaborate to render the chromatin either euchromatic—an open conformation that is highly accessible to transcriptional machinery—or heterochromatic—a highly condensed conformation that prevents interactions with transcriptional machinery [reviewed in (Campos & Reinberg, 2009; Smith & Shilatifard, 2010)].

Polycomb group proteins mediate transcriptional repression in embryonic development.

Polycomb group (PcG) proteins are traditionally known for their role in epigenetic chromatin modifications that effect transcriptional repression of developmental regulatory genes. They were originally identified in the fruitfly *Drosophila melanogaster* as repressors of the *Hox* gene family (Lewis, 1978). Molecularly, PcG proteins are classified in two main complexes, known as PRC1 and PRC2. PRC2 complexes typically include homologs of the *Drosophila* genes *Extra sex combs* (*ESC*), *Suppressor of zeste 12* (*SU(Z)12*), and the catalytically active *Enhancer of zeste* (*E(Z)*). The PhoRC complex recruits the PRC2 complex to Polycomb recognition elements (PREs) at repressed genes, where PRC2 acts to trimethylate lysine 27 of histone H3 (H3K27me3) (Cao et al., 2002; Czermin et al., 2002; Müller et al., 2002). PRC1 is made up of homologs of the *Drosophila* genes *Polycomb* (*PC*), *Polyhomeotic* (*PH*), *Posterior sex combs* (*PSC*), and *Sex combs extra* (*SCE* or *RING*). The chromodomain of PC is traditionally thought to recognize the H3K27me3 mark established by PRC2, allowing for PRC1 binding to appropriate genomic locations and subsequent monoubiquitylation at lysine 119 on histone H2A (H2A119ub) by the E3 ubiquitin ligase RING (Fischle et al., 2003; Min, Zhang, & Xu, 2003; Wang et al., 2004). In addition to establishing the repressive H3K27me3 and H2A119ub marks, Polycomb group binding can recruit additional chromatin repressing proteins, such as histone deacetylases and DNA methyltransferases, which further act to silence transcription (Mills, 2010). While the core components of PRC1 and PRC2 are conserved from *Drosophila* to vertebrates, the exact composition of the two complexes can vary according to the animal, developmental timing, and cell type (Kerppola, 2009; Schuettengruber et al., 2007).

The essential role of PcG proteins in development is conserved from *Drosophila* to mammals. PRC2 function is required for mouse embryonic viability through gastrulation (Faust et al., 1998; Faust et al., 1995; O'Carroll et al., 2001; Pasini et al., 2004). Meanwhile, in general, PRC1 loss-of-function results in less severe phenotypes in later embryonic development, such as transformation of body segments, hematopoietic defects, and neurological abnormalities (Akasaka et al., 2001; Coré et al., 1997; Endoh et al., 2008; van der Lugt et al., 1996; del Mar Lorente et al., 2000; Takihara et al., 1997). One notable exception is the PRC1 H2A ubiquitin ligase protein RING1B (known as

RNF2 in humans), whose deletion results in embryonic lethality prior to gastrulation (Voncken et al., 2003). Interestingly, PRC1 and PRC2 mutations have distinct effects in differing cell types and developmental stages, suggesting that they may have overlapping roles throughout development (Lessard et al., 1999; Park et al., 2003; Su et al., 2003).

Trithorax group complexes counteract Polycomb group function to activate developmental gene transcription.

In Drosophila, the Trithorax group (TrxG) is a heterogenous group of proteins, including the SET domain-containing proteins Trithorax (TRX) and Absent, small, or homeotic discs 1 (ASH1). This complex is thought to aid in transcriptional activation of *Hox* genes and other developmental regulators by coordinating trimethylation of H3K4 and demethylation of H3K27me2/3 at its targets and, thus, counteracting PcG repressive function (Briggs et al., 2001; Klymenko & Müller, 2004; Roguev et al., 2001). Consistent with this hypothesis, loss of TrxG function in *Drosophila* results in loss of appropriate *Hox* gene expression, but expression is restored upon PcG mutation in the TrxG mutants (Klymenko & Müller, 2004). Thus, TrxG proteins play a key role to counteract PcG function and activate gene transcription of key developmental regulators.

Both Polycomb and Trithorax group proteins are also implicated in cancer initiation and progression.

While Polycomb and Trithorax group proteins were initially identified for their key role in development, more recent studies have implicated both protein groups in a variety of human cancers (Jones & Baylin, 2007; Mills, 2010; Rajasekhar & Begemann, 2007; Sparmann & van Lohuizen, 2006). In general, Polycomb group gain-of-function and Trithorax group loss-of-function mutations in cancer highlight the respective roles of Polycomb proteins as oncogenes and Trithorax proteins as tumor suppressors [reviewed in (Mills, 2010)]. These protein complexes work together throughout development to maintain proper expression of genes involved in cell cycle, differentiation, senescence, apoptosis, and DNA damage responses, thus establishing in each cell a transcriptional

identity that is passed on to daughter cells (referred to as "cellular memory") (Boyer et al., 2006; Lee et al., 2006; Ng & Gurdon, 2008; Ringrose & Paro, 2007). The mutation of Polycomb and Trithorax group genes in such cancers frequently results in a characteristic reactivation of the developmental pattern of gene expression, which is consistent with a failure in this "cellular memory" and subsequent reversion to a developmental state (Caldas & Aparicio, 1999; Jacobs & van Lohuizen, 2002; Mills, 2010; Takihara, 2008).

BCOR is a transcriptional corepressor found in a Polycomb-like complex.

The *Bcl6-interacting corepressor*, or *BCOR*, is a corepressor that associates with Polycomb group proteins (Gearhart et al., 2006). In humans, the *BCOR* gene is composed of 16 exons over a 126 kilobase (kb) region on chromosome Xp11.4. This region encodes a unique 1755 amino acid protein that is highly conserved across higher eukaryotic organisms. The BCOR protein contains three C-terminal tandem ankyrin repeats, which canonically serve to mediate protein-protein interactions (Huynh et al., 2000). However, no other recognizable motifs have been identified. Several groups have recently purified similar BCOR-containing chromatin modifying complexes, which include several PRC1 homologs and enzymatic activities typically associated with transcriptional repression (Gearhart et al., 2006; Mueller et al., 2007; Sánchez et al., 2007). All of these BCOR-containing complexes contain a RING homolog that catalyzes H2A monoubiquitylation, and some complexes also contain an H3K36 demethylase.

BCOR interacts with the proto-oncoprotein BCL6.

BCOR was initially identified as an interacting protein with the proto-oncoprotein BCL6, a POZ/BTB (Pox virus and zinc finger/BR-C, ttk, and bab) transcriptional repressor that is required for proper lymphocyte development (Basso & Dalla-favera, 2010; Chang et al., 1996). BCL6 represses the transcription of many genes that are implicated in lymphocyte activation and differentiation, cell cycle arrest, apoptosis, and DNA damage (Baron et al., 2002; Basso et al., 2010; Ci et al., 2009; Niu, Cattoretti, & Dalla-Favera, 2003; Phan & Dalla-favera, 2004; Shaffer et al., 2000; Tunyaplin et al.,

2004). In germinal center B cells, these repressive actions function to promote B cell survival, proliferation, and antibody production (Albagli-Curiel, 2003; Fukuda et al., 1997). BCL6 is aberrantly expressed in approximately 50% of diffuse large B cell lymphomas (DLBCLs) (Lo Coco et al., 1994; Pasqualucci et al., 2003; Wang et al., 2002). This is often a result of translocations that cause BCL6 promoter substitutions, resulting in aberrant BCL6 expression (Chen et al., 1998; Ye et al., 1995). The IμHABCL6 mouse mimics such a translocation and indeed results in DLBCL, confirming the role of BCL6 as an oncoprotein that drives lymphomagenesis (Cattoretti et al., 2005).

Much of BCL6 repressive activity is derived from its amino terminal POZ domain (Albagli et al., 1996; Chang et al., 1996; Seyfert et al., 1996). It is through this domain that BCL6 interacts with its corepressors, SMRT, NCOR, and BCOR, in a mutually exclusive manner (Huynh & Bardwell, 1998; Huynh et al., 2000). Interestingly, a peptide that blocks the ability of BCL6 to bind these three corepressors disrupts BCL6 repressive function and selectively inhibits BCL6-dependent DLBCL survival (Cerchietti et al., 2010; 2009). Thus, corepressor blocking peptides present a promising approach for blocking BCL6-driven DLBCLs in human patients.

BCOR itself may play a role in oncogenesis.

Several lines of evidence suggest that BCOR, like its interacting partner BCL6, may play a role in lymphomagenesis. *BCOR* expression in B cells closely parallels that of *BCL6*, with increased expression in normal germinal center B cells, low expression levels in memory B cells, and elevated expression in a subset of diffuse large B cell lymphomas (Huynh et al., 2000) (Bardwell, unpublished data). Chromatin immunoprecipitation studies have shown that BCOR is present at 40% of the BCL6 target genes, including some key tumor suppressor genes (Melnick and Bardwell, unpublished data). Thus, it is likely that BCOR plays a role in BCL6-driven lymphomagenesis by mediating BCL6 oncogenic activity.

Additional data suggest that BCOR itself may function as an oncogene. The BCOR locus is a common retroviral integration site in B cell lymphomas (Suzuki et al.,

2006; Suzuki et al., 2002), and BCOR mRNA levels are up-regulated in such tumors (Suzuki and Bardwell, unpublished data). Furthermore, BCOR was recently reported as a novel fusion partner with RARA (t(X;17)(p11;q12)) in a variant form of acute promyelocytic leukemia (Yamamoto et al., 2010). These data provide intriguing evidence that BCOR itself can act as an oncogene, in addition to its potential oncogenic role in BCL6-driven lymphomagenesis. This BCL6-independent oncogenic activity of BCOR may relate to its interaction with Polycomb group proteins, which are known to play roles in oncogenesis (see above).

Bcor is mutated in the human MCOPS disorders Oculofaciocardiodental syndrome and Lenz microphthalmia.

In addition to its potential role in cancer, BCOR has also been implicated in human development. X-linked Microphthalmia Syndromic (MCOPS) disorders encompass the two related genetic syndromes known as Oculofaciocardiodental Syndrome (OFCD) and Lenz microphthalmia (Horn et al., 2005; Ng et al., 2004). In general, MCOPS disorders are sex-specific syndromes characterized by developmental defects in the ocular, cardiac, nervous, skeletal, craniofacial, and hematopoietic systems (Gorlin, Marashi, & Obwegeser, 1996; Hilton et al., 2009; Schulze et al., 1999). While many of these characteristics are present in both OFCD and Lenz microphthalmia, the two subtypes are distinguished by their specific clinical manifestations and associated mutations.

Oculofaciocardiodental syndrome.

The OFCD subtype can result from a range of frameshift, deletion, and nonsense mutations in *BCOR* (Hilton, Black, & Bardwell, 2007; Ng et al., 2004). Such mutations typically either create large deletions of the *BCOR* coding region or generate a premature stop codon that presumably targets the transcript for nonsense-mediated decay.

Sixty-four female OFCD patients from twenty-two families have been reported to date (Hilton, Black, & Bardwell, 2007; Hilton et al., 2007; Hilton et al., 2009). These

patients are heterozygous for a mutant *BCOR* allele and can present with a range of phenotypes. Patients most commonly present with congenital cataracts, microphthalmia, septated nasal cartilage and high nasal bridge, cardiac septation defects, and radiculomegaly of the teeth. Less common characteristics include flexion deformities of the toes, syndactyly, mental retardation, scoliosis, and hearing loss. Mother to daughter transmission of the disease has been reported. Since no male OFCD patients have been observed, hemizygosity for the null *BCOR* allele is presumed to result in embryonic lethality (Hilton et al., 2007).

Since *BCOR* is positioned on the X chromosome, random X-inactivation during embryonic development is thought to play an important role in the phenotypic variability among OFCD patients. For example, X-inactivation analysis of leukocytes from female OFCD patients displayed 96-100% skewing in favor of cells expressing the wild type *BCOR* allele (Ng et al., 2004). This observation suggests that the wild type *BCOR* allele is strongly favored over the mutant allele during hematopoiesis and suggests a distinct survival advantage for cells expressing wild type BCOR. Thus, the phenotypic severity observed in a given OFCD patient likely reflects the specific pattern of X-inactivation within the affected tissues during development.

Lenz microphthalmia.

Lenz microphthalmia is a more rare form of MCOPS whose molecular cause is still undefined. Sequence analysis from two Lenz microphthalmia patients revealed a *BCOR* missense mutation (c.254C>T), resulting in an amino acid substitution (P85L) in BCOR protein (Ng et al., 2004). However, this mutation did not reduce *BCOR* translation efficiency or the ability of BCOR to bind BCL6 *in vitro* (Ng et al., 2004). Furthermore, when tethered to a promoter through a Gal4 DNA binding domain, this P85L version of BCOR repressed transcription as well as wild type BCOR. Genomic sequencing in twenty other clinically diagnosed Lenz microphthalmia patients did not reveal any other *BCOR* mutations (Hilton et al., 2009). These findings suggest that, while mutations in

BCOR may account for a subset of Lenz microphthalmia cases, other genes are likely to play an important role in the disease's etiology.

Lenz microphthalmia is characterized clinically by microphthalmia and clinical anophthalmia, mental retardation, radioulnar synostosis, and other skeletal anomalies (Gorlin, Marashi, & Obwegeser, 1996; Hilton et al., 2009). Lenz microphthalmia has only been reported in males and is thought to result in a subclinical phenotype in females who carry a similar mutation (Hilton et al., 2009).

Several Bcor loss-of-function animal models recapitulate OFCD phenotypes.

In light of the important role for BCOR in the development of multiple human tissues, several *Bcor* loss-of-function animal models have recently been created to study this role. These models involve the use of the zebrafish *Danio rerio*, the frog *Xenopus tropicalis*, and the mouse *Mus musculus*. The study of these models has begun to elucidate important aspects of BCOR molecular function in development.

Danio rerio.

In the first of these models, antisense splice-blocking morpholinos were targeted to the orthologs of *BCOR* exons nine and ten in the zebrafish *Danio rerio* (Schulze et al., 1999). Knockdown embryos displayed ocular colobomas and skeletal deformities, such as somite disorganization and tail kyphosis—phenotypes that are reminiscent of human OFCD patient characteristics (Hilton et al., 2007). In addition, *bcor* knockdown resulted in central nervous system developmental defects, such as cerebellar abnormalities, irregularities of the optic tectum and fourth ventricle, and overgrowth of the notochord. Thus, *bcor* knockdown in zebrafish partially phenocopies the OFCD patient characteristics and confirms the role of *Bcor* in eye, skeletal, and central nervous system development.

Xenopus tropicalis.

The second model utilized antisense morpholinos to target the 5` untranslated region of the *Bcor* ortholog in *Xenopus tropicalis,* inhibiting its translation (Hilton et al., 2007). The resulting *xtBcor* knockdown embryos displayed defects in cardiovascular and gut orientation, as well as ocular colobomas and microphthalmia. Interestingly, three OFCD patients were recently identified with defects in laterality, such as dextrocardia, asplenia, and intestinal malrotation (Hilton et al., 2007). Thus, *xtBcor* knockdown recapitulates both the ocular and laterality defects found in OFCD. Also of note, left-sided expression of *xtBcor* was required to prevent laterality defects, while ocular defects did not show any left-right bias (Hilton et al., 2007). In addition, *xtBcor* knockdown downregulated expression of *xtPitx2c*, a developmental regulator of left-sided morphogenesis. This suggests that the effect of *xtBcor* on laterality determination is mediated, at least in part, through the Nodal-Pitx2c signaling pathway.

BCOR regulation of *Xenopus* laterality is likely accomplished, at least in part, through association with the transcription factor BCL6. BCL6 and BCOR work together to exclude Mastermind-like 1 (MAM1) from the Notch transcriptional complex, preventing transcription of Notch target genes (Sakano et al., 2010). This subsequently inhibits *enhancer of split related 1* (*xtEsr1*) and allows for maintained *xtPitX2* expression (Sakano et al., 2010). Thus, the laterality defects observed in OFCD patients could reflect an underlying failure in regulation of the Nodal-PitX2 signaling pathway by the BCL6/BCOR complex.

Mus musculus.

The most recent animal models of OFCD involve two different *Bcor* loss-of-function alleles in the mouse *Mus musculus* (Wamstad et al., 2008). The first of these alleles, $Bcor^{Neo}$, generated a variant of *Bcor* that splices from the third exon into a neomycin resistance coding sequence. The second *Bcor* loss-of-function allele, $Bcor^{Gt}$, results from an insertional gene trap mutation within intron six, generating a BCOR-βgeo fusion protein. The chimeric mice containing the $Bcor^{Gt}$ or $Bcor^{Neo}$ alleles have a bias in coat color contribution and tail defects. In addition, $Bcor^{Neo/+}$ female mice display lens

opacifications, suggesting the presence of cataracts like those found in OFCD patients. Interestingly, the *Bcor*^{Neo} loss-of-function allele demonstrated a strong parent-of-origin effect, in which the mutant allele may only be transmitted paternally. Since only the paternal X chromosome is inactivated in the extraembryonic tissue of developing mice, this suggests an extraembryonic requirement for BCOR in development.

In *in vitro* differentiation assays, embryonic stem cell lines harboring the *Bcor*^{Neo} and *Bcor*^{Gt} loss-of-function alleles were delayed in expression of the *Fetal liver kinase 1* (*Flk1*) and *Brachyury* mesodermal markers and in repression of the embryonic stem cell pluripotency markers *Nanog* and *Oct3/4* (Wamstad et al., 2008). Restoration of *Bcor* expression in the *Bcor*^{Neo} line reinstated normal gene expression patterns. Furthermore, both *Bcor*^{Neo} and *Bcor*^{Gt} loss-of-function embryonic stem cells showed reduced ability to form primitive erythrocyte colonies, indicating a reduced contribution to hematopoiesis.

BCOR apparently plays a contrasting role in regulating differentiation of adult multipotent mesenchymal stem cells. In mesenchymal stem cells isolated from the teeth of an OFCD patient, mutation of *BCOR* increased H3K4/36 methylation, preventing BCL-6 binding to the *AP2alpha* promoter (Fan et al., 2009). This resulted in increased *AP2alpha* expression and enhanced mesenchymal stem cell differentiation into osteogenic and dentinogenic cell fates. Therefore, these data suggest that BCOR plays distinct roles in regulating target gene expression in different tissue types as development progresses, perhaps through interaction with cell type specific transcription factors and chromatin modifying proteins.

Bcor is expressed throughout mouse embryonic development.

In the mouse, *Bcor* is expressed as four major isoforms, labeled a, b, c, and d, which encode proteins varying in size from 1707 to 1759 amino acids (Wamstad & Bardwell, 2007). In general, throughout embryonic development and adulthood, the shorter c and d isoforms are most commonly expressed, while usage of the longer a and b isoforms is more selective (Wamstad & Bardwell, 2007). In the adult mouse, *Bcor* transcript is found ubiquitously but with differential isoform usage depending upon tissue

type (Wamstad & Bardwell, 2007). In the embryonic mouse, *Bcor* transcript is first detected around E8.5 and is expressed most strongly in the extraembryonic tissue (Wamstad & Bardwell, 2007). As the embryo progresses through gastrulation and organogenesis, *Bcor* expression increases throughout multiple tissue lineages (Wamstad & Bardwell, 2007). *Bcor* transcript is most consistently found in the nervous system tissues, including the neuroectoderm, notochord, neural tube, and dorsal root ganglia. *Bcor* is also expressed in the developing tail bud, limb bud, branchial arches, lungs, teeth, eyes, heart, and liver.

A conditional null allele of Bcor was created in mouse.

To investigate the role of BCOR in developmental disorders, the Bardwell lab has generated a conditional allele of *Bcor* in mice. Upon tissue specific expression of *Cre* recombinase, this conditional allele excises exons nine and ten of *Bcor* and also splices to the out-of-frame exon eleven, generating a premature stop codon (Figure 1-1). This approach was based on clinical and molecular evidence that such a strategy would generate a null allele of *Bcor*. *BCOR* sequencing in a severely affected human OFCD patient revealed an in-frame deletion of exon ten, suggesting that this exon is required for BCOR function (Wamstad & Bardwell, 2007). Furthermore, several OFCD patients have mutations in the ninth exon of BCOR, resulting in a premature stop codon. Finally, *in vitro* reconstitution experiments have demonstrated that *Bcor* exons nine through fifteen are required for the association between BCOR, PcG proteins, and the histone demethylase FBXL10 (Corcoran & Bardwell, unpublished data) (Gearhart et al., 2006). Thus, the Bardwell lab hypothesized that removal of mouse exons nine and ten, which are homologous to human exons nine and ten, would result in a null allele of *Bcor* that fails to associate with critical complex components.

Cre-mediated removal of exons nine and ten from this allele in mouse embryonic stem cells confirmed that full-length BCOR protein was ablated and that a C-terminally truncated version of BCOR was generated (Wamstad & Bardwell, unpublished data). However, this truncated BCOR protein was not observed in other mouse tissues (Gearhart & Bardwell, unpublished data). Subsequent gene expression profiling of *Bcor*

null embryonic stem cells revealed the upregulation of many genes important for embryonic development, including *Gata4*, *Gata6*, *Sox* genes, and several homeobox genes (Wamstad & Bardwell, unpublished data). The known functions of many of these BCOR downstream genes correlate with the tissues that are affected in OFCD patients.

Bcor is required for mouse embryonic viability.

Female mice containing the $Bcor^{Fl}$ conditional null allele were crossed to male mice expressing *Cre recombinase* under the control of the ubiquitously expressed *β-actin* promoter. This removes *Bcor* exons 9 and 10 from all embryonic and extraembryonic tissues within the resulting male $Bcor^{Fl/Y}$*; β-actin-Cre* progeny. These mice exhibit developmental delay and die around embryonic day 10.5 (Bardwell lab, unpublished data). In addition, the $Bcor^{Fl/+}$*; β-actin-Cre* female progeny from this cross have random X-inactivation in the embryo proper (i.e. mosaic expression of the deleted *Bcor* allele) and paternal X-inactivation in extraembryonic tissues (i.e. exclusive expression of the deleted *Bcor* allele). These females die by embryonic day 14.5 (Bardwell lab, unpublished data).

In contrast, when male mice containing the $Bcor^{Fl}$ conditional null allele were crossed to female mice expressing *β-actin-Cre,* the resulting $Bcor^{Fl/+}$*; B-actin-Cre* female embryos also have mosaic expression of the deleted *Bcor* allele but are supported by extraembryonic tissues that exclusively express the wild type *Bcor* allele. These females are viable and bear some similar craniofacial phenotypes to human OFCD patients (Bardwell lab, unpublished data). These results show that *Bcor* is required for mouse embryonic development, although its specific role in this process remains to be defined.

Summary.

Several lines of evidence point to roles for the X-linked corepressor BCOR in both cancer and development. These roles may be mediated, at least in part, by the interaction of BCOR with known proto-oncoproteins and/or chromatin modifying proteins. However, to date, it is not fully understood how interactions between BCOR

and its associated proteins act to regulate cancer and development. I aim for a detailed understanding of the mechanisms and biological relevance of BCOR repression in cancer and development for two reasons. First, molecular mechanisms of transcriptional repression are still being elucidated, and BCOR function is a useful paradigm for the function of chromatin modifying complexes. Second, understanding BCOR function will build on our current understanding of the molecular mechanisms underlying cancer and embryonic development. Therefore, my thesis studies focus on the mechanism and roles of BCOR function in cancer and development, with particular emphasis in the following four areas:

(1) Identification of BCOR-interacting chromatin modifying proteins and transcription factors;

(2) The potential role of BCOR as an oncoprotein in lymphomagenesis

(3) The role of BCOR in the developing neural crest cell population of mice; and

(4) The role of BCOR in cardiovascular development.

Ultimately, these studies will increase our understanding of how the BCOR complex mediates development and how mutations in BCOR contribute to the molecular pathogenesis of both cancer and developmental defects. Long-term, these studies will produce a greater general understanding of the molecular mechanisms of embryonic development, potentially paving the way for diagnostic tools and therapeutic reagents that may be used to prevent or treat developmental disorders.

Figure 1-1. *Bcor* conditional allele targeting strategy.

The conditional null allele of *Bcor* contains LoxP sequences flanking *Bcor* exons nine and ten. Upon tissue specific expression of Cre recombinase, exons nine and ten are excised, resulting in splicing to the out-of-frame exon eleven, generating a premature stop codon.

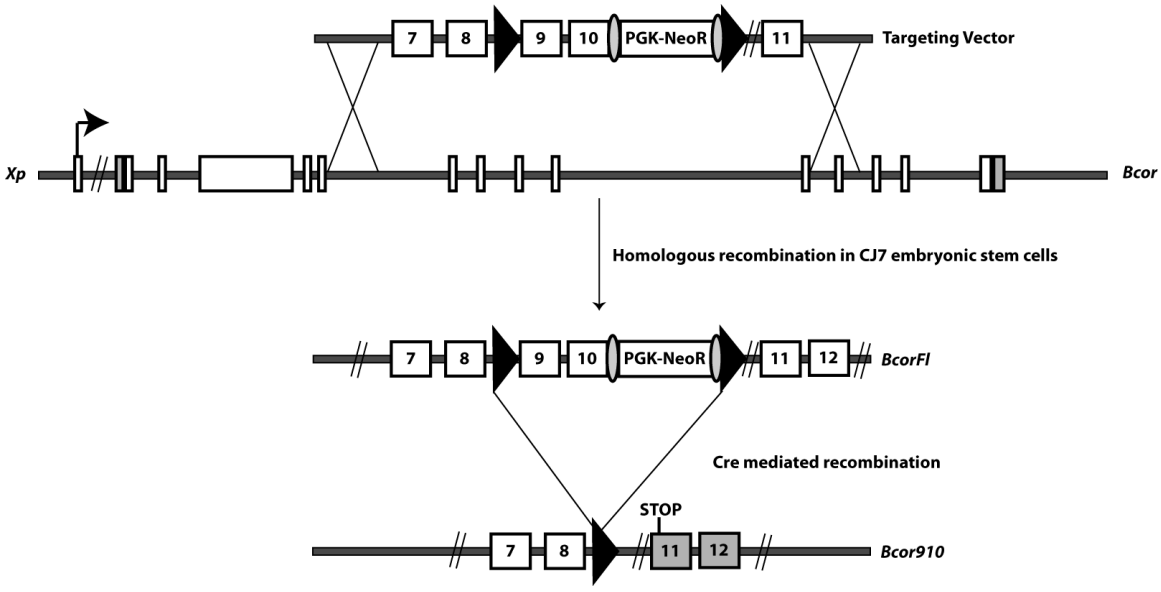
7
8
9
10
PGK-NeoR
11
Targeting Vector
Xp
Bcor
Homologous recombination in CJ7 embryonic stem cells
7
8
9
10
PGK-NeoR
11
12
BcorFl
Cre mediated recombination
STOP
7
8
11
12
Bcor910

Chapter 2.

BCOR interacts with Polycomb group proteins and several transcription factors.

Introduction.

The BCOR complex includes several chromatin modifying proteins.

To reveal BCOR-dependent repression mechanisms, the Bardwell lab previously performed biochemical analyses of the BCOR complex in the human embryonic kidney (HEK) 293 cell line and the cervical cancer HeLa cell line (Gearhart et al., 2006). Size-exclusion chromatography and silver-stain analysis of the affinity purified tandem epitope-tagged BCOR complex indicate that at least six proteins co-migrate with BCOR in a single ~800 kD complex. Mass spectrometric analysis of proteins associated with two-step affinity purified tandem epitope-tagged BCOR identified the PcG proteins NSPC1, RING1, and RNF2, as well as SKP1, a component of a Skp1-Cullin-F-BOX (SCF) E3 ubiquitin ligase (Gearhart et al., 2006). NSPC1 is a homolog of the *Drosophila* PcG protein, Posterior Sex Combs (Psc) (Gong et al., 2005; Nunes et al., 2001). Because NSPC1 had not been found in other PcG complexes, it appeared to be a unique component of the BCOR complex, and a reciprocal tagging experiment was subsequently performed. Purification of tagged NSPC1 isolated all of the associated bands observed in the BCOR complex and permitted identification of two additional bands, which were present but unidentified in the tagged-BCOR purification, as RING1-YY1-Binding protein (RYBP) (Garcia et al., 1999) and FBXL10 (JHDM1B) (Jin et al., 2004; Tsukada et al., 2006). The similarity in constituents between purifications of NSPC1 and BCOR suggests that BCOR and NSPC1 are requisite partners in HEK 293 cells. As described in more detail below, components of this complex include at least two chromatin-modifying enzymatic activities.

Protein interaction studies indicate that BCOR interacts with two sub-complexes.

To dissect the network of protein-protein interactions between BCOR and the other proteins in the complex, *in vitro* GST pull down experiments and co-immunoprecipitation assays were performed. From these studies, a model has been

derived in which BCOR recruits two sub-complexes: an SCF-like complex and a PcG complex (Gearhart et al., 2006).

BCOR interacts with an SCF-like complex that includes SKP1 and FBXL10.

SCF groups are best known as a family of E3 ubiquitin ligases, which were originally identified as required components for cell cycle progression in *Saccharomyces cerevisiae* (Feldman et al., 1997; Skowyra et al., 1997). The BCOR complex contains SKP1 and FBXL10, which appear to form an SCF-like BCOR-containing subcomplex (Gearhart et al., 2006) (Figure 2-2, blue subcomplex). In previously described SCF complexes, the Skp1/Cullin/RING protein core utilizes an associated F-BOX adapter protein to recruit specific targets for ubiquitylation and subsequent 26S proteolytic degradation (Patton, 1998; Willems, Schwab, & Tyers, 2004). A growing body of evidence indicates that these activities are intimately involved in gene control (Devoy et al., 2005; Dhananjayan, Ismail, & Nawaz, 2005; Muratani & Tansey, 2003). In addition, FBXL10, the F-BOX protein that interacts with BCOR in HEK293 cells, also has a known role in mediating H3K36me2 demethylation, allowing for more complete Polycomb group repression of targets (Tsukada et al., 2006; Yuan et al., 2011).

The BCOR-interacting SCF-like subcomplex is predicted to possess at least two enzymatic activities.

Ubiquitin ligase.

The FBXL10 and SKP1 components of the BCOR complex are presumed components of an SCF ubiquitin E3 ligase. FBXL10 is one of many F-BOX proteins containing the SKP1-interacting F-BOX domain (Dhananjayan et al., 2005). In the FBXL subfamily, leucine-rich repeats carboxy-terminal to the F-BOX recognize specific substrates that are then ubiquitylated and degraded by the 26S proteasome (Birke, 2002). The direct target of FBXL10 and whether it is poly- or mono-ubiquitylated are both

unanswered questions. A growing body of evidence indicates that ubiquitin and the proteasome are intimately involved in gene control (Eberharter et al., 2004; Jorgensen, Ben-Porath, & Bird, 2004; Voo et al., 2000).

Histone demethylase.

Unlike most other members of the FBXL subfamily, FBXL10 has additional domains that may help the BCOR complex find and modify appropriate chromatin targets. These include CXXC domains that bind unmethylated CpG sequences (Eberharter et al., 2004; Shi et al., 2007; Voo et al., 2000), PHD domains that bind methyl lysines within core histones (Eberharter et al., 2004; Tsukada et al., 2006; Wysocka et al., 2006), and the JmjC domain that serves as a histone H3K36 demethylase (Kim & Buratowski, 2007), a modification that is thought to promote transcriptional elongation (Rubnitz et al., 1994). Although there are multiple isoforms of FBXL10, the Bardwell lab has demonstrated with endogenous proteins that all of these FBXL10 isoforms co-immunoprecipitate with BCOR in 293 cells and in the Ramos B cell line (Bardwell lab, unpublished data). Importantly, ~25% of the BCOR complexes contain the longest isoform of FBXL10 and, thus, the JmjC demethylase domain.

BCOR also interacts with several Polycomb group proteins.

BCOR also interacts with several proteins that have previoiusly been described as members of Polycomb group complexes, including NSPC1, RING1, RNF2, and RYBP (Gearhart et al., 2006) (Figure 2-2, red subcomplex). Originally identified as regulators of homeotic genes in *Drosophila*, PcG complexes play important roles in mammalian development, maintenance of embryonic and adult stem cells, cell cycle regulation, and cancer (Gil, Bernard, & Peters, 2005; Raaphorst, 2005; Sauvageau & Sauvageau, 2010; Sparmann & van Lohuizen, 2006). PcG proteins are known to be part of a memory system that relies on epigenetic modification of specific histone tails to ensure faithful transmission of cell identities through cell division (Cao, Tsukada, & Zhang, 2005). In *Drosophila*, PcG proteins are found in two functionally distinct complexes, which are

thought to act sequentially in silencing. First, the PcG complex PRC2 (ESC-E(Z)) is thought to initiate repression by adding methylation marks to histone tails, and these subsequently recruit the PRC1 complex, which is involved in the maintenance of repression (Wang et al., 2004). In mammals, multiple homologs of PcG proteins exist, so there is more variability in the exact makeup of PRC2 and PRC1-like complexes (de Napoles et al., 2004).

BCOR co-purifies with RNF2 complexes.

The BCOR complex component RNF2 was initially identified as an E3 ubiquitin ligase that functions as a member of a PRC1 Polycomb complex (Lagarou et al., 2008; Ogawa et al., 2002; Sánchez et al., 2007a). However, it was also identified as a member of an E2F6.com-1 complex, suggesting that its functions extend beyond its incorporation into Polycomb complexes (Sánchez et al., 2007b). Thus, to elucidate these additional roles, biotinylated RNF2 was purified from erythroid cells, and associated proteins were identified by mass spectrometry (Jin et al., 2004). This purification confirmed that RNF2 interacts with BCOR and its associated proteins FBXL10, NSPC1, and SKP1, in addition to other previously identified PRC1 associated proteins and some previously unknown interacting proteins. A subsequent reciprocal tagging experiment with FBXL10 purified not only RNF2, but also the rest of the previously identified BCOR complex (Jin et al., 2004). Thus, these studies confirm the composition of the BCOR complex and further implicate BCOR in a chromatin-modifying role.

A similar experiment was performed to identify proteins that associate with the *Drosophila* homolog of RNF2, dRING, in *Drosophila* embryo nuclear extracts. In addition to identifying the canonical dRING-associated PRC1 complex, this purification yielded a similar but distinct dRING-containing complex that lacks PC and PH, which was named dRAF (dRING associated factors) (Willems et al., 2004). This complex bears high similarity to the BCOR complex, encompassing the RNF2 homolog and E3 ubiquitin ligase dRING, the NSPC1 homolog PSC, the FBXL10 homolog and H3K36 histone demethylase dKDM2, and a novel BCOR homolog dBCOR (unpublished, P.

Verrijzer, personal communication) (Devoy et al., 2005). This experiment further demonstrates the existence of a BCOR-containing Polycomb complex that is similar to, yet distinct from, the traditional PRC1 complex.

The BCOR complex enhances histone H2A mono-ubiquitylation activity of RNF2.

The BCOR complex PcG protein RNF2 has intrinsic E3 ligase activity for the histone protein H2A (Fang et al., 2004; Jason et al., 2005). Mono-ubiquitylated H2A (Ub-H2A) is involved in maintaining a repressed chromatin state (Cao et al., 2005; de Napoles et al., 2004; Tsukada et al., 2006; Wang et al., 2004). Consistent with the presence of RNF2, the BCOR complex purified from HEK293 cells catalyzes the addition of FLAG-tagged ubiquitin onto H2A but does so with at least 40 times the specific activity of GST-RNF2 alone (Bardwell lab, unpublished data).

Bcor interacts with the MLL fusion partners AF9 and ENL.

Finally, two recent studies have found that BCOR interacts with proteins that are commonly fused to the mixed lineage leukemia (MLL) protein in hematopoietic cancers. AF9 is a transcriptional activator that is thought to act in chromatin remodeling via incorporation into a SWI/SNF complex (Joh et al., 1996). In addition, it is one of the most common fusion partners with MLL in acute myeloid leukemias (Srinivasan, de Erkenez, & Hemenway, 2003). A recent yeast two-hybrid screen using the AF9 carboxy terminus as bait identified BCOR as an AF9 interacting protein (Srinivasan et al., 2003). BCOR interaction with AF9 is isoform-specific, suggesting that alternative splicing of *Bcor* transcript may function in regulating AF9 interaction. Furthermore, in an *in vitro* luciferase assay, the longest (‘a’) isoform of BCOR repressed AF9-mediated transactivation.

Eleven nineteen leukemia (ENL) is another common fusion partner with MLL in hematopoietic cancers. A recent purification of proteins associated with Flag-tagged ENL in human embryonic kidney cells identified BCOR, in addition to other Polycomb group

proteins (RING1 and CBX8), the histone H3 methyltransferase DOT1L, the transcriptional elongator protein pTEFb, and other MLL fusion partners (Mueller et al., 2007). This complex showed H3K79 demethylase activity, and ENL knockdown resulted in a global decrease in transcription. Thus, these studies show that BCOR is incorporated into multiple complexes involved in transcriptional activation and repression, further suggesting a regulatory role for the BCOR complex.

Summary and rationale.

Previous studies on BCOR-interacting proteins have found that BCOR interacts with the MLL fusion partners AF9 and ENL, an SCF-like subcomplex, and a PRC1-like subcomplex. However, although the described BCOR complex shares some components with previously described human PRC1-like PcG complexes (Levine et al., 2002; Levine, King, & Kingston, 2004), it does not contain all four of the core PRC1 components described in *Drosophila* (Trinkle-Mulcahy et al., 2008). In particular, it lacks a Pc component. Pc homologs have a methylated lysine-binding domain that is believed to recruit PRC1 to chromatin marked with a methyl group by the PRC2 initiator complex. One possibility is that BCOR serves the recruitment role, through its association with BCL6 or other DNA binding proteins. My experiments were designed to determine, using more sensitive mass spectrometry approaches, whether additional or alternative BCOR and NSPC1 complex components are present in HEK293 cells. This strategy differed from the previous HEK293 cell BCOR complex purification in its lower stringency and in using a Finnigan LTQ linear ion trap mass spectrometer, a new machine that is capable of analyzing more complex samples with unparalleled sensitivity. This may also help identify cell type specific transcription factors present in sub-stoichiometric amounts in the BCOR or NSPC1 complexes.

Materials and Methods.

Cloning, plasmids, and antibodies.

Bcor (full-length 'a' isoform), Fbxl10, Nspc1, Ring1, Rybp, Rnf2, and Skp1 were cloned from preexisting clones (Gearhart et al., 2006). Bcorl1 and Foxc1 were cloned by PCR amplification from HEK293 cDNA. Hey2, Tbx2, Tbx3, and Tbx20 were cloned by PCR amplification from cDNA full-length clones (Open Biosystems).

For insect cell expression, open reading frames were cloned into pIEx4-myc and pIEx4-myc-3XFlag vectors. For mammalian expression, Bcor isoform a and Bcorl1 were tagged at the N-terminus with tandem His tag, calmodulin binding peptide, and three copies of the Flag tag. N-terminally Flag-tagged human Nspc1 was cloned into pZOME-1N (Cellzome). These were then cloned into a modified version of pLentiLox3.7 containing a shortened version of the EF promoter and beta globin 5` untranslated region. This allowed us to create His-CBP-3XFlag-Bcor(a)-HA, His-CBP-3XFlag-Bcorl1-HA, ProtA2-TEV-CBP-flag-Nspc1, and His-CBP-3XFlag-HA encoding retroviruses. All nucleotides of inserts were verified by sequencing. Rabbit polyclonal antibodies were raised against BCOR, FBXL10, and NSPC1 using glutathione S-transferase (GST) fusions of human BCOR(C) (1035-1230) and human NSPC1 (128-189) and subsequently affinity purified.

BCOR and NSPC1 complex purifications.

Stable cell lines of HEK293 cells were generated by infection with His-CBP-3XFlag-Bcor(A)-HA, ProtA2 -TEV-CBP-flag-Nspc1, and His-CBP-3XFlag-HA retroviruses. Cells were cultured in Dulbecco's minimal essential medium (Cellgro) with 5% calf serum (Biosource) and 5 ug/ml blasticidin. Nuclear extracts were supplemented with 0.1% NP-40, 0.1% Tween, 2.0 mM EGTA, and 0.5 mM EDTA and incubated with M2-agarose (Sigma) overnight. Beads were washed in 50 mM Tris pH 8.0, 1.0 mM MgCl2, 1.0 mM imidazole, 0.1% NP-40, 20% glycerol, 2.0 mM dithiothreitol (DTT), 2.0

mM phenylmethylsulfonyl fluoride (PMSF), 2.0 mM EGTA, 0.5 mM EDTA, protease inhibitor cocktail (Complete EDTA-free; Roche), and 350 mM KCl (TGN350). Complexes were eluted with 30% yields using 2 mg/ml Flag peptide, substituting 2.0 mM CaCl2 for EGTA and EDTA in the TGN350 buffer, and recaptured with calmodulin-sepharose (GE HealthCare). Calmodulin beads were washed with TGN350 and stripped of protein using 100 mM Tris pH 8.5 with 8 M urea, heated at 37 degrees Celsius for 1 hour. For visualization, protein samples were resolved on a 4-12% NuPAGE Novex Bis-Tris gel in MOPS running buffer (Invitrogen) and visualized by silver staining (SilverQuest; Invitrogen) (Figure 2-1A). For mass spectrometry analysis, complexes were submitted for trypsinization and analysis at the University of Minnesota Center for Mass Spectrometry and Proteomics using liquid chromatography mass spectrometry (LC-MS) on an Orbitrap LTQ mass spectrometer. Proteins were identified using Mascot, and amenable peptides were confirmed by tandem mass spectrometry fragmentation.

BCORL1 complex purification.

Stable cell lines of HEK293 cells were generated by infection with His-CBP-3XFlag-Bcorl1-HA and His-CBP-3XFlag-HA retroviruses. Cells were cultured in Dulbecco's minimal essential medium (Cellgro) with 5% calf serum (Biosource) and 5 ug/ml blasticidin. Nuclear extracts were supplemented with 0.1% NP-40, 0.1% Tween, 2.0 mM EGTA, and 0.5 mM EDTA and incubated with M2-agarose (Sigma) overnight. Beads were washed in 50 mM Tris pH 8.0, 1.0 mM MgCl2, 1.0 mM imidazole, 0.1% NP-40, 20% glycerol, 2.0 mM dithiothreitol (DTT), 2.0 mM phenylmethylsulfonyl fluoride (PMSF), 2.0 mM EGTA, 0.5 mM EDTA, protease inhibitor cocktail (Complete EDTA-free; Roche), and 350 mM KCl (TGN350). Complexes were eluted with 30% yields using 2 mg/ml Flag peptide in the TGN350 buffer and were resolved on a 4-12% NuPAGE Novex Bis-Tris gel in MOPS running buffer (Invitrogen). Proteins were visualized by silver staining (SilverQuest; Invitrogen) (Figure 2-1B), and corresponding fragments from the experimental and control samples were excised. For mass spectrometry analysis, destained gel slices were submitted for trypsinization and analysis at the University of Minnesota Center for Mass Spectrometry and Proteomics using liquid

chromatography mass spectrometry (LC-MS) on an Orbitrap LTQ mass spectrometer.

Data analysis

Scaffold software was used to identify proteins and assign a percent confidence for identification, based on the number of peptides detected and the percent coverage for the identified protein. Proteins identified in the corresponding empty vector control purification were eliminated from each purification list. In addition, proteins previously found to bind affinity tags non-specifically were eliminated from each purification list (Trinkle-Mulcahy et al., 2008).

Insect cell co-immunoprecipitations.

Sf9 insect cells were maintained in logarithmic phase in serum-free medium at 20 degrees Celsius and 225 rpm agitation. pIEx4 plasmids were transiently transfected into Sf9 cells using Insect GeneJuice Transfection Reagent (Novagen). Cells were harvested in lysis buffer containing 1X phosphate buffered saline, 10% glycerol, 0.5% NP-40, 2 mM DTT, 2 mM sodium vanadate, 2 mM sodium fluoride, 1 mM PMSF, and complete protease inhibitor cocktail (Roche), sonicated for 15 seconds at 25% power, and incubated with M2 agarose beads (Sigma) for 3 hours. Beads were washed in lysis buffer and boiled to recover proteins, which were resolved on a 4-12% NuPAGE Novex Bis-Tris gel in MOPS running buffer (Invitrogen).

Western blots.

Proteins were transferred overnight at 4°C to a nitrocellulose membrane, blocked with non-fat dry milk and incubated with polyclonal anti-BCOR (Ng et al., 2004) and monoclonal anti-myc antibodies (Santa Cruz 9E10).

Results and Discussion.

Mass spectrometry confirms interaction between BCOR and chromatin modifying proteins.

Full-length human BCOR was tagged with the calmodulin binding peptide and 3 copies of the FLAG tag and was then stably expressed in human embryonic kidney (HEK) 293 cells. Two-step affinity purification yielded a complex mixture with enrichment for many proteins over the negative control (Figure 2-1A). Mass spectrometric analysis of the purified BCOR complex from a single purification run detected 263 BCOR interacting proteins, 35 of which were identified at greater than 95 percent confidence (Table 2-1). All of the previously identified BCOR interacting complex components, including FBXL10, RING1, RNF2, RYBP, NSPC1, and SKP1, were identified in the current purification with 100% confidence (Gearhart et al., 2006). In addition, the myeloid/lymphoid or mixed-lineage leukemia translocations 1 and 3 (MLLT1/ENL and MLLT3/AF9) and the chromobox homologs 4 and 8 (CBX4 and CBX8), which were previously present in BCOR-containing complexes but were not identified in the previous HEK293 BCOR purification, were confirmed as BCOR interacting proteins with 100% confidence (Srinivasan et al., 2003; Vandamme et al., 2011; Zhang, 2003). These data are summarized in the model for BCOR interacting proteins in Figure 2-2. Although this figure depicts the highest confidence interacting proteins as forming a single BCOR-containing complex, it is likely that BCOR can interact with different combinations of proteins in different conditions. The ability of BCOR to form complexes with different combinations of interacting proteins may play a critical role in controlling specific gene transcription throughout development and adult cellular maintenance.

Mass spectrometry identifies novel interactions between BCOR and several transcription factors.

Also identified with 100% confidence were 7 transcription factors, previously unknown to interact with BCOR (Table 2-1). Little is known regarding the transcription factors zinc finger protein 326 (ZNF326), zinc finger protein 512 (ZNF512), and zinc finger RNA binding protein (ZFR). Zinc finger protein 148 (ZNF148) is a CACCC-box binding protein capable of both transcriptional activation and repression and is involved in regulating T cell receptor gene expression (Lisowsky, 1999; Wang, Kobori, & Hood, 1993). Zinc finger protein 281 (ZNF281) shares sequence homology with ZNF148 and also is capable of both transcriptional activation and repression (Zhang, 2003). ZNF148 and ZNF281 have been shown to collaborate in regulating the expression of at least two different genes, vimentin and ornithine decarboxylase (Davis-Smyth et al., 1996; Law et al., 1999). Far upstream binding protein 3 (FUBP3) is a potent transcriptional activator known to bind sequence specifically to a single strand of the far upstream element (Honkanen, 2003).

Finally, the most well understood of these high confidence BCOR interacting transcription factors, forkhead box C1 (FOXC1), is a forkhead domain-containing transcription factor involved in regulating various aspects of embryonic development, including development of the cardiovascular, dental, craniofacial, and ocular systems. Humans with mutations in *FOXC1* develop Axenfeld-Rieger anomaly, a rare autosomal dominant syndrome most commonly characterized by anterior segment eye abnormalities, glaucoma, craniofacial defects, and tooth malformations (Mears et al., 1998; Winnier et al., 1999). Mice with mutations in *Foxc1* also develop severe cardiovascular defects, including outflow tract malformations and ventricular septal defect (Pagan et al., 2007).

Given the potential developmental relevance of the interaction between the BCOR complex and FOXC1, this interaction was examined by co-transfection and co-immunoprecipitation from Sf9 insect cells. Interestingly, immunoprecipitation of Flag-tagged FOXC1 does not co-precipitate BCOR (Figure 2-3A), suggesting that the interaction between BCOR and FOXC1 is either indirect or requires other stabilizing components. However, in the presence of BCOR, FBXL10, FOXC1, RING1, RNF2, RYBP, NSPC1, and SKP1, immunoprecipitation of Flag-tagged NSPC1 co-precipitates

FOXC1 along with the rest of the complex (Figure 2-3B). Further, elimination of either BCOR or RYBP from the complex significantly reduces FOXC1's interaction with the complex (Figure 2-3C). Therefore, this set of experiments confirms the interaction of FOXC1 with the BCOR complex in insect cells and suggests that both BCOR and RYBP are necessary for this interaction. Therefore, the ability of the BCOR complex to interact with FOXC1 may contribute to the important role of both BCOR and FOXC1 in development.

NSPC1 interacts with a similar set of chromatin modifying proteins as BCOR.

To determine the degree of overlap between BCOR and NSPC1 complex components, the NSPC1 complex was also two-step affinity purified in a similar manner to the BCOR complex (Figure 2-1A). Again, in a single purification run, purification of tagged NSPC1 isolated and identified all of the associated proteins observed in the original BCOR and NSPC1 complex purifications, including BCOR, FBXL10, RING1, RNF2, RYBP, and SKP1 (Table 2-2) (Gearhart et al., 2006). All were identified in the current purification with 100% confidence (Table 2-2). As expected, ENL/MLLT1, AF9/MLLT3, CBX4, and CBX8 were also confirmed to interact with NSPC1 with 100% confidence. FOXC1, the BCOR-interacting transcription factor described above, was also identified as an NSPC1-interacting protein with 84% confidence. The similarity in the major, high-confidence constituents between the tagged BCOR and tagged NSPC1 purifications seems to confirm that BCOR and NSPC1 do, indeed, interact with very similar complexes.

However, differences between the two complexes were also noted. Of particular importance, the NSPC1 complex purification elucidated an interaction with a protein known as BCL6 corepressor like 1 (BCORL1), which was not part of the purified BCOR complex. Bearing high homology to BCOR, BCORL1 is a transcriptional corepressor that contains a putative bipartite nuclear localization signal, tandem ankyrin repeats, and two LXXLL motifs that recruit nuclear receptor coregulators. It acts with several Class II histone deacetylases (HDACS 4, 5, and 7) and with C-terminal binding protein (CtBP) to

repress transcription (Pagan et al., 2007). BCOR-L1 is expressed at very low levels in many adult tissues, with highest expression in the adult prostate and testis (Pagan et al., 2007). These data suggest that NSPC1 might interact with BCOR and BCORL1 in a mutually exclusive fashion, and this exclusivity might play a role in regulating the functions of each complex throughout development and homeostasis.

BCORL1 interacts with NSPC1 but not BCOR.

In light of the newly elucidated interaction between BCORL1 and NSPC1, the BCORL1 complex was subsequently one-step purified from human embryonic kidney 293 cells. However, this purification of tagged BCORL1 did not work as expected, likely due to high background from the less stringent, one-step purification (Figure 2-1B). Thus, the results obtained from this purification are tentative and must still be confirmed. Tentative results suggest that BCORL1 interacts with many structural proteins, such as drebrin and myosin (Table 2-3). In addition, this purification confirmed the interaction between BCORL1 and NSPC1 but not between BCORL1 and BCOR (data not shown). In addition, BCORL1 does interact with the BCOR-interacting proteins RYBP, RING1, RNF2, SKP1, and CBX4 but does not appear to interact with the demethylase FBXL10 or the chromodomain-containing protein CBX8 (data not shown).

Summary.

BCOR interacts with an SCF-like subcomplex capable of H3K36me2 demethylation and a Polycomb-like subcomplex capable of H2A119 ubiquitylation. In addition, BCOR interacts with the MLL fusion partners AF9 and ENL, as well as several transcription factors.

NSPC1 shares many of these key BCOR-interacting chromatin modifying proteins and some BCOR-interacting transcription factors. In addition, NSPC1 interacts with the BCOR homolog BCORL1.

BCORL1 purification was not that successful. Tentative results suggest that it may interact with many structural proteins but also shares some BCOR and NSPC1 interactors.

Figure 2-1. Affinity purified NSPC1, BCOR, and BCORL1 complexes from human embryonic kidney cells.

Silver stained protein gels showing the two-step purified NSPC1- and BCOR-associated proteins (A) and one-step purified BCORL1-associated proteins (B), along with their respective negative control purifications.

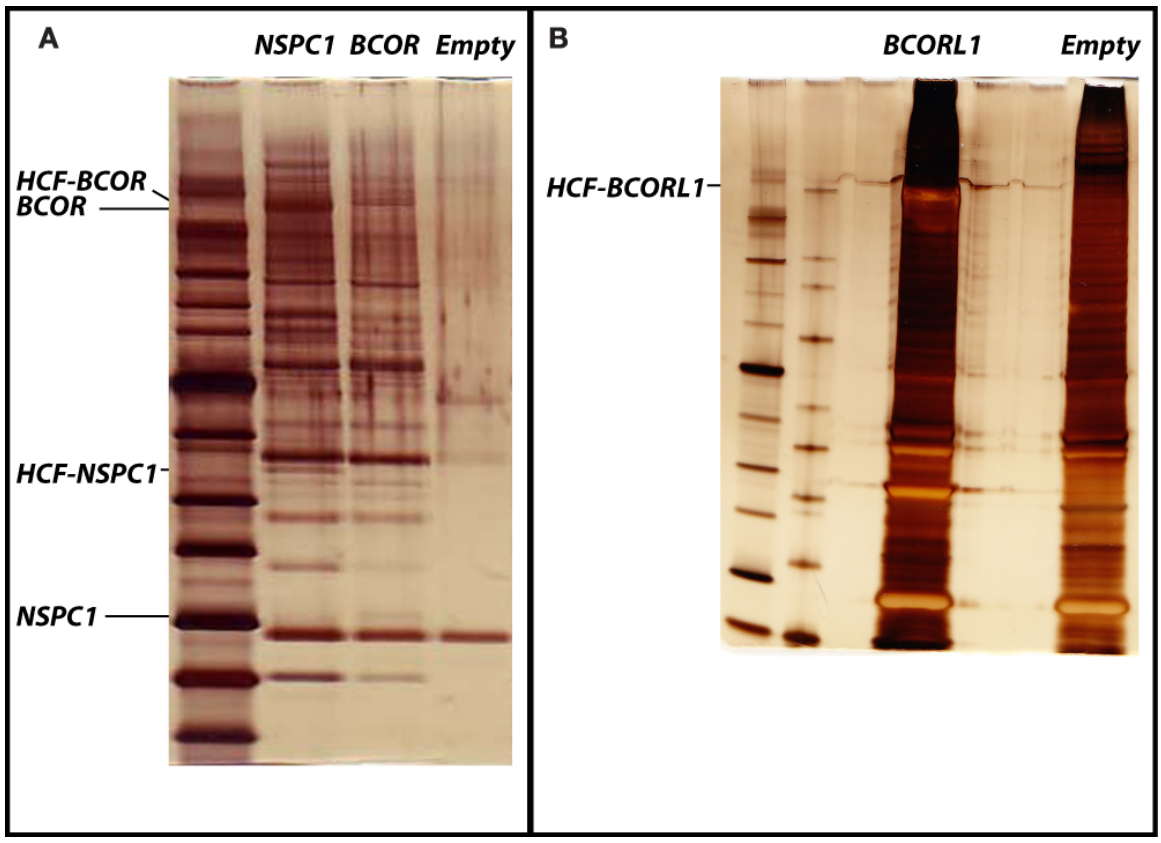
A
NSPC1
BCOR
Empty
HCF-BCOR
BCOR
HCF-NSPC1
NSPC1
B
BCORL1
Empty
HCF-BCORL1

Figure 2-2. Model for BCOR-interacting proteins.

BCOR interacts with two primary sub-complexes, an SCF-like subcomplex (blue) that demethylates H3K36 dimethyl and a Polycomb-like subcomplex (red) that ubiquitylates H2AK119. In addition, BCOR interacts with the MLL fusion partners AF9 and ENL (green), as well as a number of transcription factors (yellow). Transcription factors may have multiple contacts with the complex as in the case of FOXC1.

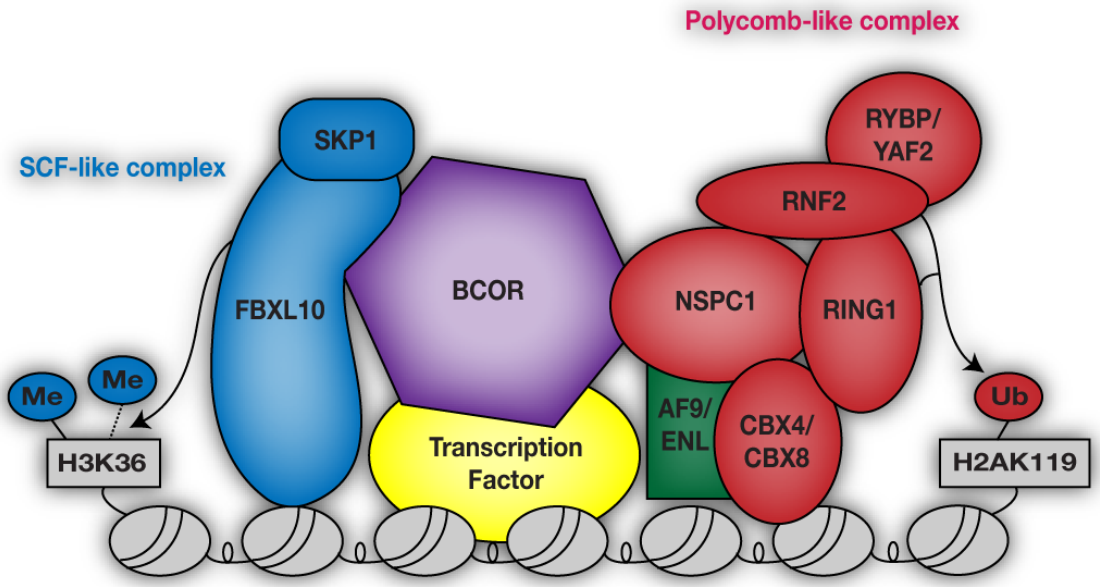
Polycomb-like complex
SCF-like complex
SKP1
RYBP/
YAF2
RNF2
FBXL10
BCOR
NSPC1
RING1
Me
Me
H3K36
Transcription
Factor
AF9/
ENL
CBX4/
CBX8
Ub
H2AK119

Figure 2-3. Western blots confirm FOXC1's interaction with the BCOR complex in vitro.

(A) Immunoprecipitation of FLAG-tagged BCL6 with and without BCOR (lanes 1 and 2) and FLAG-tagged FOXC1 with and without BCOR (lanes 3 and 4), followed by Western blotting for BCOR, BCL6, and the MYC tag. (B) Immunoprecipitation of FLAG-tagged NSPC1 in the presence of BCOR, FBXL10, FOXC1, RING1, RNF2, RYBP, NSPC1, and SKP1, followed by Western blotting for MYC. (C) Immunoprecipitation of FLAG-tagged NSPC1, omitting each of the major complex components (FOXC1, lane 1; none, lane 2; BCOR, lane 3; FBXL10, lane 4; RING1, lane 5; RNF2, lane 6; RYBP, lane 7; SKP1, lane 8), followed by Western blotting for MYC.

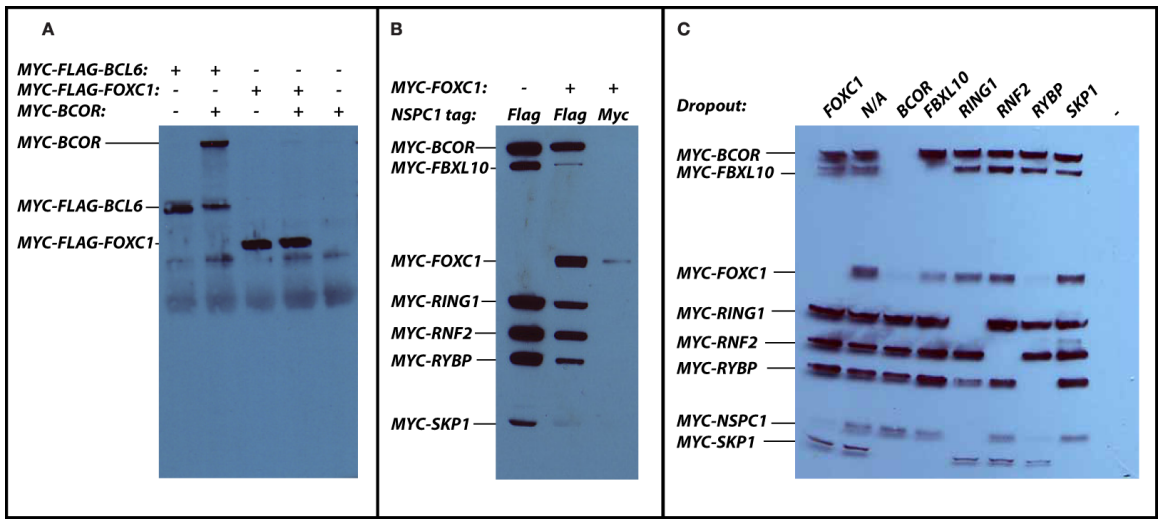
A
MYC-FLAG-BCL6: + + - - -
MYC-FLAG-FOXC1: - - + + -
MYC-BCOR: - + - + +
MYC-BCOR
MYC-FLAG-BCL6
MYC-FLAG-FOXC1
B
MYC-FOXC1: - + +
NSPC1 tag: Flag Flag Myc
MYC-BCOR
MYC-FBXL10
MYC-FOXC1
MYC-RING1
MYC-RNF2
MYC-RYBP
MYC-SKP1
C
Dropout:
FOXC1
N/A
BCOR
FBXL10
RING1
RNF2
RYBP
SKP1
MYC-BCOR
MYC-FBXL10
MYC-FOXC1
MYC-RING1
MYC-RNF2
MYC-RYBP
MYC-NSPC1
MYC-SKP1

Table 2-1. BCOR interacts with chromatin modifying proteins and transcription factors.

BCOR interacts with previously identified chromatin modifying proteins (gray rows), transcription factors (designated as "+"), and newly identified NSPC1-interacting proteins (designated by asterisks).

Gene symbol	Identified Proteins	Molecular Weight	Probability of Protein ID	Unique Peptides Identified	Protein Coverage
BCOR	BCL-6 interacting corepressor isoform c	192 kDa	100%	63	56%
FBXL10	F-box and leucine-rich repeat protein 10 isoform a	153 kDa	100%	38	42%
SKP1	S-phase kinase-associated protein 1 isoform b	19 kDa	100%	15	83%
MLLT3	myeloid/lymphoid or mixed-lineage leukemia; translocated to, 3	63 kDa	100%	15	38%
RNF2	ring finger protein 2	38 kDa	100%	15	57%
PCGF1	polycomb group ring finger 1	30 kDa	100%	11	62%
MLLT1	myeloid/lymphoid or mixed-lineage leukemia; translocated to, 1	62 kDa	100%	12	26%
HNRNPF*	heterogeneous nuclear ribonucleoprotein F	46 kDa	100%	13	52%
RYBP	RING1 and YY1 binding protein	25 kDa	100%	7	39%
RING1	ring finger protein 1	42 kDa	100%	7	24%
KIAA1967	p30 DBC protein	103 kDa	100%	8	17%
YAF2	YY1 associated factor 2	20 kDa	100%	4	37%
ZNF326*+	zinc finger protein 326 isoform 1	66 kDa	100%	6	15%
QSER1*	glutamine and serine rich 1	190 kDa	100%	9	9.20%
SFRS14	splicing factor, arginine/serine-rich 14	120 kDa	100%	6	7.00%
NOL5A*	nucleolar protein 5A	66 kDa	100%	6	15%
CBX4	chromobox homolog 4	61 kDa	100%	4	8.90%
AMOT	angiomotin isoform 1	118 kDa	100%	6	8.10%
UBAP2L	ubiquitin associated protein 2-like isoform a	115 kDa	100%	5	7.10%
ZNF148*+	zinc finger protein 148	89 kDa	100%	5	10%
CBX8	chromobox homolog 8	43 kDa	100%	4	15%
ZNF512+	zinc finger protein 512	65 kDa	100%	3	9.90%
NOP5/NOP58	nucleolar protein NOP5/NOP58	60 kDa	100%	3	8.10%
RBM9	RNA binding motif protein 9 isoform 5	47 kDa	100%	3	13%
ZC3H18*	zinc finger CCCH-type containing 18	106 kDa	100%	3	5.90%
FUBP3+	far upstream element (FUSE) binding protein 3	62 kDa	100%	3	5.20%
ZFR+	zinc finger RNA binding protein	117 kDa	100%	3	4.70%
GPATCH4	G patch domain containing 4 isoform 1	43 kDa	100%	3	11%
C11ORF30	EMSY protein	141 kDa	100%	2	1.90%
MKRN2	makorin, ring finger protein, 2	47 kDa	100%	2	7.50%
DPY30	dpy-30-like protein	11 kDa	100%	2	31%
ZNF281+	zinc finger protein 281	97 kDa	100%	2	6.70%
FOXC1+	forkhead box C1	57 kDa	100%	2	9.20%
MSI1	musashi 1	39 kDa	99%	2	8.00%
RBBP4	retinoblastoma binding protein 4	48 kDa	99%	2	9.20%
FRAS1	Fraser syndrome 1 REVERSED SEQUENCE	443 kDa	98%	2	2.70%

Table 2-2. NSPC1 interacts with chromatin modifying proteins and transcription factors.

NSPC1 interacts with previously identified chromatin modifying proteins (gray rows), transcription factors (designated as "+"), and newly identified BCOR-interacting proteins (designated by asterisks).

Gene Symbol	Identified Proteins	Molecular Weight	Probability of Protein ID	Unique Peptides Identified	Protein Coverage
BCOR	BCL-6 interacting corepressor isoform c	192 kDa	100%	99	70%
FBXL10	F-box and leucine-rich repeat protein 10 isoform a	153 kDa	100%	49	44%
BCORL1	BCL6 co-repressor-like 1	183 kDa	100%	47	40%
SKP1	S-phase kinase-associated protein 1 isoform b	19 kDa	100%	18	88%
RNF2	ring finger protein 2	38 kDa	100%	10	35%
RYBP	RING1 and YY1 binding protein	25 kDa	100%	9	39%
RING1	ring finger protein 1	42 kDa	100%	7	36%
PCGF1	polycomb group ring finger 1	30 kDa	100%	8	46%
HNRNPF*	heterogeneous nuclear ribonucleoprotein F	46 kDa	100%	9	44%
CBX4	chromobox homolog 4	61 kDa	100%	7	15%
YAF2	YY1 associated factor 2	20 kDa	100%	4	37%
QSER1*	glutamine and serine rich 1	190 kDa	100%	5	3.90%
MORC4	zinc finger, CW type with coiled-coil domain 2 isoform a	106 kDa	100%	4	7.50%
YLPM1	YLP motif containing 1	242 kDa	100%	4	4.10%
OTUD4	OTU domain containing 4 protein isoform 3	117 kDa	100%	3	5.00%
NOL5A*	nucleolar protein 5A	66 kDa	100%	4	6.10%
MLLT3	myeloid/lymphoid or mixed-lineage leukemia; translocated to, 3	63 kDa	100%	3	6.70%
ZC3H18*	zinc finger CCCH-type containing 18	106 kDa	100%	3	5.70%
ABCB7	highly divergent homeobox	77 kDa	100%	2	4.30%
CBX8	chromobox homolog 8	43 kDa	100%	2	10%
ZNF148*+	zinc finger protein 148	89 kDa	100%	2	3.00%
MLLT1	myeloid/lymphoid or mixed-lineage leukemia; translocated to, 1	62 kDa	100%	2	5.00%
CTCF+	CCCTC-binding factor	83 kDa	99%	2	2.90%
SETD2	huntingtin interacting protein B	231 kDa	99%	2	1.70%
CYFIP1	cytoplasmic FMR1 interacting protein 1 isoform a REVERSED SEQUENCE	145 kDa	99%	2	4.20%
ZNF326*+	zinc finger protein 326 isoform 1	66 kDa	98%	2	4.80%

Table 2-3. BCORL1 interacts primarily with structural proteins.

BCORL1 interacts with many structural proteins, as well as some shared BCOR- and NSPC1-interacting proteins (asterisks).

Gene Symbol	Identified Proteins	Molecular Weight	Unique Peptides Identified	Peptides Identified in Negative
BCORL1	BCL-6 corepressor-like protein 1 OS	183 kDa	116	1
DBN1	Drebrin OS	71 kDa	36	0
MYO18A	Myosin-XVIIIa OS	233 kDa	24	0
FLII	Protein flightless-1 homolog OS	145 kDa	20	0
CYTSA	Cytospin-A OS	125 kDa	18	0
MYO1D	Myosin-Id OS	116 kDa	17	0
LMO7	LIM domain only protein 7 OS	193 kDa	15	0
MYO5A	Myosin-Va OS	215 kDa	15	0
FHL1	Four and a half LIM domains protein 1 OS	36 kDa	15	1
RAI14	Ankycorbin OS	110 kDa	10	0
TPM1	Tropomyosin alpha-1 chain OS	33 kDa	10	0
PELP1	Proline-, glutamic acid- and leucine-rich protein 1 OS	120 kDa	9	1
BCORL1	Isoform 3 of BCL-6 corepressor-like protein 1 OS	191 kDa	9	1
AMOT*	Angiomotin OS	118 kDa	8	0
MPRIP	Myosin phosphatase Rho-interacting protein OS	117 kDa	8	0
IRS4	Insulin receptor substrate 4 OS	134 kDa	8	1
U2AF2	Splicing factor U2AF 65 kDa subunit OS	54 kDa	7	0
RING1*	E3 ubiquitin-protein ligase RING1 OS	42 kDa	7	1
CGGBP1	CGG triplet repeat-binding protein 1 OS	19 kDa	6	0
SR140	U2-associated protein SR140 OS	118 kDa	6	0
TEX10	Testis-expressed sequence 10 protein OS	106 kDa	6	1
UBA1	Ubiquitin-like modifier-activating enzyme 1 OS	118 kDa	6	1

Chapter 3.

Bcor expression must be properly regulated for mouse embryogenesis and is tightly controlled in mouse germinal center B cells.

Introduction.

BCL6 is a proto-oncoprotein that contributes to lymphomagenesis.

The proto-oncoprotein BCL6 is a POZ/BTB transcriptional repressor that is required for proper lymphocyte development. BCL6 is aberrantly expressed in approximately 50% of diffuse large B cell lymphomas (DLBCLs) (Lo Coco et al., 1994; Pasqualucci et al., 2003; Wang et al., 2002). This is often a result of translocations that cause BCL6 promoter substitutions (Chen et al., 1998; Ye et al., 1995). The IμHABCL6 mouse mimics such a translocation and indeed results in DLBCL, confirming the role of BCL6 as an oncoprotein that drives lymphomagenesis (Cattoretti et al., 2005).

The interaction of BCOR with BCL6 suggests a potential oncogenic role.

The transcriptional corepressor BCOR (BCL6 interacting corepressor) interacts with BCL6 (Huynh et al., 2000) and functions by recruiting polycomb group (PcG) and other chromatin modifying proteins (Gearhart et al., 2006). *BCOR* expression in B cells closely parallels that of *BCL6*, with increased expression in normal germinal center B cells, low expression levels in memory B cells, and elevated expression in a subset of diffuse large B cell lymphomas (Bardwell lab, unpublished data). Chromatin immunoprecipitation studies have shown that BCOR is present at forty percent of the BCL6 target genes, including some key tumor suppressor genes (Melnick & Bardwell, unpublished data). Thus, it is likely that BCOR plays a role in BCL6-driven lymphomagenesis by mediating BCL6 oncogenic activity.

BCOR itself may play an oncogenic role independently of BCL6 misexpression.

In addition to its potential role in mediating BCL6 oncogenic activity, BCOR itself may be a proto-oncoprotein. Several mouse retroviral insertion screens have identified the BCOR locus as a common retroviral integration site in B cell lymphomas (Mohan et al., 2010; Suzuki et al., 2006), and BCOR mRNA levels are up-regulated in

such tumors (Suzuki & Bardwell, unpublished data). This strongly suggests that BCOR itself is capable of acting as an oncoprotein.

Summary and rationale.

Bcor's pattern of expression, interaction with BCL6, role in BCL6-mediated repression, and common retroviral integration in B cell lymphomas make it a strong candidate oncogene in lymphomagenesis, working either independently or in collaboration with BCL6. To investigate the potential role of *Bcor* as an oncogene, we attempted to generate mice that either express *Bcor* ubiquitously or that overexpress *Bcor* specifically in the mature germinal center B cells, the cells from which BCL6 driven lymphomas arise. To accomplish this, we created a conditional allele of *Bcor* to constitutively express *Bcor* upon activation of *Cre* recombinase. This allele was utilized in combination with the ubiquitously expressed *βactin-cre* to obtain mice that express *Bcor* ubiquitously. In addition, the conditional allele of *Bcor* was used in combination with a *CD21-cre*, which is expressed in mature germinal center B cells and follicular dendritic cells, to obtain mice that overexpress *Bcor* in mature germinal center B cells (Kraus et al., 2004). We expected that an analysis of rates of tumor formation in these animals would allow us to determine whether *Bcor* constitutive expression can drive oncogenesis, either in the whole animal or specifically in mature B cells. In addition, we hoped to breed these animals to IμHABCL6 mice to determine if *Bcor* misexpression can increase or accelerate BCL6-driven B cell lymphomagenesis.

Materials and Methods.

Targeting vector design.

We generated a conditional myc-tagged Bcor targeting vector in which a splice acceptor and a LoxP-flanked transcriptional "stop" cassette ("BigT," provided by Dr. Shankar Srinivas) are engineered upstream of the myc-Bcor sequence (Figure 3-1A). The BigT transcriptional "stop" cassette contains a PGK-driven neomycin resistance allele followed by multiple polyadenylation sites and is excised upon expression of Cre recombinase, allowing for expression of the *myc-Bcor* coding sequence. To generate the targeting vector, the BigT-myc-Bcor sequence was then inserted into the ROSA26PA plasmid (AddGene), which flanks the inserted region with 5` and 3` Rosa26 homology arms of 1.1 and 4.3 kb, respectively (Kraus et al., 2004). This targeting vector was linearized with Kpn1 and electroporated into CJ7 embryonic stem (ES) cells. ES cell clones containing a copy of the homologously recombined $Rosa26^{Bcor}$ allele were identified by Southern blot (see "Genomic Southern blot evaluation of targeted Bcor ES cells") and were provided to the University of Minnesota Mouse Genetics Laboratory for injection into blastocysts and generation of chimeras. Chimeras were bred to obtain $Rosa26^{Bcor}$ heterozygotes ($Rosa26^{Bcor/+}$).

Genomic Southern blot evaluation of targeted Bcor *ES cells.*

Following neomycin selection, genomic DNA was prepared from 384 neomycin resistant colonies. DNA was then digested with EcoRV, separated by agarose gel electrophoresis, and transferred to positively charged nylon membranes. These membranes were then hybridized to radiolabeled DNA probes designed to detect both wild type (11.5 kb 5` and 11.5 kb 3`) and targeted (4.1 kb 5` and 16.5 kb 3`) alleles (5` arm Figure 3-1B, 3` arm not shown). Primer sequences are as follows:

5` Arm Forward: 5` – AATACCCAGGCAAAAAGGGGAGACC – 3`

5` Arm Reverse: 5` – GCTCAGAGACTCACGCAGCCCTAGT – 3`

3` Arm Forward: 5` – CTGTCTGAGCAGCAACAGGTCTTCG– 3`

3` Arm Reverse: 5` – CACAATATTGCTCGCACCAACACAA– 3`

Mouse breeding.

To generate mice that express *Bcor* ubiquitously, $Rosa26^{Bcor}$ heterozygotes were bred to mice containing a Cre recombinase transgene whose expression is driven by the ubiquitously expressed beta actin promoter (*βactin-cre*). $Rosa26^{Bcor}$ heterozygotes containing the *βactin-cre* allele were utilized as experimental animals while $Rosa26^{Bcor}$ heterozygotes without the *βactin-cre* allele were controls.

To overexpress *Bcor* specifically in mature germinal center B cells, $Rosa26^{Bcor}$ heterozygotes were bred to mice containing a Cre recombinase transgene whose expression is driven by the mouse complement receptor 2 promoter (*CD21-cre*) (Kraus et al., 2004). The resulting $Rosa26^{Bcor}$ heterozygotes were then interbred to obtain $Rosa26^{Bcor/+}$; *CD21-cre* and $Rosa26^{Bcor/Bcor}$; *CD21-cre* experimental animals and $Rosa26^{Bcor/+}$ controls.

To identify cells in which Cre is expressed, we obtained mice containing a Cre-responsive YFP reporter ($Rosa26^{YFP}$). $Rosa26^{YFP}$ homozygotes were bred with $Rosa26^{Bcor/+}$*; CD21-cre* animals to generate $Rosa26^{Bcor/YFP}$*; CD21-cre* experimentals and $Rosa26^{Bcor/YFP}$ and $Rosa26^{+/YFP}$*; CD21-cre* controls.

Determination of mouse and embryo genotypes.

Genotypes of offspring were identified based on two different polymerase chain reactions (PCR) on DNA prepared from either mouse tails or embryonic yolk sacs. The wild type Rosa26 allele was identified by PCR using the following primers, which generate an 800 base pair product:

Rosa26 Forward: 5'- GCTCTCCCAAAGTCGCTCTGAG -3'

Rosa26 Reverse: 5'- GCCCCAGCTACAGCCTCGATTTGTG-3'

The Rosa26 insertion allele was identified by PCR using the following primers, which generate a 320 base pair product:

Rosa26 Forward: 5'- GCTCTCCCAAAGTCGCTCTGAG -3'

Rosa26 Insert Reverse: 5'- AAGACCGCGAAGAGTTTGTC-3'

The Rosa26-Bcor and Rosa26-YFP alleles were then distinguished by PCR using the following primers, which generate 240 base pair and 430 base pair products, respectively:

BigT Forward: 5'- TCATGTCTGGATCCCCATCAAGCTG-3'

Rosa26Bcor Reverse: 5'- CCACACATGCGGACCCTCTCG-3'

Rosa26YFP Reverse: 5'- CTTCGGGCATGGCGGACTTG-3'

The presence of the Cre allele was also ascertained by PCR using the following primers, which generate a 300 base pair product:

Cre Forward: 5'- CCTGATGGACATGTTCAGGGATCG-3'

Cre Reverse: 5'- TCCATGAGTGAACGAACCTGGTCG-3'

Isolation of splenocytes.

To isolate splenocytes, whole spleens were dissected from adult animals and halved. Cells were dissociated through steel mesh using a plunger, passed over 70 um nylon mesh, rinsed in phosphate buffered saline (PBS), rinsed with ACK lysis buffer (0.15 M ammonium chloride, 10 mM potassium carbonate, 0.1 mM sodium EDTA) to lyse red blood cells, and resuspended in PBS containing 2% fetal bovine serum and 2 mM EDTA.

Western blot for BCOR protein.

To determine relative BCOR protein levels in *Rosa26*$^{Bcor/+}$*; CD21-cre* splenocytes and *Rosa26*$^{Bcor/Bcor}$*; CD21-cre* splenocytes compared to *Rosa26*$^{Bcor/Bcor}$splenocytes,

protein was prepared from an equal number of isolated splenocytes for each sample using TriZol.

To determine relative Bcor protein levels in *Rosa26*$^{Bcor/YFP}$*; CD21-cre* mature germinal center cells compared to *Rosa26*$^{+/YFP}$*; CD21-cre* mature germinal center cells, YFP positive splenocytes were isolated by fluorescence activated cell sorting (FACS), and protein was prepared from an equal number of cells for each sample using TriZol.

In both cases, proteins were resolved on a NuPAGE 3-8% Tris-Acetate gel (Invitrogen) and transferred to nitrocellulose membranes at 4`C overnight. Membranes were blocked in Odyssey blocking buffer (Li-COR Biosciences) and incubated with rabbit polyclonal anti-Bcor antibody (D. Ng et al 2004), mouse monoclonal anti-myc 9E10 antibody (Santa Cruz sc-40), and/or mouse monoclonal anti-β–actin antibody (Abcam 8226). Membranes were then incubated with anti-rabbit Rockland IRDIS 800 and/or anti-mouse Alexa 680 secondary antibodies, and proteins were detected using the Odyssey Infrared Imaging System.

Quantitative RT-PCR.

Total RNA was isolated from splenocytes using TriZol, and cDNA was generated using MMLV reverse transcriptase (Invitrogen). Bcor PCR was performed using the following primers:

Bcor N-terminus Forward: 5'- CGCATGTGTGGAACAAGTGA -3'

Bcor N-terminus Reverse: 5'- ACGATGTTTCCAGGGACCC -3'

Bcor C-terminus Forward: 5'- CACATACTCAGGGAGAACCATCATG-3'

Bcor C-terminus Reverse: 5'- TCATCTGGGTCTTCTGGTCCTG-3'

Bcor Endogenous Forward: 5'- CAGGGCTCCCTGCCTACTTC -3'

Bcor Endogenous Reverse: 5'- GAAGCGTCGCCATCATTCAC -3'

HPRT was used as a loading control for analysis of Bcor RT-PCR results. HPRT PCR was performed using the following primers:

HPRT forward: 5’-AGCTACTGTAATGATCAGTCAACG-3’

HPRT reverse: 5’-AGAGGTCCTTTTCACCAGCA-3’.

Results and Discussion.

Generation of the conditional Bcor overexpressing mouse.

To generate mice that overexpress Bcor either ubiquitously or in mature germinal center B cells, we utilized a knock-in approach to insert a conditional *Bcor* expressing cassette into the murine *Rosa26* locus (generating a $Rosa26^{Bcor}$ allele). Knock-in to the *Rosa26* locus is frequently used to drive transcription of inserted genes, and such insertion does not result in any detrimental effect to the animal. Expression of Cre recombinase excises the LoxP-flanked transcriptional "stop" cassette, allowing for expression of the *myc-Bcor* coding sequence (See Methods and Figure 3-1 A). Homologous recombination of targeted embryonic stem cells was identified by genomic Southern blot (Figure 2-1 B).

Proper Bcor expression levels are required for mouse embryonic development.

To assess the potential role of *Bcor* as an oncogene in the whole mouse, mice containing the $Rosa26^{Bcor}$ allele were crossed to mice expressing a *Cre* recombinase transgene under the control of the ubiquitously expressed beta actin promoter (*β–actin-cre*). This generated $Rosa26^{Bcor/+}$*; β–actin-cre* mice that express *Bcor* ubiquitously from early embryonic stages. At postnatal day (P) 0, no $Rosa26^{Bcor/+}$*; β–actin-cre* mice were recovered (Figure 3-2 A).

Since $Rosa26^{Bcor/+}$*; β–actin-cre* embryos seem to die prenatally, litters were dissected from pregnant dams at various embryonic time points to determine an age and cause of death. When embryos were dissected from pregnant dams at embryonic day (E) 11.5, live $Rosa26^{Bcor/+}$*; β–actin-cre* mice were recovered at expected Mendelian ratios (data not shown) and were morphologically similar to their $Rosa26^{Bcor/+}$ littermates (Figure 3-2 B, C). There was also no difference in yolk sac vascularization and placental architecture between mutants and wild type littermates (data not shown). Therefore, a

failure to establish these nutrient-providing structures is not a likely cause of death for these embryos.

However, as embryonic development progressed, *Rosa26*$^{Bcor/+}$*; β–actin-cre* animals were smaller and developmentally delayed compared to *Rosa26*$^{Bcor/+}$ littermates (Figure 3-2 D-G). The ubiquitous misexpression of *Bcor* uniformly resulted in death by E14.5 (Figure 3-2 H, I). These dead E14.5 mutants were similar in size and morphology to E12.5-E13.5 control embryos, suggesting that the developmental process was interrupted within this timeframe. Preliminary histological analysis of E11.5 control and mutant embryos suggested that the mutant animals had severe neurological abnormalities, which likely caused their death (data not shown). Therefore, proper regulation of *Bcor* expression is required for mouse neurological development and embryonic viability past E13.5, suggesting that BCOR is involved in regulating genes that are important to neurological development.

The Rosa26 conditional overexpression system fails to elevate BCOR protein levels in mouse germinal center B cells.

To determine the role of BCOR as an oncoprotein in B cell lymphomagenesis, mice containing the *Rosa26*^{Bcor} allele were crossed to mice expressing the *Cre* recombinase transgene under the control of the mouse complement receptor 2 promoter (*CD21-cre*) (Helms, Cordero, & Tapadia, 2005). This breeding strategy was intended to generate *Rosa26*$^{Bcor/+}$*; CD21-cre* mice that overexpress *Bcor* specifically in mature germinal center B cells and follicular dendritic cells. At P21, *Rosa26*$^{Bcor/+}$*; CD21-cre* mice were recovered at expected Mendelian ratios and lived normal lifespans compared to control littermates (data not shown).

To assess levels of *Bcor* expression in whole spleens, total protein was extracted from *Rosa26*$^{Bcor/+}$*; CD21-cre*, *Rosa26*$^{Bcor/Bcor}$*; CD21-cre*, and *Rosa26*$^{Bcor/Bcor}$ whole spleens. BCOR protein levels were then ascertained by Western blot using an anti-BCOR rabbit polyclonal antibody to detect total BCOR and an anti-MYC mouse monoclonal antibody to detect exogenous BCOR. Results showed the expression of MYC tagged

BCOR protein in *Rosa26*$^{Bcor/+}$*; CD21-cre* and *Rosa26*$^{Bcor/Bcor}$*; CD21-cre* spleens (Figure 3-3 A). However, BCOR total protein levels were not elevated in *Rosa26*$^{Bcor/+}$*; CD21-cre* or *Rosa26*$^{Bcor/Bcor}$*; CD21-cre* spleens compared to control *Rosa26*$^{Bcor/Bcor}$ spleens (Figure 3-3 A). This result was confirmed in three separate experimental and control pairs of littermates (data not shown).

One possible cause for this lack of BCOR elevation within the spleen is that BCOR protein is only slightly elevated in B cells, resulting in a negligible difference in the whole spleen. Thus, to assess levels of *Bcor* expression only within *Cre* positive B cells, *Rosa26*$^{Bcor/+}$*; CD21-cre* animals were bred with *Rosa26*$^{YFP/YFP}$ mice, which contain a Cre-responsive YFP reporter under the control of the ubiquitously expressed *Rosa26* promoter (*Rosa26*^{YFP}). This generated *Rosa26*$^{Bcor/YFP}$*; CD21-cre* experimental animals and *Rosa26*$^{Bcor/YFP}$ and *Rosa26*$^{+/YFP}$*; CD21-cre* controls, in which YFP-positive cells contain the active *Cre* transgene. YFP-positive cells were isolated by fluorescence activated cell sorting, and BCOR protein levels of the sorted population were ascertained by Western blot. However, BCOR protein was not elevated in the sorted population of *Rosa26*$^{Bcor/YFP}$*; CD21-cre* experimental animals compared to *Rosa26*$^{+/YFP}$*; CD21-cre* controls (Figure 3-3 B). Thus, the Rosa26 conditional overexpression system fails to elevate BCOR protein levels even in the intended mouse germinal center B cell population.

Bcor transcript levels are tightly controlled in mouse germinal center B cells.

One potential cause for this system's failure to overexpress BCOR is tight transcriptional control of *Bcor* within the intended germinal center B cell population. Therefore, total and endogenous *Bcor* transcript levels from whole spleens were ascertained by quantitative reverse transcriptase polymerase chain reaction. Results indicate a slight elevation in total *Bcor* transcript in *Rosa26*$^{Bcor/Bcor}$*; CD21-cre* spleens compared to *Rosa26*$^{Bcor/+}$*; CD21-cre* and *Rosa26*$^{Bcor/Bcor}$ spleens (Figure 3-4 A). However, endogenous *Bcor* transcript is downregulated in *Rosa26*$^{Bcor/Bcor}$*; CD21-cre* and *Rosa26*$^{Bcor/+}$*; CD21-cre* spleens compared to *Rosa26*$^{Bcor/Bcor}$ spleens (Figure 3-4 B). This

suggests that the expression from the induced *Bcor* allele downregulates the endogenous *Bcor* allele, providing a potential explanation for the similar total BCOR protein levels. This is likely since, by chromatin immunoprecipitation analysis, BCOR binds its own promoters in human lymphoma cell lines (Bardwell and Melnick, unpublished). Therefore, in mouse B cells, regulation of *Bcor* expression must have an additional "level" of control that is not present in other tissue types at earlier developmental stages. Unfortunately, this tight regulation of BCOR levels in splenocytes prevents us from using this experimental system to determine whether *Bcor* overexpression accelerates oncogenesis in murine mature germinal center B cells.

Summary.

Misexpression of *Bcor* throughout the developing embryo results in prenatal lethality between E12.5 and E14.5. Thus, proper regulation of *Bcor* expression is required for mouse embryonic development.

Bcor transcript levels are tightly controlled within murine mature germinal center B cells, inhibiting upregulation of BCOR protein levels and preventing a proper assessment of the oncogenic potential of *Bcor* in the B cell population.

Figure 3-1. Generation of the conditional *Bcor* overexpressing mouse.

The *Bcor* conditional overexpression allele was generated by insertion of a LoxP-flanked transcriptional "stop" sequence followed by a myc-tagged *Bcor* coding sequence downstream of a splice acceptor site. (A) Homologous recombination was used to insert this sequence into intron one of the *Rosa26* genomic locus ($Rosa26^{Bcor}$). Tissue-specific expression of Cre recombinase can excise the LoxP-flanked transcriptional "stop" sequence, allowing for expression of myc-tagged *Bcor* driven by the *Rosa26* promoter. (B) Mouse embryonic stem cells containing the *Bcor* conditional overexpression allele were identified by genomic Southern blot of DNA digested with EcoRV. The blot shown was performed using the 5` probe (pictured in panel A), which detects an 11.4 kb wild type fragment and a 4.1 kb recombined fragment.

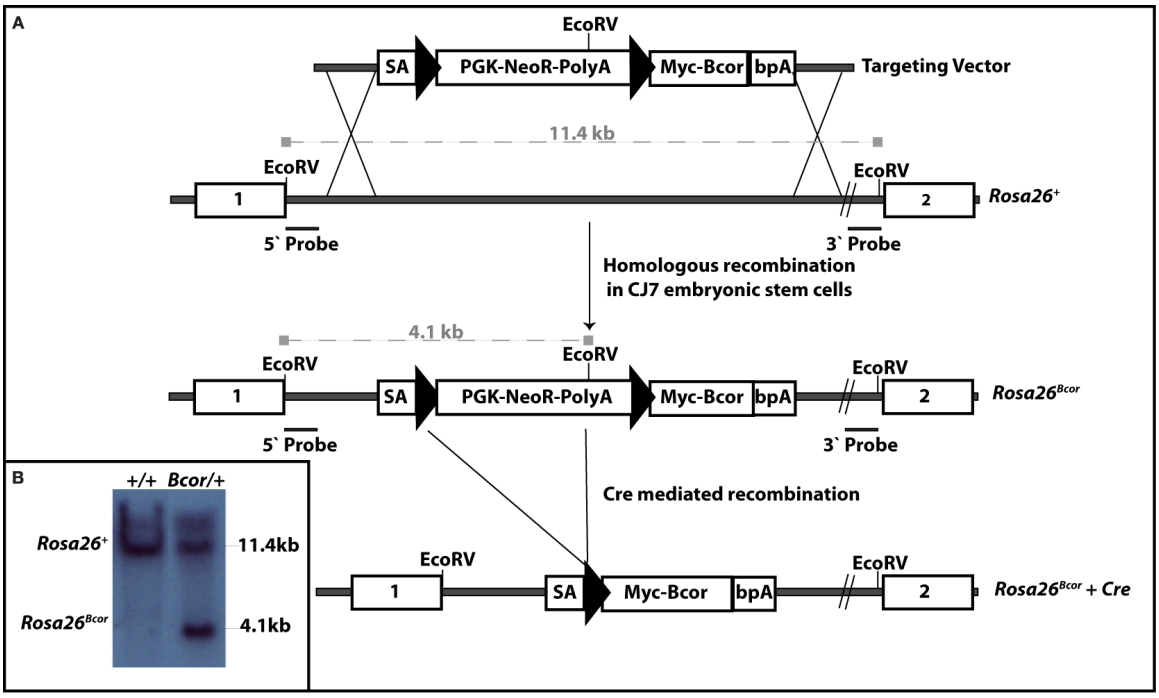
A
EcoRV
SA
PGK-NeoR-PolyA
Myc-Bcor
bpA
Targeting Vector
11.4 kb
EcoRV
EcoRV
1
2
Rosa26+
5` Probe
3` Probe
Homologous recombination
in CJ7 embryonic stem cells
4.1 kb
EcoRV
EcoRV
EcoRV
1
SA
PGK-NeoR-PolyA
Myc-Bcor
bpA
2
Rosa26Bcor
5` Probe
3` Probe
B
+/+ Bcor/+
Rosa26+
11.4kb
Rosa26Bcor
4.1kb
Cre mediated recombination
EcoRV
EcoRV
1
SA
Myc-Bcor
bpA
2
Rosa26Bcor + Cre

Figure 3-2. Mice that express *Bcor* ubiquitously are embryonic lethal.

(A) Mice that express *Bcor* ubiquitously do not survive to birth. (B-C) Mice that express *Bcor* ubiquitously are viable to E11.5, when they are similar in size and morphology to wild type littermates. (D-I) Mice that express *Bcor* ubiquitously experience developmental arrest around E12.5-13.5 and death by E14.5.

A

***Rosa26*$^{Bcor/+}$ X *Rosa26*$^{+/+}$*; Bactin-cre* (n=62)**

	Bcor/+	*Bcor/+; Cre*
Expected	**31**	**31**
Observed	**62**	**0**

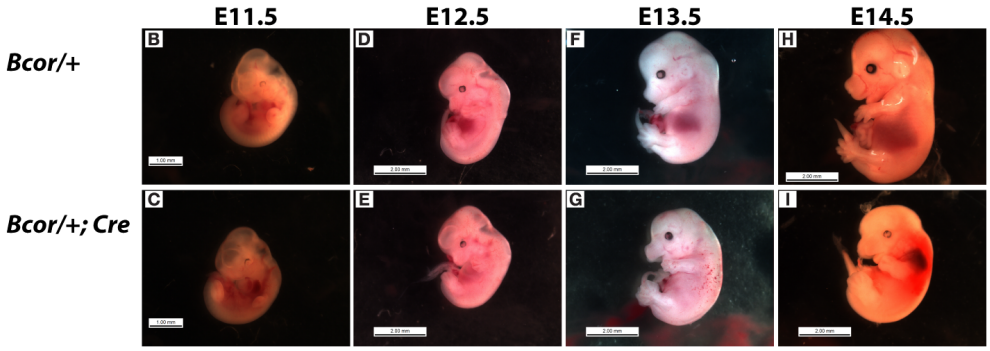

Figure 3-3. BCOR is not overexpressed at the protein level in *Rosa26*^{Bcor} *; CD21-cre* splenocytes.

Western blots for MYC-BCOR (yellow), endogenous BCOR (green), and ACTIN (red). (A) In whole spleen, mice containing both the *Bcor* conditional overexpression allele and *CD21-cre* have similar levels of total BCOR protein to Cre negative animals. However, more BCOR protein is found in the myc-tagged exogenous form (yellow) than in the endogenous form (green). (B) In isolated B cells, mice carrying both the *Bcor* conditional overexpression allele and *CD21-cre* have similar levels of total BCOR protein to mice carrying only *CD21-cre*. However, more BCOR protein is found in the myc-tagged exogenous form (upward shifted yellow band) than in the endogenous form (lower green band).

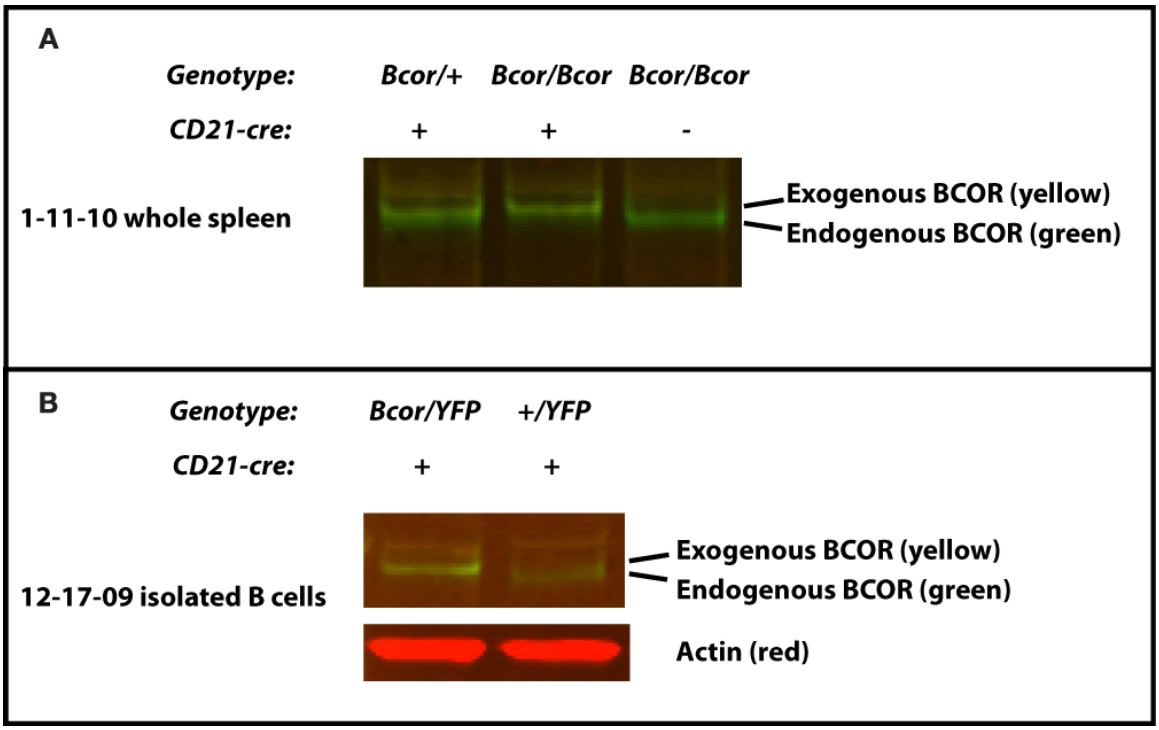
A
Genotype:
Bcor/+
Bcor/Bcor
Bcor/Bcor
CD21-cre:
+
+
-
1-11-10 whole spleen
Exogenous BCOR (yellow)
Endogenous BCOR (green)
B
Genotype:
Bcor/YFP
+/YFP
CD21-cre:
+
+
12-17-09 isolated B cells
Exogenous BCOR (yellow)
Endogenous BCOR (green)
Actin (red)

Figure 3-4. Exogenous *Bcor* expression downregulates expression from the endogenous locus in *Rosa26*^{Bcor} *; CD21-cre* splenocytes.

RT-PCR for *Bcor* transcript from isolated splenocytes. (A) Total *Bcor* transcript in *Rosa26*$^{Bcor/Bcor}$*; CD21-cre* spleens is slightly elevated compared to *Rosa26*$^{Bcor/+}$*; CD21-cre* and *Rosa26*$^{Bcor/Bcor}$ spleens. (B) Endogenous *Bcor* transcript is downregulated in *Rosa26*$^{Bcor/Bcor}$*; CD21-cre* and *Rosa26*$^{Bcor/+}$*; CD21-cre* spleens compared to *Rosa26*$^{Bcor/Bcor}$ spleens.

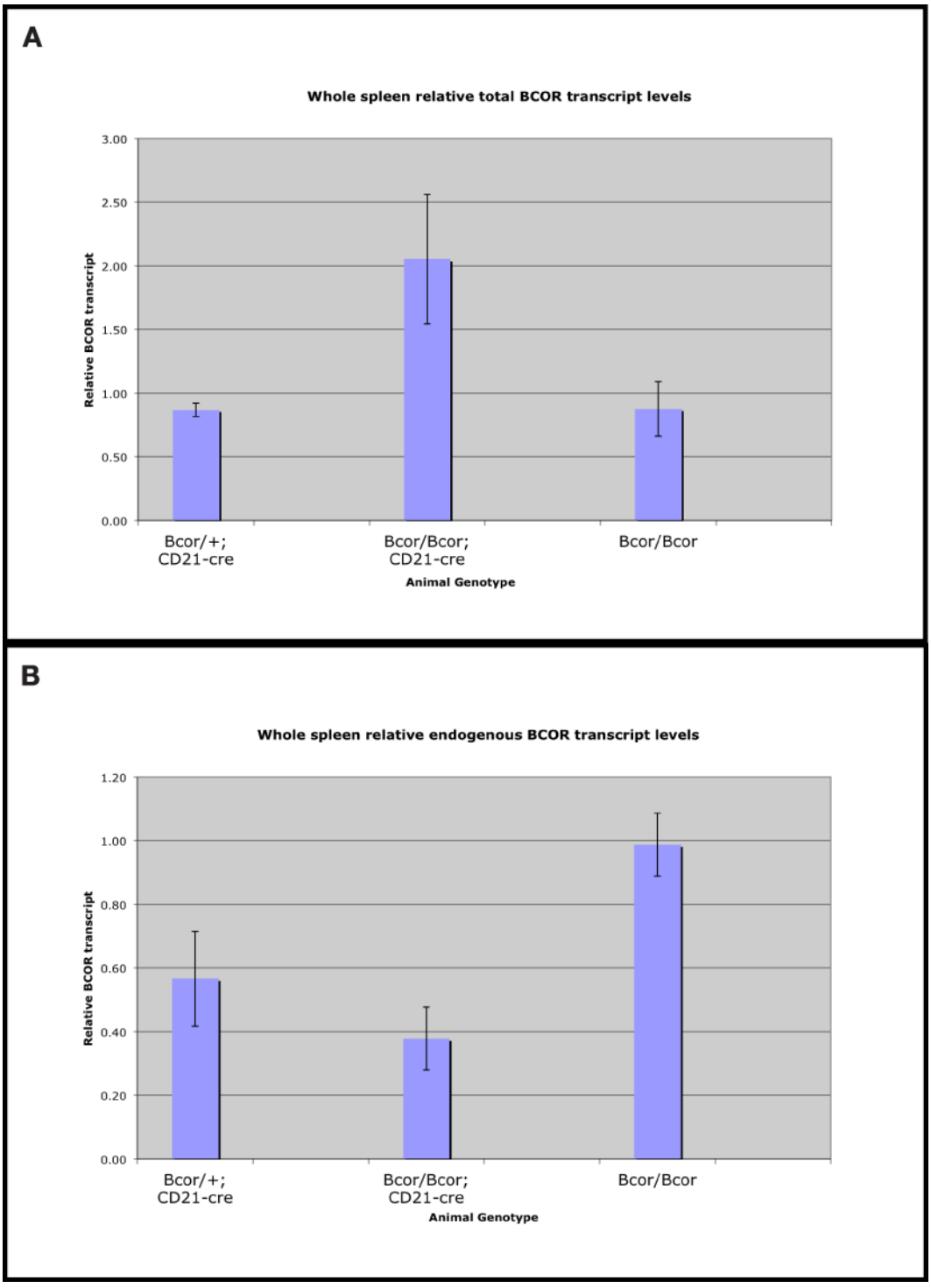
A
Whole spleen relative total BCOR transcript levels
Relative BCOR transcript
3.00
2.50
2.00
1.50
1.00
0.50
0.00
Bcor/+; CD21-cre
Bcor/Bcor; CD21-cre
Bcor/Bcor
Animal Genotype
B
Whole spleen relative endogenous BCOR transcript levels
Relative BCOR transcript
1.20
1.00
0.80
0.60
0.40
0.20
0.00
Bcor/+; CD21-cre
Bcor/Bcor; CD21-cre
Bcor/Bcor
Animal Genotype

Chapter 4:

BCOR is required in the neural crest cell lineage for mouse craniofacial development.

Introduction.

An overview of mammalian craniofacial development.

Craniofacial development is highly complex and depends on interactions between multiple tissues and cell types. The tissues of the head are derived from all three germ layers (ectodermal, mesenchymal, and endodermal). These three layers are strategically juxtaposed within the embryo in seven prominences that reorganize for normal facial morphogenesis. In the embryo, these are the midline frontonasal prominence and three paired derivatives of the first branchial arch, which each give rise to key facial structures (Helms et al., 2005). At E10 in mice, the ventral frontonasal prominence forms paired nasal placodes, which then invaginate to create paired medial and lateral nasal prominences (Figure 4-1 A). These grow and migrate to form the forehead, nose, lip philtrum, and primary palate. Meanwhile, the first branchial arch derivatives form the maxillary and mandibular processes that then give rise to the maxilla and mandible (Figure 4-1 A) (Burstyn-Cohen et al., 2004). Each branchial arch is made up of a paraxial mesoderm "core" that is surrounded by cranial neural crest cells and encased in ectoderm (Figure 4-1 B, C). The pharyngeal endoderm lies on the medial aspect of the branchial arches, just posterior to the midline lateral mesoderm.

Cranial neural crest cells.

Neural crest cells (NCCs) are key players in the process of craniofacial development. NCCs are a pluripotent cell population that arises from the lateral ridges of the neural plate, at the boundary between neural ectoderm and surface ectoderm. In embryonic development, BMPs signal through the Wnt pathway to induce epithelial to mesenchymal transformation of these cells, conferring upon them their NCC state (Le Douarin et al., 2004). These cells then migrate from the dorsal neural tube throughout the embryo, where they give rise to a host of differentiated cell types, each specified according to signaling interactions with the surrounding endoderm, ectoderm, and mesoderm. Neural crest derived cells have a variety of functions in the adult body,

including peripheral and enteric nervous system coordination, protection from the environment, and craniofacial formation (Couly et al., 2002).

To form the craniofacial structure, NCCs migrate ventrolaterally and proliferate to form the frontonasal process and branchial arch precursor swellings, as well as to contribute to the head and neck mesenchyme. During this process, NCCs remain plastic until they receive external cues from pharyngeal endoderm, branchial arch ectoderm, or the brain's isthmic organizer at their final destination. This then induces the NCCs to take on their final identity, eventually forming most of the bony structures of the head.

The pharyngeal endoderm and orofacial ectoderm.

Evidence from a variety of animal models indicates that the pharyngeal endoderm plays a critical role in craniofacial patterning. Ablation of this region in chick embryos results in a range of facial defects, including absence or reduction of the nasal capsule, Meckel's cartilage (mandibular precursor), and first branchial arch (Haworth et al., 2004). The pharyngeal endoderm is thought to effect its role in craniofacial development primarily through other cell types. Specifically, it prepatterns the orofacial ectoderm to direct NCC-derived mesenchymal patterning (Trokovic et al., 2003).

Following its induction by the pharyngeal endoderm, the orofacial ectoderm subdivides into proximal and distal domains. These domains act through different growth and transcription factor signaling pathways to create a suitable environment for and define the fate of NCCs upon their population of the branchial arch (Figure 4-2 A, B) (Trokovic, Trokovic, & Partanen, 2005; Tucker & Sharpe, 1999). For example, *Fibroblast growth factor 8* (*Fgf8*) signaling controls downstream Lim-homeobox domain genes *Lhx6* and *Lhx7* in the NCC-derived ectomesenchyme (Clouthier et al., 1998), Endothelin-1 controls the expression of *Goosecoid* (*Gsc*) to pattern the mandible (Chen et al., 1996), and BMP signaling regulates *Msx1* in the NCC-derived ectomesenchyme (Helms et al., 2005). In addition, FGF and BMP signaling are both responsible for defining the proximal-distal axis within the oral ectoderm of the first branchial arch. In the upper and middle oral ectoderm, Sonic hedgehog (SHH) and FGF signaling pathways

are critical for patterning the frontonasal process into adult craniofacial structures (Miletich & Sharpe, 2004). NCC-derived mesenchymal cells later crosstalk with the overlying orofacial epithelium to aid in patterning of the epithelium and development of the teeth (Couly, Coltey, & Le Douarin, 1992).

Paraxial mesoderm.

The cranial paraxial mesoderm is made of the following two main cell types: the unsegmented preotic head mesoderm and the occipital somites, which form some of the neck muscles, the pharyngeal and laryngeal muscles, and the tongue (Ferguson & Graham, 2004; Mootoosamy & Dietrich, 2002). Intercellular signaling from the ectoderm, endoderm, and cranial neural crest cells all contribute to the determination of paraxial mesoderm cells. In turn, the paraxial mesoderm directs cranial neural crest cell movement and helps form a proper environment for migrating cranial neural crest cells within the branchial arch (Ferguson & Graham, 2004). In addition, the paraxial mesoderm plays a key role in signaling pharyngeal endoderm development.

Mammalian palatal development.

The mammalian palate derives from two main structures: a primary palate, which is found in the anterior, medial portion of the adult hard palate, and the secondary palate, which makes up the rest of the adult hard and soft palate. The primary palate forms by E12.5 in mice from the medial nasal and maxillary processes. Development of the secondary palate begins at E11.5 when the maxillary process extends bilateral primordial palatal shelves, which grow in an anterior-posterior direction within the lateral oropharynx. Between E12.5 and E14.5, these palatal shelves grow into an elongated, vertical position along either side of the tongue (Figure 4-2 C, D) and then migrate to a horizontal position above the tongue (Figure 4-2 E). At E14.5, the bilateral palatal shelves meet horizontally in the midline and fuse along their medial edge epithelia to create a medial epithelial seam (Figure 4-2 F). The palatal shelves also fuse with the nasal septum dorsally and with the primary palate anteriorly. Palatal development is completed

by E16.5, at which point the anteriorly located hard palate and more posterior soft palate separate the oral cavity from the nasal cavity (Figure 4-2 G).

Polycomb group proteins and epigenetics in craniofacial development.

A recent analysis of gene expression changes throughout early mouse craniofacial development revealed a key role for Polycomb and Trithorax group proteins throughout this process. Specifically, from E10.5 to E12.5, expression shifted from genes that drive cell proliferation to genes implicated in cell differentiation (Feng et al., 2009). This shift was accompanied by a decrease in the expression of Polycomb group members *Pcgf6*, *Cbx1*, and *Cbx2*, which are involved in maintaining cell potency, and an increase in the expression of *Asxl3*, *Cbx4*, *Cbx6*, and *Mll5*, which promote cell differentiation.

Further evidence for the role of Polycomb group proteins in craniofacial development is found in both patients and animal models with Polycomb group loss-of-function mutations. Mice that are deficient in *Rae28*, the mouse homolog of Drosophila Polyhomeotic (PH), are perinatally lethal and display craniofacial defects, in addition to skeletal transformation, ocular defects, and cardiac abnormalities (Takihara et al., 1997). Furthermore, chromatin immunoprecipitation of the PRC2-associated protein poly(ADP-ribose) polymerase 3 (PARP3) from human neuroblastoma cell lines reveals that PARP3 occupies the promoter regions of genes involved in craniofacial development, including key genes from the HoxC, Fox, Sox, Dlx, Irx, and bHlh gene families (Rouleau et al., 2011). Finally, an analysis of global chromatin changes in human ICF (immunodeficiency, centromere instability, and facial anomalies) syndrome revealed a loss of the repressive H3K27 trimethylation and H2AK119 ubiquitylation patterns, accompanied by an increase in the activating H3K9 acetylation and H3K4 trimethylation marks (Jin et al., 2008). Interestingly, the T-box proteins, which are implicated in a variety of human syndromes involving craniofacial disorders, have a conserved T-box DNA binding domain that interacts with H3K27 demethylase and H3K4 methyltransferase complexes (Miller et al., 2008; Miller, Mohn, & Weinmann, 2010; Miller & Weinmann, 2009). These findings suggest a key role for Polycomb group

proteins and their associated repressive chromatin modifications in regulating the dynamic balance between appropriate gene activation and repression throughout the process of craniofacial development.

Congenital craniofacial defects.

Defects in the craniofacial region account for three quarters of all human congenital birth defects. These defects vary widely and may affect each of the craniofacial region's major functions, which include holding and protecting the brain, serving as a scaffold for sensory organs, and acting as a center for food intake. Thus, due to the great importance of this region, craniofacial defects are associated with a high degree of morbidity and mortality.

One of the most common craniofacial defects, cleft lip with or without cleft palate, is found in 1 out of every thousand live human births in North America. Clefting results from failure in fusion of any of the major facial prominences (lateral, medial, or maxillary), which may result in either unilateral or bilateral cleft formation. Clefting of the secondary palate can also occur when the maxillary prominence-derived palatal shelves fail to proliferate, elevate, or fuse in the midline. These defects have a variety of causes, including both heritable disorders and environmental offenses. However, due to our insufficient understanding of the underlying causes and processes, prevention and prenatal detection remain elusive. Thus, in light of the severe morbidity and mortality associated with such defects, a greater understanding of the molecular pathogenesis of cleft lip/palate and other craniofacial defects is essential.

Craniofacial defects in human oculofaciocardiodental syndrome.

OFCD patients commonly display a distinctive craniofacial phenotype that involves facial asymmetry, midfacial hypoplasia, and narrowing of the facies (Hilton, Black, & Bardwell, 2007). Nearly all patients have septate nasal cartilage and broadening of the nasal region (Hilton, Black, & Bardwell, 2007; Hilton et al., 2009).

In addition, OFCD patients very commonly have palatal and jaw abnormalities. A 2007 study found cleft palate in 17 of 28 patients examined, often associated with bifurcations of the uvula and tongue (Hilton, Black, & Bardwell, 2007). However, a more recent study found palatal defects in only 8 of 26 patients examined (Hilton et al., 2009). Mandibular asymmetry and prominence are also found.

Other defects of the craniofacial region are also found with variable penetrance. Patients occasionally have macrocephaly (large head) or microcephaly (small head) (Hilton, Black, & Bardwell, 2007). OFCD patients may display mild mental retardation or developmental delay, although most are within the normal range of intelligence. Dental findings are very common in OFCD patients, with delay in dentition, radiculomegaly (extended tooth root growth), oligodontia (missing teeth), tooth duplication, and tooth fusion being the most common findings. Patients may also have abnormalities of ear structure, and around 15% of patients have mild conductive or sensorineural hearing loss (Hilton, Black, & Bardwell, 2007; Hilton et al., 2009).

Bcor is expressed in neural crest derived tissues and the developing craniofacial region.

Although *Bcor* is widely expressed in adult tissues, it has more restricted expression early in development. The Bardwell lab has shown by *in situ* analysis that *Bcor* is expressed beginning at mouse embryonic day 8.5 (E8.5) in the neuroectoderm (Wamstad & Bardwell, 2007). In subsequent days, *Bcor* becomes more widely expressed, with strong expression detected in the branchial arches, limb buds, and neural tube by E9.5 (Wamstad & Bardwell, 2007). By E13.5, *Bcor* is expressed at low levels throughout much of the embryo proper, with particularly high levels detected in the neural tube, olfactory epithelium, teeth primordia, retina, and lens of the eye (Wamstad & Bardwell, 2007). Thus, the expression pattern of *Bcor* in the developing embryo indicates a possible role in the development of neural crest derived tissues.

More recently, an analysis of the embryonic maxilla and mandible shows that *Bcor* is expressed in these regions as well. From E11.5-14.5, whole mount *in situ*

hybridization reveals strong *Bcor* expression in the tongue and mandibular teeth primordia (Cai et al., 2010). At E13.5, *Bcor* is expressed at the medial edge epithelium (MEE) of the palatal shelves (Cai et al., 2010). At E14.5, *Bcor* expression is found in the palatal ruggae and MEE fusion, as well as in the whisker primordia (Cai et al., 2010). Therefore, its pattern of expression within the developing palate and mandibular regions suggests that *Bcor* may be involved in the formation of these structures.

Summary and rationale.

The pattern of *Bcor* expression in mouse neural crest tissues and craniofacial region, in addition to the characteristic craniofacial phenotype of OFCD patients with *BCOR* mutations, strongly suggest that BCOR plays a key role in neural crest cells and subsequent craniofacial development. Thus, a mouse conditional null allele for *Bcor* (see Chapter 1, Figure 1-1) was utilized in combination with either a *Pax3-Cre recombinase* or a *Wnt1-Cre recombinase* to remove BCOR from the neural crest derived population.

The *Pax3-Cre* allele contains *Cre* recombinase inserted into the first exon of the endogenous *Pax3* locus, creating a null *Pax3* allele (Lang et al., 2005; Tucker, 2007). When *Pax3-Cre* mice are bred with mice containing a *Cre*-responsive *LacZ* reporter, *B-galactosidase* expression is detected in the developing dorsal neural tube, somites, pharyngeal arches, and cardiac outflow tract, which are the major regions of neural crest cell contribution in the developing embryo (Engleka et al., 2005; Lombaert, Knox, & Hoffman, 2011).

The *Wnt1-Cre* transgene contains the *Cre* recombinase coding region downstream of the *Wnt1* promoter/enhancer sequence. This results in Cre recombinase activity starting at E8.5 within the *Wnt1*-expressing developing neural tube tissues (Danielian et al., 1998).

These experiments provide a thorough analysis of the role of BCOR in the neural crest lineage and its contributions to mouse craniofacial development. Based on the phenotypes observed in OFCD patients, we expected that removal of *Bcor* from the

neural crest cell lineage would result in cleft palate and midfacial hypoplasia, mimicking the craniofacial defects observed in OFCD patients. By establishing a mouse model for the craniofacial defects observed in OFCD, we hope to further our understanding for the molecular basis for these defects and eventually aid the diagnosis and treatment of OFCD patients.

Materials and Methods.

Mouse care and breeding.

Mice were maintained in conventional housing facilities under protocols approved by the University of Minnesota Institutional Animal Care and Use Committee. To generate mice that are null for *Bcor* in the neural crest cell population, the conditional null allele of *Bcor* ($Bcor^{Fl}$) was utilized (described in Chapter 1, Figure 1-1). $Bcor^{Fl/Fl}$ females from a mixed background were bred to mixed background male mice containing *Cre recombinase* driven by either the *Pax3* endogenous promoter or the *Wnt1* promoter/enhancer transgene (Danielian et al., 1998a; Lang et al., 2005). The resulting $Bcor^{Fl/+}$ heterozygotes and $Bcor^{Fl/Y}$ hemizygotes were utilized as controls and $Bcor^{Fl/+}$ mice containing *Pax3-Cre* or *Wnt1-Cre* and $Bcor^{Fl/Y}$ mice containing *Pax3-Cre* or *Wnt1-Cre* were utilized as experimentals.

Tissue processing.

Tissues from mutant and control mice were harvested at embryonic days 7.5-18.5 and postnatal days 21 and greater. Tissues were immersion-fixed in 4% paraformaldehyde fixative (Fisher) overnight at 4 degrees. Following fixation, tissues were ethanol dehydrated, cleared in CitriSolv (Fisher), and infiltrated with paraffin wax (Fisher) at 60 degrees and 20 psi. Following infiltration, tissues were embedded in Paraplast Xtra paraffin wax (McCormick Scientific) and cut into 6-micron sections, using a microtome (Leica).

Hematoxylin and eosin staining.

Mutant and control sections were rehydrated in a decreasing ethanol series. Rehydrated tissue was stained with hematoxylin (Sigma), acid washed, and eosin (Sigma) stained. Stained sections were then dehydrated, and a cover slip was attached using Permount mounting medium (Fisher). Images were captured using a Leica microscope

with a Zeiss camera and Axiovision (release 4.6) software (Zeiss). Captured images were then further processed using Adobe Photoshop CS3.

Skeletal preparations.

Newborn or E18.5 mice were fixed in 95% ethanol for 24 hours, eviscerated, and fixed in 95% ethanol for another 24 hours. They were then stained for 1 week at room temperature in a staining solution consisting of 0.15 mg/ml Alcian blue 8GX (Sigma) in 75% ethanol. After washing in 95% ethanol for 24 hours, they were treated with 1% potassium hydroxide for 72 hours to fully remove skin and muscle. Preparations were then washed in water for 7-8 hours, stained for 8 hours in 1 mg/ml alizarin red S (Sigma) in 1% potassium hydroxide, washed in water for 7-8 hours, and again treated with 20% glycerol in 1% potassium hydroxide at room temperature until cleared. The specimens were taken through an ethanol:glycerol series (3 days in 12.5%:50%, 3 days in 25%:50%, 3 days in 37.5%:50%, 3 days in 50%:50%,) and stored in 100% glycerol at room temperature.

PCR primers.

A multiplexing PCR strategy was used to genotype wild type *Bcor*, $Bcor^{Fl}$, and $Bcor^{\Delta}$ alleles from genomic DNA isolated from tails in adult mice and yolk sacs in embryos. Primers C, G and J generate a wild type amplicon of 424 bp, a $Bcor^{Fl}$ amplicon of 570 bp, and a $Bcor^{\Delta}$ amplicon of 519 bp.

VBp1539 C: 5'-GATGTCGACGTATGCAGAGACCACCTCTTGGC-3'

VBp1543 G: 5'-ACGGTACCGTCAGGGTAGAAAAACCAAAGCAAG-3'

VBp1546 J: 5'-CATCAGCCGCGGTGTGGATCATGCAGGCTTGG-3'

Results and Discussion.

Conditional deletion of Bcor in the Pax3-expressing neural crest cell lineage.

Ubiquitous deletion of *Bcor* in mice results in early embryonic lethality by E9.5 [Wamstad, Corcoran, Hamline, Bardwell, in preparation]. To bypass this early embryonic requirement for *Bcor* and to analyze the role of *Bcor* in the neural crest cell population, we deleted *Bcor* conditionally using *Pax3-Cre*, which is expressed in the neural crest cells, as well as somites of developing embryos (Engleka et al., 2005).

Mutant animals were found at Mendelian ratios throughout embryonic development, but no surviving mutants were observed at weaning (data not shown). Upon observation of birthing litters, mutant animals were appropriately birthed at normal size compared to wild type littermates (data not shown). However, they uniformly failed to thrive, exhibited a pale gray coloring, and died without milk spots within a few hours of birth (data not shown). To confirm that this lethality was due to a role in neural crest cells, *Bcor* was also removed from the neural crest cell lineage using a *Wnt1-Cre* transgene, which resulted in an identical phenotype and timing of perinatal lethality (data not shown). This confirms that *Bcor* is required in the neural crest cell lineage for postnatal survival. Given the overlapping expression of the *Wnt1-Cre* and *Pax3-Cre* within the developing neural tube and previous description of BCOR as a corepressor, these observations indicate that BCOR likely plays a role in repressing target genes in neural crest progenitors and that disruption of this repression results in perinatal lethality.

Bcor neural crest cell mutants exhibit severe cleft palate.

Because of the perinatal lethality of *Bcor* neural crest cell mutants, we undertook a thorough analysis of these animals to determine the cause of death. Upon dissection of E18.5 animals, *Bcor* mutants in both the *Pax3* and *Wnt1* expressing lineages were observed to have striking cleft palate defects, which is a common cause of death within the perinatal period (Figure 4-3 A,E; n= 10 and data not shown). Hematoxylin and eosin

staining of E18.5 transverse and frontal sections revealed that the cleft palate involved both the hard and soft portions of the palate (Figure 4-3 B-H, Figure 4-4; n=2). Skeletal preparations of E18.5 animals further confirmed palatal clefting in the mutant animals, showing the failure of Alizarin red stained bony structures to fuse in the palatal midline (Figure 4-5 A,E; n=3). Given the timing of death in these mutants, as well as their external appearance within the perinatal period, this cleft palate defect is a likely cause for the perinatal lethality of these mutants. These data suggest that *Bcor* is required in the neural crest cell lineage for appropriate formation of the palate. Therefore, BCOR likely functions to repress key target genes within the neural crest cell contributors to the palatal tissue at some point in development.

Bcor neural crest cell mutants have tongue defects and ectopic salivary glands.

Frontal sections of E18.5 animals unexpectedly revealed additional craniofacial soft tissue defects in the mutant animals. These included ankyloglossia, which is a fusion of the tongue to the underlying mucosa, and ectopic salivary glands present in the submandibular region (Figure 4-4; n=3). Salivary glands are formed from a complex series of interactions between oral epithelium and mesenchyme, which specify a subpopulation of salivary gland progenitor cells (Lombaert et al., 2011; Tucker, 2007). These cells then proliferate and differentiate to form the endothelial, epithelial, mesenchymal, myoepithelial, and neuronal cell types that are found in the fully formed salivary gland. Recent work has focused on identifying and defining the specific progenitor cell pool that gives rise to these diverse cell types within salivary glandular tissue (Arany et al., 2011; Hai et al., 2010). The sufficiency of *Bcor* mutation in inducing ectopic salivary gland formation suggests that it may play a key repressive role in salivary gland progenitors, providing a potential basis for regenerative therapy.

Mutant palatal shelves fail to elevate in embryonic development.

To ascertain the timing and cause of the cleft palate defect, mutant and wild type mice were dissected at various stages of embryonic development. Frontal sections of

E13.5 palates revealed wild type palatal histology, with vertical palatal shelves of normal size and shape descending on either side of the tongue (Figure 4-6 A,D; n=2). However, by E14.5, the mutant tongue failed to descend within the oral cavity, and the palatal shelves failed to rise to their horizontal positioning over the tongue (Figure 4-6 B,E; n=2). This phenotype persists at E15.5, when the palatal shelves of wild type animals have met and begun to fuse in the midline (Figure 4-6C,F, n=2). BrdU incorporation assays and TUNEL staining performed at each of the above timepoints (E13.5, E14.5, E15.5) detected no difference in proliferative or apoptotic activity in mutant palatal shelves compared to those of wild type littermates (n=2 per time point, data not shown). This suggests a primary mechanical defect in palatal shelf elevation, unrelated to cell proliferation or apoptosis within the palatal shelves. Therefore, *Bcor* must play a role either within the palatal shelves themselves or in the surrounding neural crest cell derived structures to allow for palatal shelf elevation.

Bcor neural crest cell mutants have additional defects of the tympanic bone and mandible.

Skeletal preparations of E18.5 animals revealed additional defects in craniofacial bony and cartilaginous structures. Specifically, the mutant tympanic bone and mandible both appeared shortened compared to the wild type structures (Figure 4-5 C, D and G, H; n=3). Of note, by defining the shape of the oral cavity, the proper formation of the mandible plays a key role in craniofacial development. We hypothesized that BCOR function within the early developing mandible contributes to the failure of palatal shelf elevation. Thus, to assess the potential role of mandibular defects in the overall *Bcor* mutant craniofacial phenotype, mandibular development in the *Bcor* mutants was further analyzed.

Bcor neural crest cell mutants have defective Meckel's cartilage development.

Meckel's cartilage is a cartilaginous structure that arises from the neural crest cell contribution within the mandibular prominence mesoderm and forms a template for

mandibular ossification (Chai et al., 2000; Frommer & Margolies, 1971). Through its key role in patterning the mandibular region, Meckel's cartilage permits proper tongue alignment within the oral cavity and, thus, allows for proper palatal shelf elevation at the appropriate time in development (Chai & Maxson, 2006). Given the defects in palatal shelf elevation during development and in adult mandible morphology, *Bcor* neural crest cell mutants were analyzed for proper Meckel's cartilage formation in development.

Alcian blue staining of embryos at E14.5 highlights the developing cartilaginous structures. By this timepoint, Meckel's cartilage in control embryos has taken on an elongated shape that forms an apex at the midline of the developing mandible (Figure 4-7A,B, n=3). However, Meckel's cartilage from mutant animals failed to properly elongate and has taken on a broadened, rounded shape in the developing mandibular region (Figure 4-7C,D, n=3). This suggests that the mandibular defects observed in E18.5 animals derive from an earlier defect in Meckel's cartilage formation. Therefore, BCOR plays a role in regulating Meckel's cartilage formation and subsequent mandibular patterning, likely through a role in transcriptional repression that allows for proper Meckel's cartilage outgrowth. Furthermore, similar Meckel's cartilage defects have been previously implicated in failed palatal shelf elevation, suggesting that it is a likely contributing factor to cleft palate defects in the *Bcor* neural crest cell mutants.

Summary.

Bcor neural crest cell mutants die perinatally with severe cleft palate defect, ectopic salivary glands, mandibular deformities, tympanic bone malformations, and tongue defects.

Mutant palatal shelves fail to elevate in development but show no evidence for defects in proliferation or apoptosis.

Mutant Meckel's cartilage fails to elongate, possibly preventing subsequent tongue depression and palatal shelf elevation in *Bcor* neural crest cell mutant animals.

Figure 4-1. Overview of mouse craniofacial development.

(A) A frontal view of the major events of mouse craniofacial development are pictured from embryonic day 9.5 through 13.5. (B) A sagittal view of an E9.5 mouse embryo, with emphasis on the primary craniofacial contributors. A cross section at the level of the dashed line is shown in (C), showing the paraxial mesoderm "core" (pink) surrounded by cranial neural crest (purple) and ectoderm. [Adapted from Chai and Maxson, 2006.]

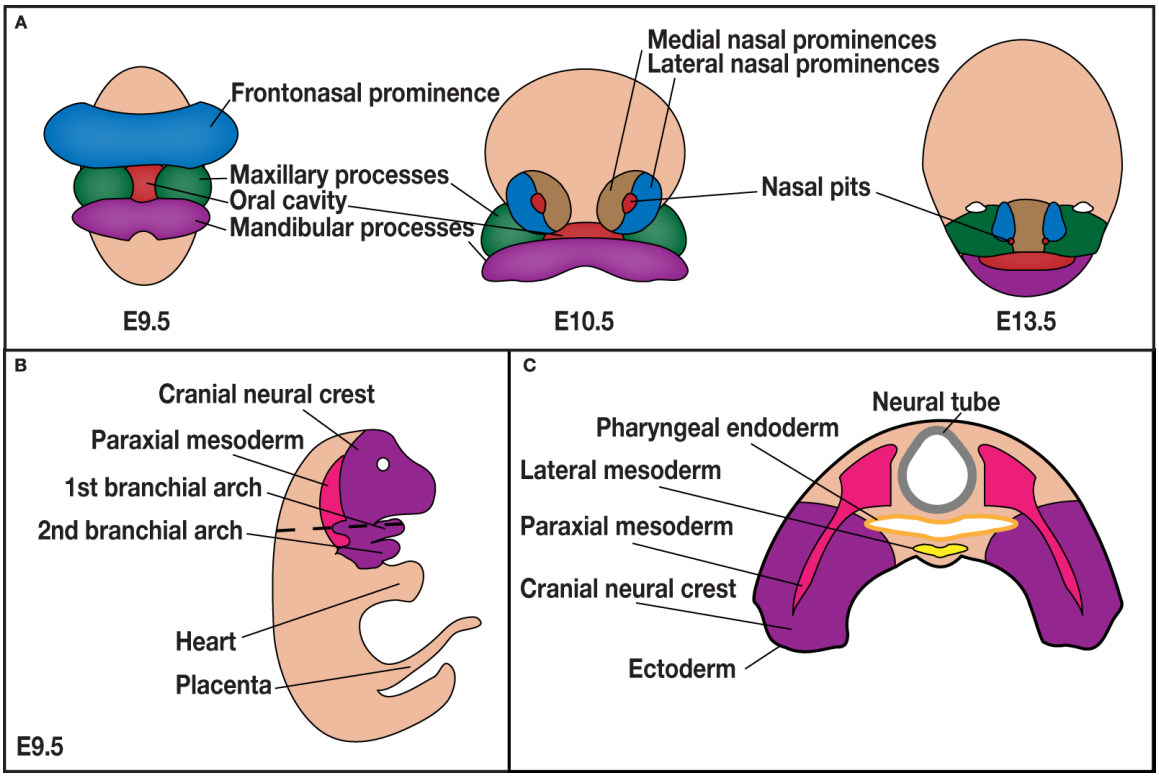
A
Frontonasal prominence
Maxillary processes
Oral cavity
Mandibular processes
Medial nasal prominences
Lateral nasal prominences
Nasal pits
E9.5
E10.5
E13.5
B
Cranial neural crest
Paraxial mesoderm
1st branchial arch
2nd branchial arch
Heart
Placenta
E9.5
C
Neural tube
Pharyngeal endoderm
Lateral mesoderm
Paraxial mesoderm
Cranial neural crest
Ectoderm

Figure 4-2. Overview of mouse mandibular and palatal development.

(A) A frontal view of the E10.5 mouse craniofacial region. The boxed mandibular processes are pictured in molecular detail in (B), showing *Bmp4* and *Fgf8* expression in the surface ectoderm (blue). In the distal domain, *Bmp4* promotes *Msx1* and *Msx2* expression while inhibiting *Barx1* expression in the proximal domain. Meanwhile, *Fgf8* in the proximal domain activates *Lhf6, Lhf7*, *Barx1*, and *Dlx2* expression. *Gsc,* which is expressed in the proximal aboral domain, is also required for mandibular patterning and is regulated by *Endothelin-1*. (C-G) Mouse palatogenesis begins with the vertical outgrowth of palatal shelves (labeled "P") by E13 (C). The tongue's depression within the oral cavity at E13.5 (D) allows for palatal shelf elevation to the horizontal position by E14 (E). The shelves then grow together at the midline by E14.5 (F) and fuse by E15.5 (G). [Adapted from Chai and Maxson, 2006.]

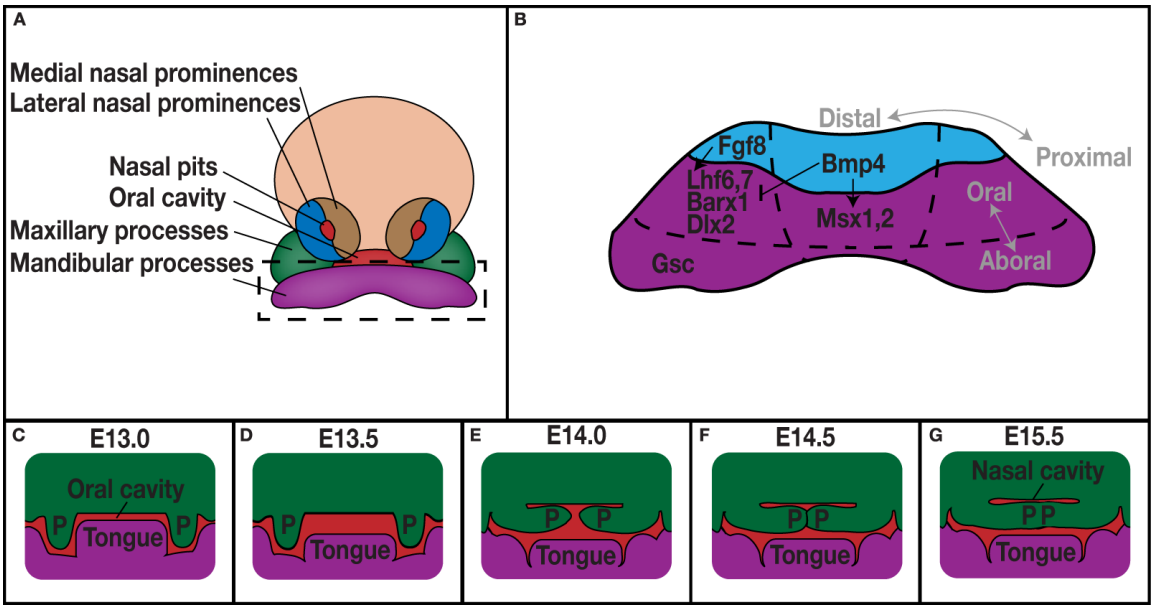
A
Medial nasal prominences
Lateral nasal prominences
Nasal pits
Oral cavity
Maxillary processes
Mandibular processes
B
Distal
Proximal
Fgf8
Bmp4
Lhf6,7
Barx1
Dlx2
Msx1,2
Oral
Aboral
Gsc
C
E13.0
Oral cavity
P
Tongue
P
D
E13.5
P
Tongue
P
E
E14.0
P
P
Tongue
F
E14.5
P P
Tongue
G
E15.5
Nasal cavity
P P
Tongue

Figure 4-3. *Bcor* neural crest cell mutants have cleft palate defects.

Gross morphology of the maxillary region (mandibles removed) in control and mutant mice reveals cleft palate (white arrows, A vs. E). Hematoxylin and eosin staining of transverse sections through E18.5 heads reveals normal nasal septum morphogy (black arrowheads, B vs. F) but confirms the involvement of both hard palate (white arrowheads, C vs. G) and soft palate (black arrows, D vs. H).

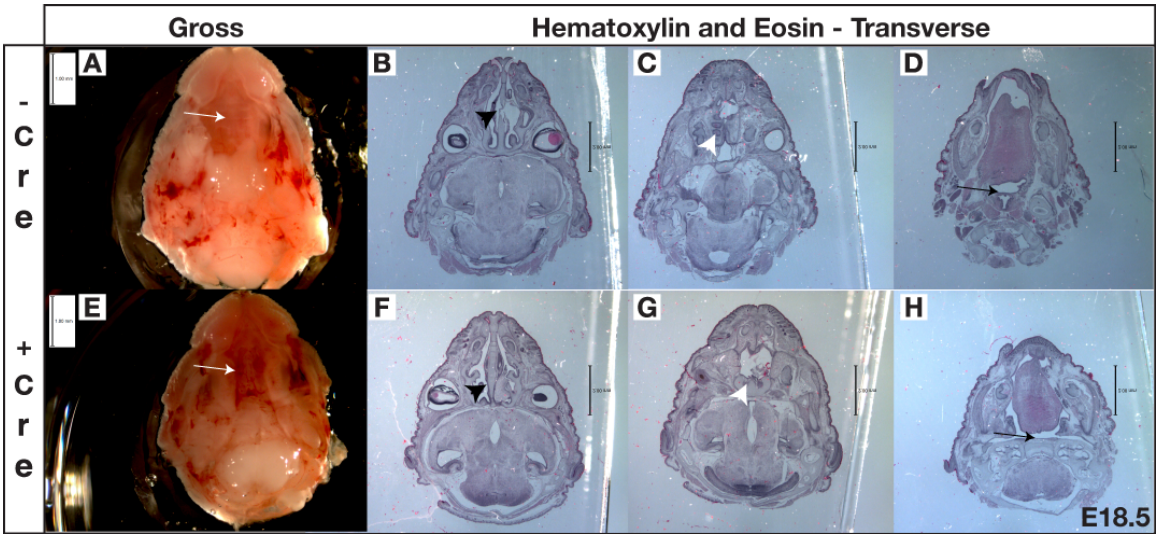
Gross
Hematoxylin and Eosin - Transverse
-cre
+cre
A
B
C
D
E
F
G
H
E18.5

Figure 4-4. *Bcor* neural crest cell mutants have disorganized tongue morphology and ectopic salivary glands.

Hematoxylin and eosin staining of frontal sections through E18.5 heads confirms cleft palate in mutants (C,D) compared to wild types (A,B). In addition, mutants have disorganized tongue morphology (arrowheads) and ectopic salivary glands in the submandibular region (arrows). P = palatal shelves, T = tongue

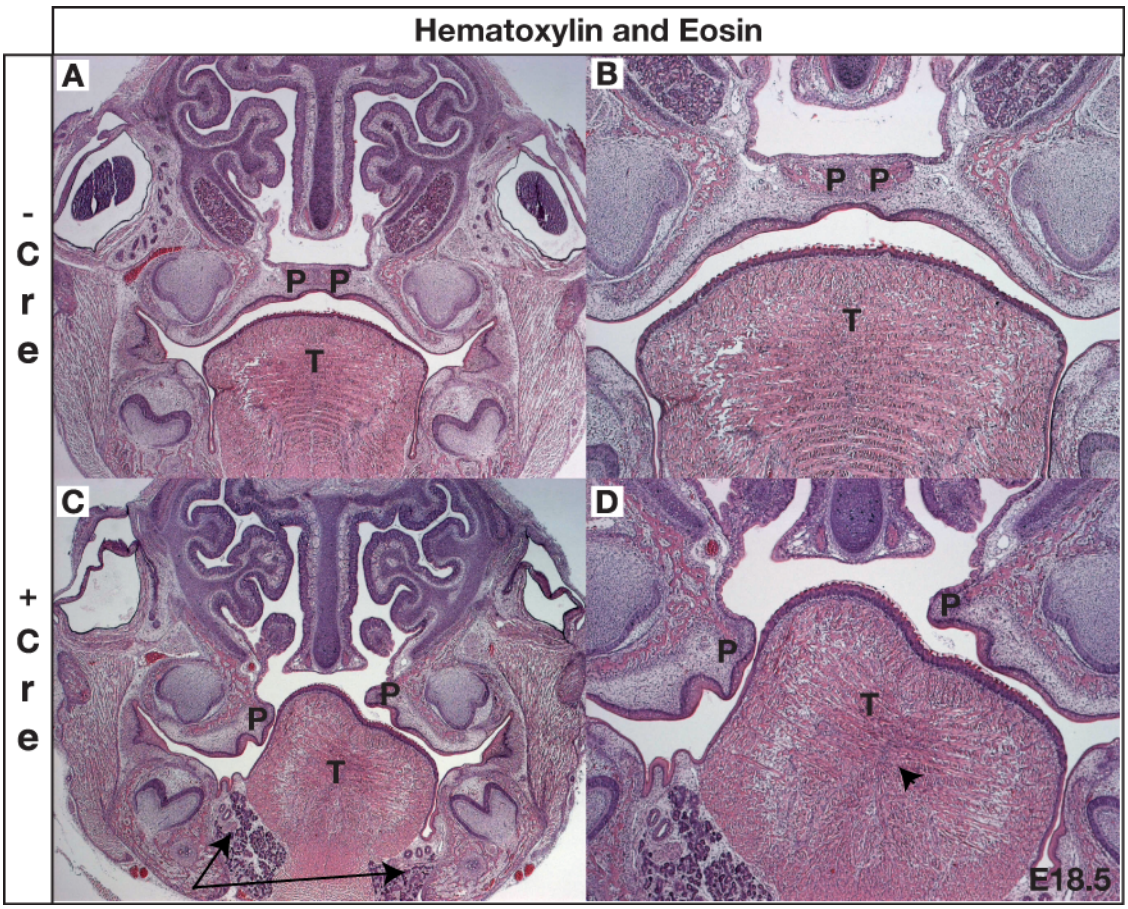
Hematoxylin and Eosin
-
C
r
e
+
C
r
e
A
B
C
D
P
P
T
E18.5

Figure 4-5. *Bcor* neural crest cell mutants have bony defects of the palate, tympanic bone, and mandible.

Skeletal preparations of E18.5 control and mutant heads confirm cleft palate defect (white arrowheads, A vs. E), as well as bony defects of the tympanic bone (white arrows, B,C vs. F,G) and mandible (black arrowheads, B,D vs. F,H). Cartilage is stained with Alcian blue, while bone is stained with Alizarin red.

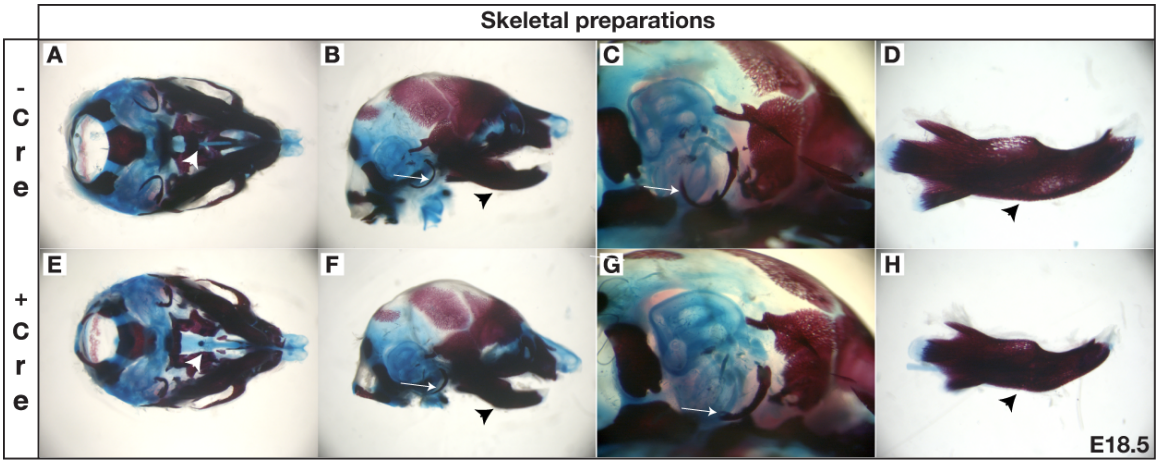
Skeletal preparations
-Cre
+Cre
A
B
C
D
E
F
G
H
E18.5

Figure 4-6. Palatal shelves from *Bcor* neural crest cell mutants fail to elevate.

Hematoxylin and eosin staining of frontal sections through control and mutant palates at E13.5 (A, D), E14.5 (B,E), and E15.5 (C,F) reveals a failure in palatal shelf elevation that persists throughout development.

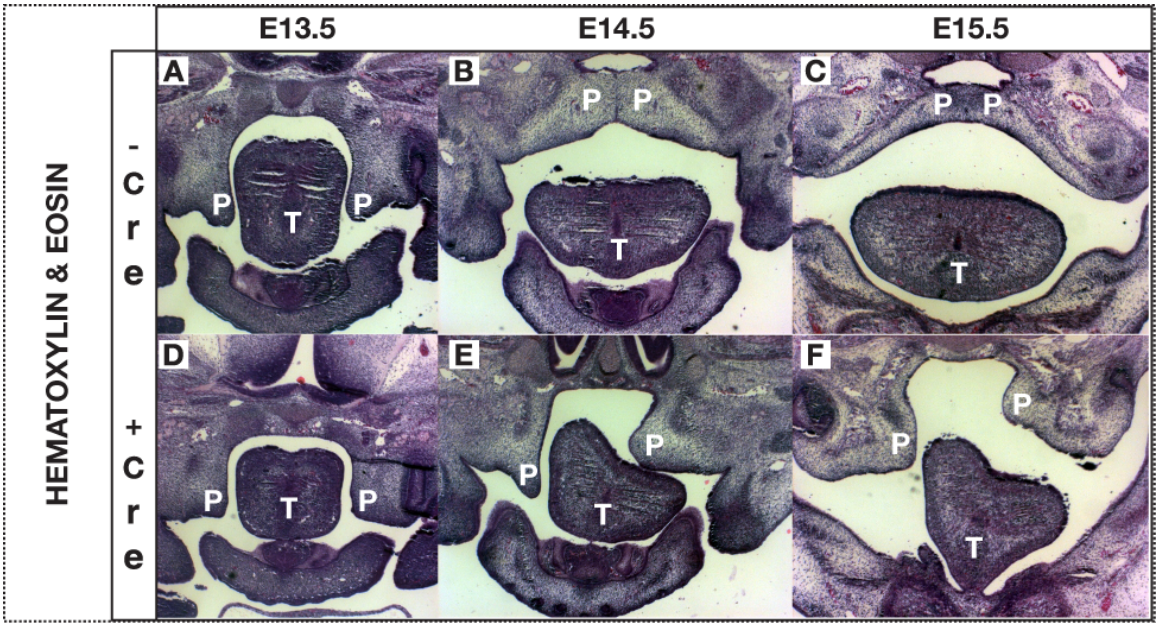
HEMATOXYLIN & EOSIN
E13.5
E14.5
E15.5
-cre
+cre
A
B
C
D
E
F
P
T

Figure 4-7. *Bcor* neural crest mutants have defects in Meckel's cartilage formation.

Alcian blue staining of cartilaginous structures in E14.5 control (A,B) and mutant (C,D) mice reveals defective Meckel's cartilage formation (arrows). Inset photographs in A and C highlight the difference in Meckel's cartilage structure in the control (A) versus the mutant (C).

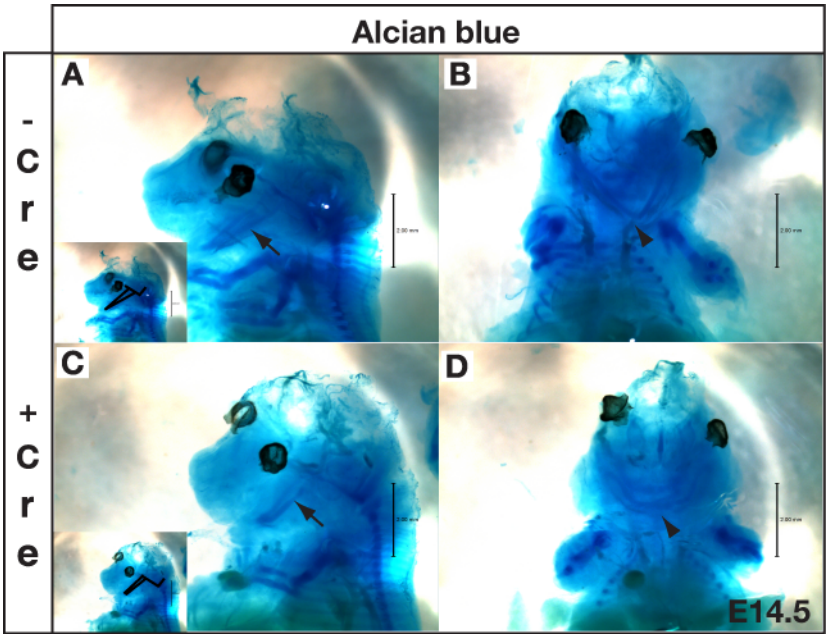
Alcian blue
A
B
C
D
- Cre
+ Cre
E14.5

Chapter 5:

BCOR is required for mouse cardiovascular development and function.

Introduction.

Basic anatomy and physiology of the cardiovascular system.

In both mice and humans, the heart is a muscular structure that is primarily responsible for oxygenating and pumping blood to the body's tissues. Thus, in order to carry out this important function, the heart and its outflow vessels must be capable of separating deoxygenated from oxygenated blood. To accomplish this, the linear heart tube that is formed very early in development is septated by adulthood. This septation results in a four-chambered adult cardiovascular structure, with two distinct outflow vessels (Figure 5-1 A).

Blood flows into the right side of the heart in its deoxygenated form. It is pumped from the right atrium, through the tricuspid valve to the right ventricle, and out of the heart through the pulmonary valve. The pulmonary artery then carries the blood to the lungs, where it becomes oxygenated. Now in its oxygenated form, blood is carried to the left side of the heart through the pulmonary vein. It is pumped from the left atrium, through the bicuspid valve to the left ventricle, and back out of the heart through the aortic valve. The aorta then carries the oxygenated blood to the body's tissues. Because of their important role in transporting blood away from the heart, the pulmonary artery and aorta are often collectively referred to as the "outflow tract," a term that will be used throughout the remainder of this chapter.

Congenital heart defects.

Congenital heart disease (CHD) is one of the most common abnormalities of human development, occurring in one percent of all live births, and accounts for more infant deaths than any other birth defect (Hoffman & Kaplan, 2002). Although most causes are unknown, these defects can result from a wide variety of genetic and environmental abnormalities and can occur either alone or in combination with other abnormalities.

CHDs are commonly classified into two main subtypes: cyanotic and non-cyanotic (reviewed in Hoffman & Kaplan, 2002). Cyanotic CHDs are named for the associated loss of oxygen delivery to the body's tissues, resulting in a blue discoloration of the skin. These may include the following disorders:

-Transposition of the great vessels: a defect in which the pulmonary artery and aorta are transposed, such that the pulmonary artery provides for left ventricular outflow while the aorta provides for right ventricular outflow.

-Tetralogy of Fallot: a combination of ventricular septal defect, pulmonary artery narrowing, hypertrophy (thickening) of the right ventricle, and an aorta that overrides both ventricles.

-Tricuspid or pulmonary atresia: abnormal development of the tricuspid or pulmonary valves, respectively, preventing normal flow through the valve or allowing for backflow of blood through the valve.

-Truncus arteriosus: a defect in which the pulmonary artery and aorta are fused in one common vessel, which overrides the right and left ventricles.

-Total anomalous pulmonary venous return: a defect in which the pulmonary veins (which carry oxygenated blood from the lungs back to the left side of the heart) are not connected to the left atrium.

Non-cyanotic CHDs do not typically compromise oxygen delivery to an extent that affects skin coloration. These defects include the following:

-Atrial or ventricular septal defects: a defect in formation of the interatrial or interventricular septum, allowing for blood flow between the right and left atria or ventricles, respectively (Figure 5-1 B, C).

-Aortic or pulmonic stenosis: a defect in aortic or pulmonary valve opening, resulting in decreased flow through the respective valve.

-Patent ductus arteriosus: a defect in which the embryonic ductus arteriosus fails to close, allowing for direct communication between the pulmonary artery and aorta.

-Aortic coarctation: narrowing of the aorta, which decrease blood flow out of the heart and to the body's tissues.

Four major progenitor populations contribute to the developing mammalian heart.

The formation of the mammalian cardiovascular system is a complex process that involves the integration and cooperation of several distinct progenitor populations throughout development. The cardiovascular progenitor cells are derived primarily from the anterior primitive streak (Lawson, Meneses, & Pedersen, 1991; Tam et al., 1997). By E7.5 in mice, cells from the anterior primitive streak coalesce at the midline to form the early mesodermal cardiac crescent, a region referring to the crescent-shaped first heart field (FHF), which forms a scaffold for cardiac growth and remodeling (Figure 5-1 D) (Vincent & Buckingham, 2010). The second heart field (SHF) is also derived from the anterior primitive streak and lies medially and posteriorly to the crescent (Srivastava, 2006a; Vincent & Buckingham, 2010). These SHF cells migrate to and build upon the FHF scaffold to form a beating linear heart tube, which is composed of an interior endocardial and an exterior myocardial cell layer (Figure 5-1 E) (Buckingham, Meilhac, & Zaffran, 2005; Srivastava, 2006). The bilaterally symmetrical linear heart tube then loops and septates throughout development to form the adult cardiovascular structure (Figure 5-1 F, G). Lineage tracing experiments suggest that the FHF primarily populates the left ventricle, while SHF descendants make the major contribution to the right ventricle and atria (Cai et al., 2003).

At least two other cell populations are thought to contribute to embryonic cardiovascular development. The neuroectoderm-derived cardiac neural crest cells (cNCCs) migrate from the dorsal neural tube to make up a major component of the pharyngeal arches (Brown & Baldwin, 2006). In both mouse and human, the pharyngeal arches form in five symmetrical pairs, each of which houses a single arch artery at the embryo's ventral midline (Brown & Baldwin, 2006). The cNCCs comprise the smooth muscle of these pharyngeal arch arteries, which are remodeled to form the heart's asymmetrical outflow tract, composed of a pulmonary artery anterior to a left-looping

aorta (Brown & Baldwin, 2006). The SHF makes a contribution to the endothelium of the pharyngeal arch arteries and, thus, collaborates with cNCCs in cardiac outflow tract formation (Vincent & Buckingham, 2010). Cardiac NCCs also populate the endocardial cushions, which form the valves of the heart (Vincent & Buckingham, 2010). Thus, cNCCs are involved in multiple aspects of cardiovascular development, including cardiac outflow tract and ventricular septation and myocardialization, valve formation, and innervation (Hutson & Kirby, 2007; Vincent & Buckingham, 2010; Waldo et al., 2005).

Meanwhile, the mesenchymal proepicardial organ (PEO) is a transitory structure that arises from the coelomic mesenchyme of the septum transversum, an embryonic structure that precedes the diaphragm and foregut ventral mesentery (Männer et al., 2001). The PEO is responsible for forming the epicardium, an outer layer of the heart that also makes contributions to the coronary vessel smooth muscle and cardiac interstitium (Vincent & Buckingham, 2010).

Transcriptional regulation and markers of cardiovascular progenitor cells.

The process of cardiovascular development is regulated by a highly complex and only partially understood network of transcriptional activation and repression. These transcriptional regulators, which include the homeodomain, T-box, and GATA transcription factor families, are often expressed at multiple points in cardiovascular development, and crosstalk between regulators is common.

Many of these transcriptional pathways appear to be particularly important for regulating SHF development. One of these key regulatory networks is centered on the LIM- and homeodomain-containing transcription factor known as insulin gene enhancer protein, or *Islet1* (*Isl1*), (Cai et al., 2003). Fate mapping studies have shown that *Isl1*-derived cells contribute to both myocardium and endocardium within the right ventricle, outflow tract, and atria, with more minor contributions to the left ventricle (Cai et al., 2003; Moretti et al., 2006). *Isl1* mouse mutants still form a primitive heart tube but have impaired cardiac looping and absence of SHF identities, such as outflow tract and right ventricle (Cai et al., 2003). However, although *Isl1* is not required for the earliest stages

of heart development, recent studies have shown that *Isl1*-derived cells are more widely distributed within the cardiac progenitor population than originally thought and also play a minor role within the FHF (Ma, Zhou, & Pu, 2008; Prall et al., 2007; Sun et al., 2007).

The homeodomain transcription factor Nkx2-5 is another key upstream element in the cardiac regulatory cascade. Expressed in both the FHF and SHF at the time of myocardial differentiation, Nkx2-5 is involved in formation of cardiac endocardium, the myocardial chambers, and conduction system (Habets et al., 2002; Lyons et al., 1995; Jay et al, 2004; Pashmforoush et al., 2004; Stanley et al., 2002; Tanaka et al., 1999). Lineage mapping shows that Nkx2-5-derived cells are found throughout the developing heart, including the atria, ventricles, and outflow tract (Ma, Zhou, & Pu, 2008; Moses et al., 2001; Stanley et al., 2002).

Establishment of left-right asymmetry in cardiovascular development.

The *Nodal* signaling pathway, leading to activation of the transcription factor *Pitx2c*, is primarily responsible for establishment of left-right asymmetry within the developing heart. Within the heart proper, *Pitx2c* functions to establish left-right asymmetry in several capacities, including repression of right atrial identity in the left SHF, repression of proliferation in the sinus venosus, and initiation of pulmonary vein formation (Franco, 2003; Galli et al., 2008; Tessari et al., 2008). In the outflow tract, *Pitx2c* also establishes left-right asymmetry by controlling the rotation and, thus, final positioning of the outflow vessels, as well as downstream laterality signaling (Bajolle et al., 2006; Yashiro, Shiratori, & Hamada, 2007).

Several recent studies have suggested that laterality defects are an underlying cause of some forms of congenital heart disease (Bamford et al., 2000; Ozcelik et al., 2006; Ramsdell, Bernanke, & Trusk, 2006). Specifically, defects in laterality are often found in association with cardiac outflow tract defects, such as double inlet left ventricle and double outlet right ventricle (Franco, 2003). Thus, establishment of left-right asymmetry appears to be important for proper alignment of the cardiac chambers and outflow vessels.

A role for epigenetics in cardiovascular development.

The importance of timing and crosstalk between cardiovascular transcriptional regulatory pathways highlights a need for careful fine-tuning of transcriptional regulation throughout this process. Thus, by programming temporal- and tissue-specific gene expression as development progresses, regulation of chromatin state plays a key role in cardiovascular development. Mouse mutant analyses suggest that chromatin regulation affecting cardiovascular development occurs at several levels. These include chromatin remodeling by Polycomb groups and ATP-dependent SWI/SNF, ISWI, CHD, and INO80 complexes, as well as covalent histone modifications made by histone deacetylases, acetyltransferases, demethylases, methyltransferases, and poly (ADP-ribose) polymerases (Han et al., 2011).

Polycomb group proteins.

Several recent studies have suggested a role for Polycomb group proteins in regulating embryonic cardiovascular development. Mutation of the Polycomb/Trithorax enhancer gene *Additional sex combs like 2* (*Asxl2)* results in enlarged hearts, interstitial cardiac fibrosis, and disorganized cardiomyocytes, as well as anterior and posterior transformations of the skeleton (Baskind et al., 2009). These phenotypes are found in addition to an overall decreased level of trimethylated H3K27, suggesting that mutation of *Asxl2* disturbs Polycomb repressive activity and, thus, disrupts cardiovascular development.

Another Polycomb group protein, RAE28, has also been shown to be important for cardiac morphogenesis. Mutation of *Rae28*, the mouse homolog of *polyhomeotic* in *Drosophila melanogaster*, results in perinatal lethality, in association with posterior skeletal transformations, ocular defects, cleft palate, and cardiovascular defects (Takihara et al., 1997). Cardiac defects include tetralogy of Fallot, pulmonary and aortic stenosis, overriding aorta, double outlet right ventricle, right ventricular hypoplasia, and ventricular septal defects. Subsequent studies have shown that *Rae28* acts in

cardiovascular development by sustaining the expression of *Nkx2.5* throughout development after its initial activation, a sustenance that is required for proper cardiac morphogenesis (Shirai et al., 2002). Therefore, these studies suggest an important role for Polycomb group proteins in establishing and maintaining proper gene expression throughout cardiovascular development.

Covalent histone modifications.

The relationship between cardiovascular development and covalent histone modifying enzymes, in particular, is still under investigation. However, several intriguing associations between these two processes have recently been identified. T-box transcription factors have been shown to interact with the MLL complex subunit Rbbp5 to promote H3K4 dimethylation (H3K4me2, an "activating" mark) while also interacting with the Jmj domain protein Jmjd3 to demethylate trimethylated H3K27 (H3K27me3, a "repressing" mark) (Miller et al., 2010). Furthermore, reprogramming of fibroblasts to activated cardiomyocytes by the transcription factors TBX5, GATA4, and Mef2c involves loss of H3K27me3 and enrichment of H3K4me2 (Ieda et al., 2010). Finally, the H3K36 methyltransferase WHSC1 interacts dose-dependently with the cardiac transcription factor Nkx2-5 and is required for normal cardiovascular structure in mice (Nimura et al., 2009). These results indicate that covalent chromatin modifications play an important, but currently ill defined, role in cardiovascular development.

Recent studies on the BAF chromatin remodeling complex provide one potential clue to how histone modifying proteins affect cardiovascular development. The BAF complex subunit Baf45c is enriched in the heart during embryonic development and is required for normal heart function and somite formation in zebrafish (Lange et al., 2008). Interestingly, Baf45c binds methylated and acetylated histone lysine residues, offering one potential link between covalent chromatin modifications and chromatin remodeling in cardiovascular development (Lange et al., 2008).

Bcor is expressed in the developing heart

Although *Bcor* is widely expressed in adult tissues, it shows more restricted expression early in development. The Bardwell lab has shown by in situ analysis that *Bcor* is expressed in the mouse embryo beginning at embryonic day 8.5 (E8.5) and in the developing ventricles at E9.5 (Wamstad & Bardwell, 2007). Furthermore, previous studies have shown that *BCOR* mRNA is highly expressed in the human fetal heart (Huynh et al., 2000). Thus, the expression of *BCOR* in the developing heart indicates a possible role for BCOR in maintaining proper cardiovascular development.

Over 85% of human oculofaciocardiodental syndrome patients have cardiovascular defects.

Further evidence that BCOR plays a role in the developing cardiovascular system derives from analysis of the cardiovascular systems of OFCD patients. Of the OFCD patients in whom cardiac function has been studied, over 80 percent have at least one cardiovascular defect (Hilton, Black, & Bardwell, 2007; Hilton et al., 2009). Although the specific defects vary, atrial septal defect is most common and is found in over 80% of OFCD patients with cardiovascular anomalies (Hilton, Black, & Bardwell, 2007; Hilton et al., 2009). Ventricular septal defect is also highly common, though it is found at lower incidence than atrial septal defect (Hilton, Black, & Bardwell, 2007). Atrial and ventricular septal defects are pathologic holes in the septa separating the right and left atria or ventricles, respectively, allowing for mixing of deoxygenated and oxygenated blood. Other cardiovascular defects observed in OFCD patients at lesser frequencies include pulmonary artery stenosis, hypoplasia of the aortic arch, mitral valve prolapse, right ventricular hypertrophy, double outlet right ventricle, and patent ductus arteriosus (Hilton, Black, & Bardwell, 2007; Hilton et al., 2009). Defects may be observed in isolation or concurrently, with two or more defects in the same patient.

Recent studies on OFCD patients have suggested a role for BCOR in cardiovascular laterality determination. Three OFCD patients were recently identified with laterality defects, including dextrocardia, asplenia, and intestinal malrotation (Hilton et al., 2007). Given the high association of laterality defects with congenital heart disease, the

identification of OFCD patients with laterality defects provides further evidence that BCOR plays an important role in cardiovascular development (Ramsdell, 2005).

BCOR is involved in laterality specification in Xenopus.

Very few studies have focused on the role of BCOR specifically in cardiovascular development. However, a recent study in *Xenopus tropicalis* supports a role for BCOR in the establishment of left-right asymmetry (Hilton et al., 2007). In this study, morpholino oligonucleotides were used to block translation of *xtBcor*, the Xenopus ortholog of BCOR. Upon injection of *xtBcor* morpholino into the left side of two-to-four cell embryos, ~86% of embryos exhibited laterality defects, including reversed cardiac orientation in ~50% of embryos (Hilton et al., 2007).

BCOR likely regulates *Xenopus* laterality, at least in part, through association with the transcription factor BCL6, which together exclude MAM1 from the Notch transcriptional complex in *Xenopus* and, thus, prevent transcription of Notch target genes (Sakano et al., 2010). In this way, the BCL6/BCOR complex inhibits *enhancer of split related 1* (*ESR1*) and allows for maintained *PitX2* expression (Sakano et al., 2010). Thus, the cardiac defects observed in OFCD could reflect an underlying deformity in left-right axis asymmetry.

Summary and rationale for studies.

Several lines of evidence support a role for BCOR in mediating proper cardiovascular development. First, females heterozygous for X-linked BCOR mutations exhibit OFCD, a multisystemic syndrome that often involves cardiovascular defects. Second, BCOR is part of a Polycomb-like chromatin-modifying complex, and other chromatin modifiers have known roles in cardiovascular development. Third, BCOR is expressed in the developing mouse heart. Finally, xtBcor appears to be involved in the establishment of *Xenopus* left-right axis asymmetry, a process that is essential for proper cardiovascular development and the prevention of congenital heart disease. However,

these observations do not reveal the specific role of BCOR in mediating cardiovascular development, and this remains an open and important question.

In order to further dissect this role of BCOR in cardiovascular development, a conditional *Bcor* null allele in the mouse (see Chapter 1, Figure 1-1) was utilized in combination with mice expressing *Cre* recombinase under the control of various cardiac promotors. The resulting progeny are null for *Bcor* in several different cardiac precursor cell lineages, allowing for a thorough dissection of the role of BCOR in each of these lineages.

Specifically, a *Tie2-Cre* recombinase was used to remove *Bcor* from the endothelium. The *Tie2-Cre* transgene is composed of the *Tie2* promoter, *Cre* cDNA, MT-1 poly-adenylation sequence, and *Tie2* intron 1 enhancer (Kisanuki et al., 2001). It is used to drive the expression of Cre recombinase within the endothelium, including the endocardial tissues but not the endocardial cushions of the developing heart, beginning at E7.5 (Kisanuki et al., 2001).

The *Pax3-Cre* recombinase was used to remove *Bcor* from the neural crest cells. The *Pax3-Cre* allele contains *Cre* recombinase inserted into the first exon of the endogenous *Pax3* locus, creating a null *Pax3* allele (Lang et al., 2005; Tucker, 2007). When *Pax3-Cre* mice are bred with mice containing a *Cre*-responsive *LacZ* reporter, *B-galactosidase* expression is detected in the developing dorsal neural tube, somites, pharyngeal arches, and cardiac outflow tract (Engleka et al., 2005; Lombaert, Knox, & M. Hoffman, 2011).

Several *Cre* recombinase alleles with overlapping expression patterns were used to remove *Bcor* from the myocardium. The *xMlc2-Cre* transgene is driven by a 3 kb fragment of the *Xenopus myosin light chain 2* promoter (Breckenridge et al., 2007). It is expressed from E7.5 in the cardiac crescent and, by E12.5, is found in the cardiomyocytes of all four developing chambers. In addition, *Bcor* deletion using two different *Nkx2.5-Cre* alleles was analyzed. The first contained an *Nkx2.5-Cre* knock-in to the endogenous *Nkx2.5* locus and is expressed starting at E7.5 in the cardiac crescent (Moses et al., 2001). The second, *Nkx2.5-IRES-Cre,* is a *Cre* recombinase coding

sequence linked to an internal ribosome entry site (IRES), which is knocked into the endogenous *Nkx2.5* 3` untranslated region (Stanley et al., 2002). The *Nkx2.5-IRES-Cre* is expressed starting at the E7.5 cardiac crescent stage in both myocardium and endocardium throughout the heart. Finally, the *Isl1-Cre* knock-in to the endogenous *Isl1* locus was utilized to drive Cre expression in the early cardiac crescent beginning by E7.5 and throughout the four chambers and outflow tract (Sun et al., 2007; Yang et al., 2006).

Based on the cardiovascular defects observed in OFCD patients and the known participation of BCOR in a Polycomb-like chromatin-modifying complex, we hypothesized that BCOR functions in murine cardiovascular progenitor cells to repress key cardiovascular target genes. The OFCD cardiovascular phenotype suggests that this repression most likely takes place in the myocardial precursors, endocardial precursors, and/or neural crest cells that contribute to the cardiovascular system. This work aims to understand the role of *Bcor* in each of these murine cardiovascular precursors, adding to our understanding of cardiovascular development and of the cardiovascular pathogenesis of OFCD.

Materials and Methods.

Mouse care and breeding.

Mice were maintained in conventional housing facilities under protocols approved by the University of Minnesota Institutional Animal Care and Use Committee. To generate mice that are null for *Bcor* in specific cardiac precursors, the conditional null allele of *Bcor* ($Bcor^{Fl}$) was utilized (described in Chapter 1, Figure 1-1). $Bcor^{Fl/Fl}$ females from a mixed background were bred to mixed background male mice containing *Cre* recombinase whose expression is driven by the cardiac-inclusive *Tie2*, *Pax3*, *xMlc2*, *Nkx2.5*, or *Isl1* promoters. The resulting $Bcor^{Fl/+}$ heterozygotes and $Bcor^{Fl/Y}$ hemizygotes were utilized as controls and $Bcor^{Fl/+}$ containing *Cre* and $Bcor^{Fl/Y}$ containing *Cre* were utilized as experimentals.

Tissue processing.

Tissues from mutant and control mice were harvested at embryonic days 7.5-18.5 and postnatal days 21 and greater. Embryonic tissues were immersion-fixed in 4% paraformaldehyde fixative (Fisher) overnight at 4 degrees Celsius. For processing of postnatal heart tissue, hearts were perfusion fixed with 10% formalin (Fisher), followed by immersion fixation in 10% formalin overnight at room temperature. Following fixation, tissues were ethanol dehydrated, cleared in CitriSolv (Fisher), and infiltrated with paraffin wax (Fisher) at 60 degrees Celsius and 20 psi. Following infiltration, tissues were embedded in Paraplast Xtra paraffin wax (McCormick Scientific) and cut into 6-micron sections, using a microtome (Leica).

Hematoxylin and eosin staining.

Mutant and control sections were rehydrated in a decreasing ethanol series. Rehydrated tissue was stained with hematoxylin (Sigma), acid washed, and eosin (Sigma) stained. Stained sections were then dehydrated, and a cover slip was attached using

Permount mounting medium (Fisher). Images were captured using a Leica microscope with a Zeiss camera and Axiovision (release 4.6) software (Zeiss). Captured images were then further processed using Adobe Photoshop CS3.

In-situ hybridization.

In situ hybridization analysis was performed as previously described (Wamstad & Bardwell, 2007). Briefly, the digoxigenin-labeled antisense and sense riboprobes were synthesized by *in vitro* transcription using the MEGAscript T7 kit (Ambion, Austin, TX). The *Sox9* plasmid used for riboprobe synthesis has been previously described (Zhao et al., 1997). The *Sox9* sequence was confirmed by restriction enzyme digestion and DNA sequencing.

Echocardiography.

Cardiac ultrasound was performed in mice under inhaled isoflurane anesthesia, utilizing a 30 MHz probe and a Vevo 660 high-resolution ultrasound bio-microscope (VisualSonics, Toronto, Ontario, Canada). B-mode imaging of the aortic root was obtained in modified right parasternal long-axis view. Doppler interrogation was performed in both the long- and short-axis beneath the aortic valve to determine aortic insufficiency (AI), and in the high right parasternal position to determine aortic diastolic retrograde flow, as a measure of severe aortic regurgitation (AR).

PCR primers.

A multiplexing PCR strategy was used to genotype wild type *Bcor*, $Bcor^{Fl}$, and $Bcor^{\Delta}$ alleles from genomic DNA isolated from tails of adult mice and yolk sacs of embryos. Primers C, G and J generate a wild type amplicon of 424 bp, a $Bcor^{Fl}$ amplicon of 570 bp, and a $Bcor^{\Delta}$ amplicon of 519 bp.

VBp1539 C: 5’-GATGTCGACGTATGCAGAGACCACCTCTTGGC-3’

VBp1543 G: 5’-ACGGTACCGTCAGGGTAGAAAAACCAAAGCAAG-3’

VBp1546 J: 5’-CATCAGCCGCGGTGTGGATCATGCAGGCTTGG-3’

Gene expression analysis.

Tissues were harvested from E13.5 mouse embryos on ice, placed directly into Trizol (Invitrogen), homogenized by mortar and pestle, and stored at -80 degrees Celsius. For hindlimb analysis, hindlimbs from three animals were pooled in each of two $Bcor^{F/Y}$ control and $Bcor^{F/Y}$*;Isl1-Cre* experimental samples. For heart analysis, hearts and proximal outflow tracts from three animals were pooled in each of three $Bcor^{F/Y}$ control and $Bcor^{F/Y}$*;Isl1-Cre* experimental samples. Each of the $Bcor^{F/Y}$*;Isl1-Cre* experimental hearts displayed common outflow tracts upon dissection. Samples were run in triplicate. Total RNA was prepared using a phase-lock column (5Prime) and Purelink RNA Mini Kit (Invitrogen). Total RNA concentration and quality were determined by Nanodrop spectroscopy and Agilent BioAnalyzer, respectively.

The University of Minnesota Biomedical Genomics Center performed cDNA synthesis, dye labeling, and hybridization to MouseRef8 v2.0 Expression Beadchip microarrays (Illumina). All expression data for 25697 probes were 1) quantile normalized and 2) averaged when probes that mapped to identical gene symbols. This left 18138 values, which were then used to conduct statistical analyses for differential expression using two group t-tests.

Results and Discussion.

Conditional deletion of Bcor in the Isl1-expressing lineage.

Ubiquitous deletion of *Bcor* in mice results in embryonic lethality by E9.5 [Wamstad, Corcoran, Hamline, Bardwell, in preparation]. To bypass this early embryonic requirement for *Bcor* and to analyze the role of *Bcor* in cardiovascular development, we deleted *Bcor* conditionally using an *Isl1-cre* knock-in allele, which is expressed in a subset of hindlimb and cardiac progenitors begininning at E7.5 (Yang et al., 2006). No mutant animals were observed at birth. Mutants were observed at just under Mendelian ratios at E13.5, but few surviving mutants were observed by E15.5 (Table 5-1 A). Since limb defects alone do not typically result in lethality, based on the expression pattern of *Isl1-cre*, we speculated that the embryonic lethality of these mutants resulted from an essential role for *Bcor* in the *Isl1*-expressing cardiovascular progenitors.

Hearts mutant for Bcor in the Isl1-expressing lineage fail to undergo ventricular and outflow tract septation.

Gross dissection at E13.5 revealed a common outflow tract in 65% of mutant hearts (Figure 5-2 A-C and E-G, Table 5-1 B, C). An additional 13% of hearts displayed other outflow tract abnormalities, such as interruption of the aortic arch or rightward looping aorta (Table 5-1 B,C). Histological analysis of mutant hearts at E13.5 confirmed a common outflow tract and, in addition, revealed a ventricular septal defect and decreased ventricular wall thickness (Figure 5-2 D,H). Earlier histological analysis at E12.5 revealed atrioventricular cushion defects, associated with a failure to form two distinct great vessels (Figure 5-3). These data, along with the most common cardiovascular phenotypes of OFCD patients, suggest that *Bcor* plays a key role in *Isl1*-expressing progenitors for the proper septation of the cardiovascular atrioventricular canal and outflow tract. Given the known participation of BCOR in a Polycomb-like chromatin-modifying complex, we hypothesized that BCOR acts as a transcriptional corepressor in *Isl1* positive cardiac ventricular and outflow tract progenitors.

Hearts mutant for Bcor in the Isl1 lineage express a panel of cardiac stress response genes.

To elucidate the molecular function of BCOR in cardiovascular development, mutant and wild type hearts were dissected from E13.5 mice and analyzed for gene expression by microarray. Taking a $p \leq 0.05$ cutoff, 49 genes were either up- or down-regulated by 1.5-fold in the mutant hearts compared to wild type controls (Table 5-2). Of the up-regulated genes, many are implicated in the cardiovascular response to disease or stress, such as *Aldoa*, *Mest*, *Atp5d*, *Tcp1*, and *Ankrd1*. Thus, these are likely indirect effects of *Bcor* mutation, caused by developmental stress to the cardiovascular structure, as opposed to the direct effects of *Bcor* loss. Some of the down-regulated genes appear to be of greater developmental relevance. These include *Myocyte specific enhancer factor 2c* (*Mef2c*), which is expressed in the precardiogenic mesoderm from E7.75 and is required for proper mouse cardiac development and vasculogenesis (Bi, Drake, & Schwarz, 1999; Lin et al., 1997). In addition, the *E1A binding protein* (*Ep300*) gene is a histone acetyltransferase that is involved in chromatin remodeling and is required for expression of key cardiac genes (Slepak et al., 2001). While their downregulation with *Bcor* mutation makes these genes unlikely direct BCOR targets, they may represent cardiovascular pathways that are impacted by BCOR in development.

Conditional deletion of Bcor in the Nkx2.5-expressing lineage.

Given the clear role of *Bcor* in *Isl1*-expressing cardiovascular cells, we next undertook an analysis of *Bcor* deletion using the *Nkx2.5-IRES-Cre* knock-in allele. The *Nkx2.5-IRES-Cre* expression pattern is reportedly very similar to that of *Isl1-Cre* throughout the developing heart beginning at the early cardiac crescent stage (Stanley et al., 2002). Therefore, we expected mice with removal of *Bcor* using the *Nkx2.5-IRES-Cre* to have a very similar phenotype to those with *Bcor* removed from the *Isl1*-expressing lineage.

However, unexpectedly, live mice were observed at expected Mendelian ratios (data not shown, n=16). Therefore, *Bcor* is not required within the *Nkx2.5*-expressing cardiovascular lineage for survival. Echocardiography was performed at 5 months of age to assess heart function. Echocardiography revealed severe aortic runoff and aortic insufficiency in 50% of mutants, as well as increased ventricular volume and decreased shortening fraction in 100% of mutants (Figure 5-4, n=4). We hypothesized that this decrease in cardiovascular function resulted from an underlying defect in cardiovascular structure, suggesting that *Bcor* is required in the *Nkx2.5*-expressing lineage for either embryonic cardiovascular development or adult cardiovascular homeostasis.

To better understand the pathology underlying these functional defects, mutant and littermate control mice were sacrificed at 2 months of age. Hearts were dissected, sectioned in the sagittal plane, and hematoxylin and eosin stained. Mutant hearts were of similar size to the hearts of wild type littermates but took on an abnormal, rounded shape (Figure 5-5 G-K, n=4), as opposed to the apex shape of wild type hearts (Figure 5-5 A-E). The right and left ventricles of mutant hearts were severely hypertrophied, and blood remained pooled in the left ventricle (Figure 5-5 I-K). In addition, higher magnification of the aortic valve revealed thickening of the mutant aortic valve leaflets (Figure 5-5 L compared to 5-5 F). Therefore, *Bcor* is required in the *Nkx2.5*-expressing lineage for proper cardiac function, as evidenced by both the functional defects on echocardiography and cardiac hypertrophy on histology. We hypothesize that this reflects a role for *Bcor* in earlier cardiovascular development, perhaps in aortic valve formation or the development of outflow tract smooth muscle. These possibilities are under ongoing investigation.

Conditional deletion of Bcor in the Pax3-expressing neural crest cell lineage.

To further understand the role of *Bcor* in other cardiovascular precursor cells, we deleted *Bcor* conditionally using *Pax3-Cre*, which is expressed in the neural crest contributors to the developing cardiac outflow tract (Lang et al., 2005). While no viable $Bcor^{Fl/Y}$*; Pax3-Cre* mice were observed at weaning (see previous chapter), dissection of embryos at E18.5 produced $Bcor^{Fl/Y}$*; Pax3-Cre* embryos at expected Mendelian ratios

(data not shown, n=10). Hematoxylin and eosin staining of frontal sections through *Bcor*$^{Fl/Y}$*; Pax3-Cre* hearts revealed bilateral atrial enlargement and blood congestion, which was not present in *Bcor*$^{Fl/Y}$ littermates (Figure 5-6 A,C, n=4). In two of eight mutants examined, injection of India ink into the left ventricle revealed a blockage in blood flow within the pulmonary artery (Figure 5-6 B,D). These data reveal a role for *Bcor* in the neural crest derived cardiac outflow tract, suggesting that *Bcor* is involved in repression of cardiac target genes within the neural crest cell population.

Conditional deletion of Bcor in the Tie2-expressing endocardial lineage and xMlc2-expressing myocardial lineage.

Mice containing *Bcor* deletions in the *Tie2*-expressing endocardial and *xMlc2*-expressing myocardial lineages had no observable phenotype (data not shown). Mutant lifespans were comparable to those of wild type littermates (data not shown). Upon dissection and histological analysis, mutant hearts were similar in size and morphology to wild type hearts (data not shown). This suggests either that *Bcor* plays no role in these endocardial and myocardial lineages or that there is redundancy for *Bcor* function in these cell types.

Hindlimbs mutant for Bcor in the Isl1-expressing lineage are delayed in development and fail to undergo mesenchymal condensation.

In addition to cardiovascular defects, oculofaciocardiodental syndrome (OFCD) patients also have a high incidence of skeletal defects, including radioulnar synostosis (fusion of the bones in the forelimb), hammer toes, and syndactyly of the toes (Hilton et al., 2009; Ng et al., 2004). *Bcor* is also expressed in the mouse limb buds beginning at E9.5 (Wamstad & Bardwell, 2007). Thus, the expression of *Isl1-Cre* in the hindlimb provided an opportunity to investigate the role of *Bcor* in mouse hindlimb development.

Deletion of *Bcor* within the *Isl1* lineage resulted in a delay in hindlimb development, as evidenced by the delay in digit formation upon hematoxylin and eosin

staining of hindlimb sections (Figure 5-7 A,B versus D,E, n=3). Skeletal development within the limb occurs in four stages: cell migration to the site of skeletogenesis, epithelial-mesenchymal interactions, cell condensations, and differentiation into chondroblasts and osteoblasts (Hall & Miyake, 2000). SOX9 is a transcription factor that controls the formation of mesenchymal condensations at future sites of skeletogenesis by regulating the expression of *collagen 2α1*. In-situ hybridization for *Sox9* shows broadened *Sox9* expression in mutant hindlimbs (Figure 5-7 C versus D, n=3). Thus, these data suggest that *Bcor* is involved in regulating the formation of mesenchymal condensations in the developing hindlimb upstream of *Sox9*. We further hypothesize that BCOR regulates hindlimb mesenchymal condensation through its role as a transcriptional repressor.

Bcor mutant hindlimbs in the Isl1 lineage misexpress several members of the Hox gene family.

To elucidate the molecular function of BCOR in hindlimb development, mutant and control hindlimbs were dissected from E13.5 littermates and analyzed for gene expression by microarray. Taking a $p \leq 0.05$ cutoff, 17 genes were either up- or down-regulated by 1.3-fold in the mutant hindlimbs compared to wild type controls (Table 5-3). Among the upregulated set were several *Hox* genes, including *Hoxc6*, *Hoxa5*, *Hoxa2*, *Hoxc9*, and *Hoxc10*. *Hoxc6* plays a role in fish fin positioning and is also expressed in hindlimb buds of *Xenopus* and mouse (Jegalian et al., 1992; Savard, Gates, & Brockes, 1988; Tanaka et al., 2005). Both *Hoxc9* and *Hoxc10* play key roles in distinguishing hindlimb from forelimb identity (Logan & Tabin, 1999; Rodriguez-Esteban et al., 1999; Takeuchi et al., 1999). Upregulation of *Hoxa2* in the *Bcor* mutant hindlimbs holds particular relevance, given its defect in mesenchymal condensation. *Hoxa2,* which is regulated by bone morphogenetic proteins (BMPs), has multiple roles in the formation of hindlimb condensations, including establishment of the condensation boundary, induction of condensation growth, and the prevention of cell differentiation that terminates condensation (Hall & Miyake, 2000).

Downregulated genes in *Bcor* mutant hindlimbs included *Hoxd12*, as well as the *Limb bud and heart development regulator homolog* (*Lbh*). *Hoxd12* is involved in regulating bone formation and ossification and also has a known role in regulating digit formation (Sheth, Bastida, & Ros, 2007). The highly conserved transcription cofactor *Lbh* modulates *Runx2* and *Vegf* expression to regulate bone ossification and vascular invasion (Conen et al., 2009). These results provide evidence that BCOR may be functioning as a key regulator of *Hox* gene expression in the hindlimb. This function is consistent with the known interaction between BCOR and Polycomb group proteins and provides a possible molecular basis for limb defects observed in OFCD patients.

Summary.

Bcor mutants in the *Isl1*-expressing cell lineage die prenatally with cardiac outflow tract defects and ventricular septal defect, suggesting that *Bcor* is required in *Isl1*-expressing cells for both ventricular and outflow tract septation. These mutants also have delayed hindlimb development and fail to undergo mesenchymal condensation, suggesting that *Bcor* is also required in *Isl1*-expressing cells for proper hindlimb formation.

Bcor mutants in the *Pax3*-expressing neural crest cell lineage have bilateral atrial enlargement and blockage of pulmonary arterial bloodflow, suggesting that *Bcor* is required in neural crest cells for establishing appropriate cardiovascular circulation.

Bcor mutants in the *Nkx2.5*-expressing cell lineage have aortic insufficiency, bilateral ventricular hypertrophy, and thickening of the aortic valve leaflets. Thus, *Bcor* is required in the *Nkx2.5* expressing lineage for efficient cardiovascular function.

Bcor mutants in the *Tie2*-expressing endocardial cell lineage or *xMlc2*-expressing myocardial cell lineage have no observable cardiovascular phenotype, suggesting that *Bcor* has either a redundant or a negligible role in these cell types.

Figure 5-1: Overview of mouse cardiovascular structure, septal defects, and development.

(A) The wild type, four-chambered adult heart separates deoxygenated (blue arrows) from oxygenated (red arrows) blood. (B) Atrial and (C) ventricular septal defects allow for mixing of deoxygenated and oxygenated blood (purple arrows). (D) The mouse E7.5 cardiac crescent, with the first heart field shown anteriorly (light grey) and the second heart field posteriorly (dark grey). (E) The E8.5 linear heart tube, which loops and septates throughout development into the adult structure (F-G). V=ventricle, A=atrium, COFT=common outflow tract, RA=right atrium, LA=left atrium, RV=right ventricle, LV=left ventricle. [Adapted from Srivastava, 2006.]

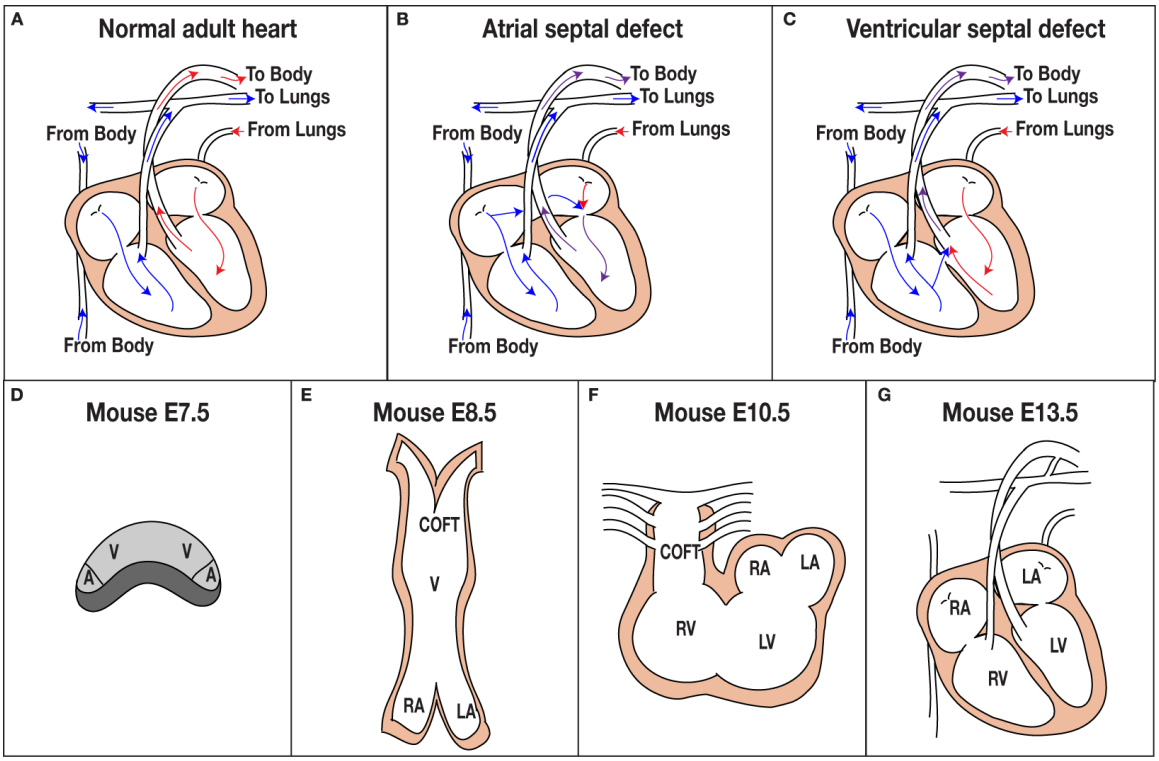
A
Normal adult heart
To Body
To Lungs
From Body
From Lungs
From Body
B
Atrial septal defect
To Body
To Lungs
From Body
From Lungs
From Body
C
Ventricular septal defect
To Body
To Lungs
From Body
From Lungs
From Body
D
Mouse E7.5
V
V
A
A
E
Mouse E8.5
COFT
V
RA
LA
F
Mouse E10.5
COFT
RA
LA
RV
LV
G
Mouse E13.5
LA
RA
LV
RV

Figure 5-2: Bcor mutant hearts in the *Isl1*-expressing cell lineage have outflow tract defects and ventricular septal defect.

Gross dissection at E13.5 reveals a common outflow tract in *Bcor*$^{Fl/Y}$*; Isl1-Cre* hearts (A, E). Scanning electron microscopy confirms the presence of a common outflow tract in *Bcor*$^{Fl/Y}$*; Isl1-Cre* hearts (B,C versus F,G). Hematoxylin and eosin staining of *Bcor*$^{Fl/Y}$*; Isl1-Cre* hearts at E13.5 confirmed a common outflow tract and, in addition, revealed a ventricular septal defect and decreased ventricular wall thickness (D, H). Ao = aorta, PA = pulmonary artery, COFT = common outflow tract, RA = right atrium, LA = left atrium, RV = right ventricle, LV = left ventricle.

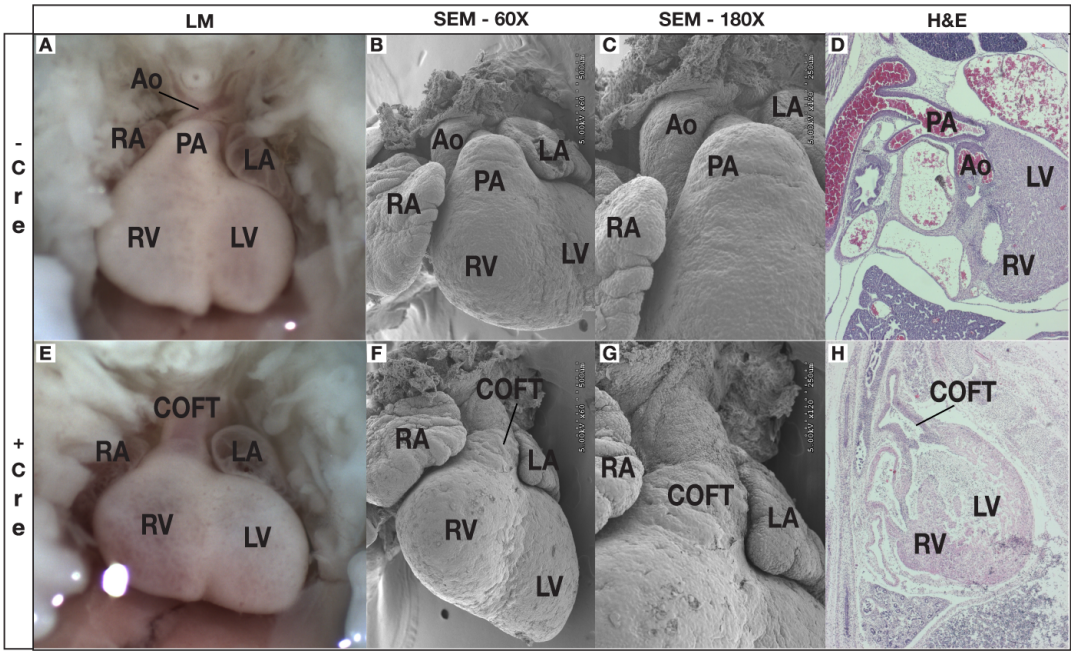
LM
SEM - 60X
SEM - 180X
H&E
-cre
+cre
A
B
C
D
E
F
G
H
Ao
RA
PA
LA
RV
LV
COFT

Figure 5-3: *Bcor* mutant hearts in the *Isl1*-expressing cell lineage have defective atrioventricular cushion development and fail to form a septated outflow tract.

Hematoxylin and eosin staining of frontal (A-J) and sagittal (K-T) sections through E12.5 $Bcor^{Fl/Y}$*; Isl1-Cre* and $Bcor^{Fl/Y}$ hearts reveals atrioventricular cushion defects (AVC) and failure to form two distinct great vessels (COFT). Black arrows denote normally developing atrioventricular cushions in wild type hearts (B-D) and poorly formed atrioventricular cushions in mutants (G-I). Pink arrows denote normally developing outflow tract cushions in wild type hearts (B-C, K-L) and poorly formed outflow tract cushions in mutants (G-H, P-Q). Pink arrowheads show the wild type, septated outflow tract (D,E,M) compared to mutant common outflow tracts (I,J,R). Ao = aorta, PA = pulmonary artery, COFT = common outflow tract, RA = right atrium, LA = left atrium, RV = right ventricle, LV = left ventricle, AVC = atrioventricular cushions, OTC = outflow tract cushions, IVS = interventricular septum.

HEMATOXYLIN & EOSIN - FRONTAL
- Cre
+ Cre
Anterior
Posterior
A
B
C
D
E
F
G
H
I
J
RV
LV
OTC
AVC
Ao
PA
Ao/PA
RA
LA
COFT

HEMATOXYLIN & EOSIN - SAGITTAL
- Cre
+ Cre
Right
Left
K
L
M
N
O
P
Q
R
S
T
OTC
RA
RV
LV
Ao PA
PA
IVS
LA
COFT

Figure 5-4: *Bcor* mutant hearts in the *Nkx2.5* expressing cell lineage have severe aortic regurgitation as adults.

B-mode image and Doppler interrogation of aortic root and aorta in $Bcor^{Fl/Y}$ (A, B) and $Bcor^{Fl/Y}$*; Nkx2.5-IRES-Cre* (C, D) mice. Baseline is defined at a frequency and velocity of 0, when no blood flow occurs over the interrogated region. In wild type mice, deviations from baseline show aortic valve opening and subsequent blood flow through the aortic valve and aorta, followed by aortic valve closing and cessation of blood flow. $Bcor^{Fl/Y}$ mice demonstrate normal blood flow over the aortic valve (A) and through the aorta (B). $Bcor^{Fl/Y}$*; Nkx2.5-IRES-Cre* mice have aortic regurgitation, which is detected as constant deviations from baseline flow at the aortic root (C) and severe backflow through the aorta (D).

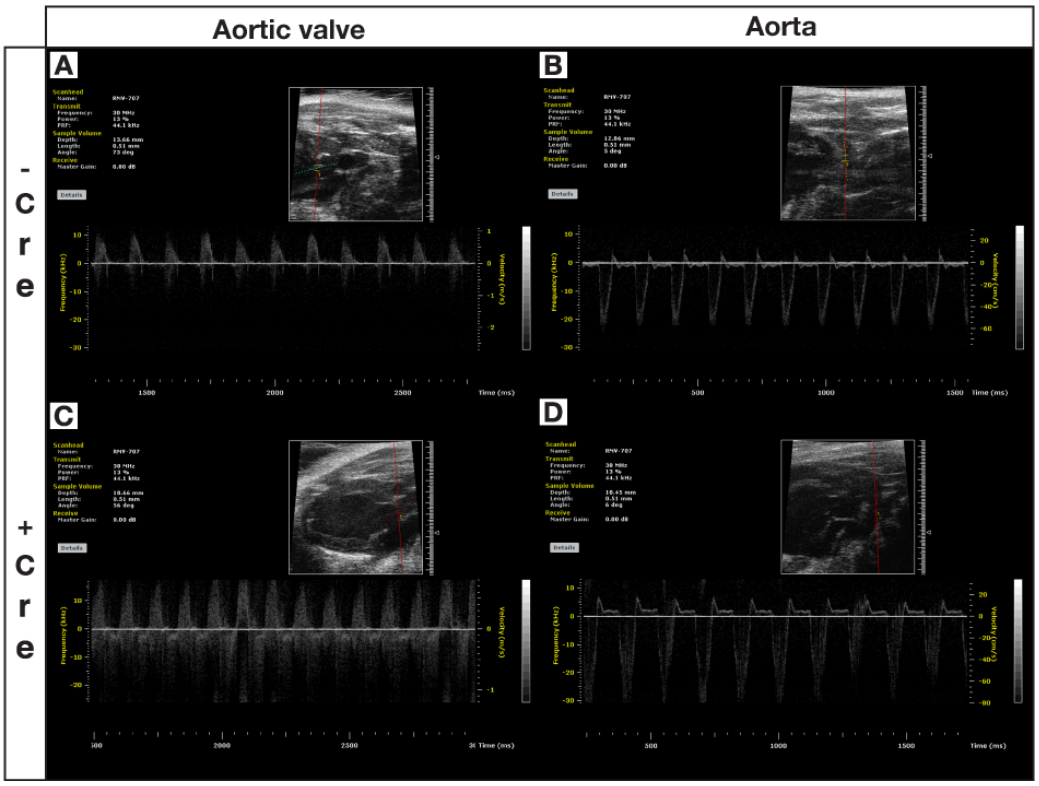
Aortic valve
Aorta
-Cre
+Cre
A
B
C
D

Figure 5-5: *Bcor* mutant hearts in the *Nkx2.5* expressing cell lineage have bilateral ventricular hypertrophy and thickened aortic valve leaflets.

Hematoxylin and eosin staining of sagittal sections from $Bcor^{Fl/Y}$ (A-F) and $Bcor^{Fl/Y}$*; Nkx2.5-IRES-Cre* (G-L) mice. $Bcor^{Fl/Y}$*; Nkx2.5-IRES-Cre* mice have hypertrophy of the ventricles (black arrows, G-K), blood stasis in the left ventricle (black arrowheads, I-K), and thickening of the aortic valve leaflets (L). Ao = aorta, PA = pulmonary artery, RA = right atrium, LA = left atrium, RV = right ventricle, LV = left ventricle, IVS = interventricular septum, AVL = aortic valve leaflets.

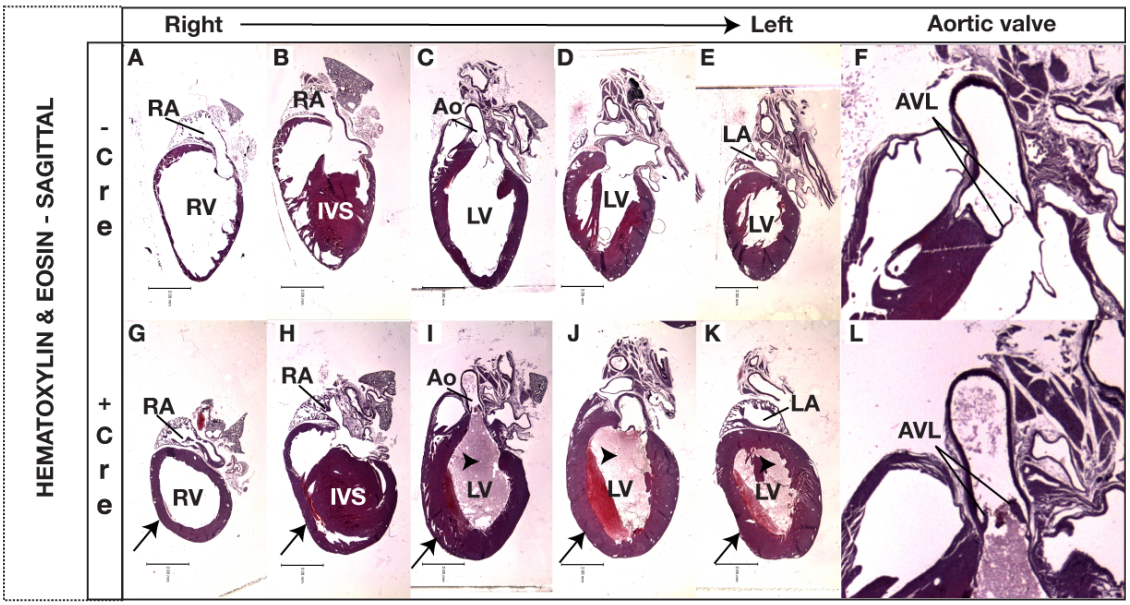
HEMATOXYLIN & EOSIN - SAGITTAL
Right
Left
Aortic valve
- Cre
+ Cre
A
RA
RV
B
RA
IVS
C
Ao
LV
D
LV
E
LA
LV
F
AVL
G
RA
RV
H
RA
IVS
I
Ao
LV
J
LV
K
LA
LV
L
AVL

Figure 5-6: *Bcor* mutant hearts in the *Pax3*-expressing cell lineage have biatrial enlargement and blood congestion.

Hematoxylin and eosin staining of frontal sections through $Bcor^{Fl/Y}$; *Pax3-Cre* hearts reveals bilateral atrial enlargement and blood congestion (A versus C). Injection of India ink into the left ventricle revealed blocked pulmonary arterial blood flow (B versus D, arrow denotes blockage).

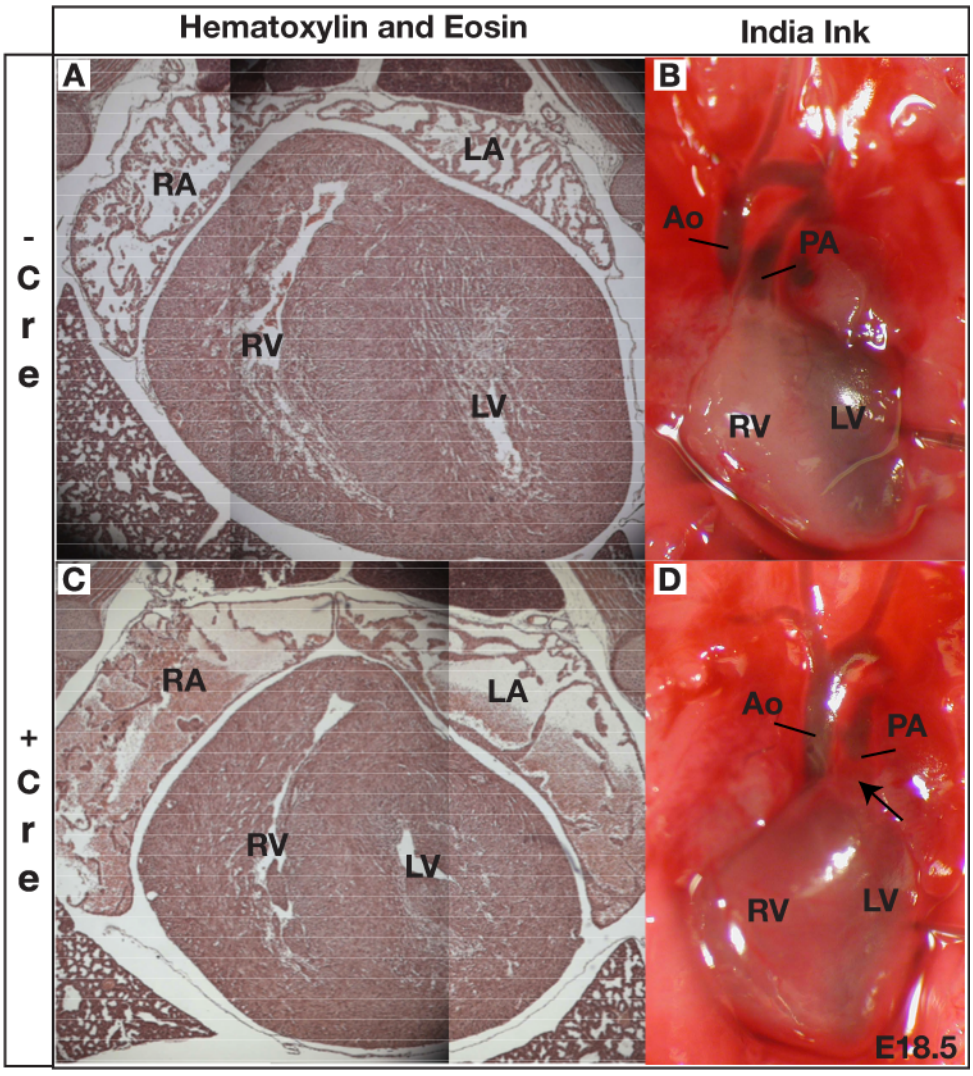
Hematoxylin and Eosin
India Ink
-cre
+cre
A
B
C
D
RA
LA
RV
LV
Ao
PA
E18.5

Figure 5-7: *Bcor* mutant hindlimbs in the *Isl1*-expressing cell lineage are delayed in development and fail to undergo mesenchymal condensation.

Hematoxylin and eosin staining reveals a delay in hindlimb digit formation in *Bcor*$^{Fl/Y}$*; Isl1-Cre* hindlimb development (A,B versus D,E). In-situ hybridization for the mesenchymal condensation marker *Sox9* reveals broadened *Sox9* expression in *Bcor*$^{Fl/Y}$*; Isl1-Cre* hindlimbs (C versus D).

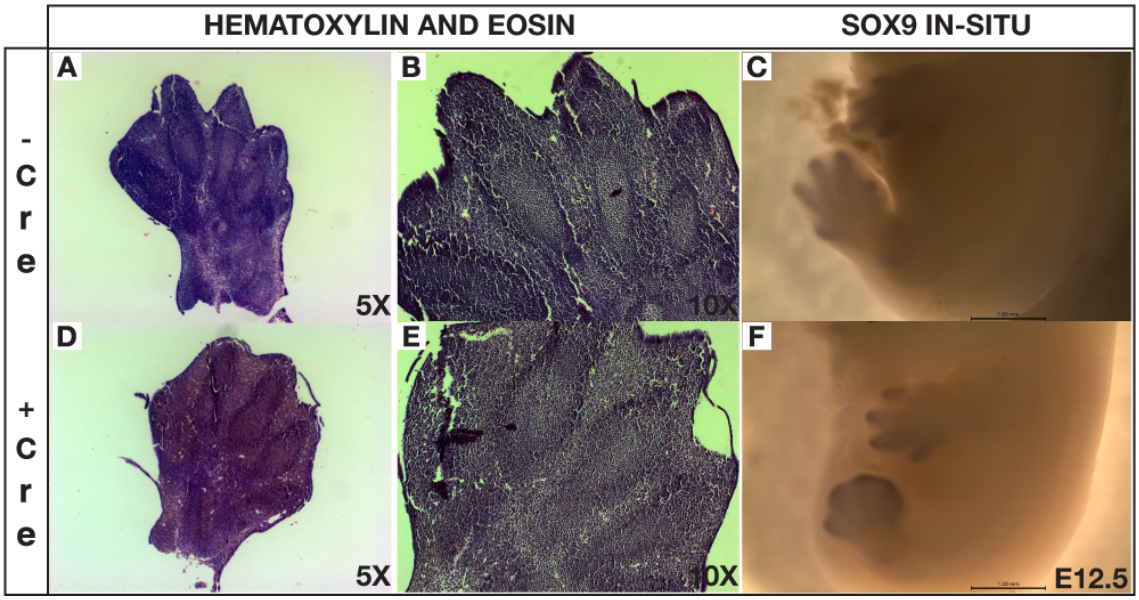
HEMATOXYLIN AND EOSIN
SOX9 IN-SITU
-Cre
+Cre
A
B
C
D
E
F
5X
10X
5X
10X
E12.5

Table 5-1. *Bcor* mutants in the *Isl1*-expressing cell lineage are found at less than Mendelian ratios and have a high incidence of heart defects.

(A) Observed and expected ratios of genotypes from crosses between $Bcor^{Fl/Fl}$ females and *Isl1-Cre* males. (B) Incidence of heart defects in E13.5 embryos from $Bcor^{Fl/Fl}$ females and *Isl1-Cre* males crosses. (C) Breakdown of heart defects observed in E13.5 embryos from (B).

A

Genotype	E13.5 Expected	E13.5 Observed		E15.5 Expected	E15.5 Observed
$Bcor^{Fl/Y}$ live	69.25	70		5.75	7
$Bcor^{Fl/+}$ live	69.25	79		5.75	11
$Bcor^{Fl/Y}$ Isl1-Cre live	69.25	57		5.75	2
$Bcor^{Fl/+}$ Isl1-Cre live	69.25	57		5.75	2
$Bcor^{Fl/Y}$ dead	0	1		0	0
$Bcor^{Fl/+}$ dead	0	0		0	0
$Bcor^{Fl/Y}$ Isl1-Cre dead	0	10		0	1
$Bcor^{Fl/+}$ Isl1-Cre dead	0	3		0	0
Totals	277	277		23	23

B

Genotype	Total Hearts Observed	Total Hearts Affected	Percentage Hearts Affected	Percentage Common Outflow Tract
$Bcor^{Fl/Y}$	62	0	0	0
$Bcor^{Fl/+}$	56	0	0	0
$Bcor^{Fl/Y}$ Isl1-Cre	55	43	78	65
$Bcor^{Fl/+}$ Isl1-Cre	41	3	7	7
Totals	214	46	85	73

C

Genotype	Wild Type Heart Anatomy	Common Outflow Tract	Rightward Looping Aorta	Vertically Branching Aorta
$Bcor^{Fl/Y}$	62	0	0	0
$Bcor^{Fl/+}$	56	0	0	0
$Bcor^{Fl/Y}$ Isl1-Cre	12	36	1	6
$Bcor^{Fl/+}$ Isl1-Cre	38	3	0	0
Totals	168	39	1	6

Table 5-2. Misexpressed genes in hearts that are mutant for *Bcor* in the *Isl1*-expressing cell lineage.

49 genes were significantly ($p \leq 0.05$) up- or down-regulated by 1.5-fold in the $Bcor^{Fl/Y}$; *Isl1-Cre* mutant hearts compared to $Bcor^{Fl/Y}$ wild type controls. Genes that are upregulated in mutants are shaded; downregulated genes are white.

Gene ID	Fold Change (Mutant/WT)	P-Value
Aldoa	2.2	0.05
Mest	2.0	0.02
Atp5d	1.9	0.03
Tcp1	1.9	0.03
Ankrd1	1.9	0.02
Sumo2	1.8	0.01
Uap1	1.8	0.02
EG625054	1.8	0.05
Ywhaq	1.7	0.01
Ndufb3	1.6	0.04
Tubb6	1.6	0.05
Immt	1.6	0.04
4930403O06Rik	1.6	0.03
Degs1	1.6	0.05
Fhl2	1.6	0.02
Elp2	1.6	0.05
Shfm1	1.6	0.05
Uchl3	1.6	0.005
Timm8a1	1.6	0.04
Gypc	1.6	0.04
LOC100047998	1.6	0.04
Pno1	1.6	0.03
Vdac2	1.6	0.04
Nup62	1.6	0.03
Cox5a	1.6	0.03
Pdk3	1.5	0.003
Col4a2	1.5	0.03
Clip4	1.5	0.04
LOC100044862	1.5	0.002
Psat1	1.5	0.01
Pdia4	1.5	0.01
Cacna2d1	0.67	0.04
Rgs5	0.66	0.00003
E2f2	0.66	0.004
Zfp326	0.66	0.04
Ppap2b	0.66	0.04
Glg1	0.65	0.04
Pfdn2	0.65	0.04
Zfp91	0.65	0.02
Hspb6	0.64	0.01
Rsrc2	0.64	0.02
Ep300	0.64	0.001
Bach2	0.64	0.01
Irs2	0.62	0.01
Mef2c	0.62	0.02
Actb	0.60	0.001
Ddc	0.58	0.05
BC017647	0.58	0.01
Tbc1d20	0.41	0.01

Table 5-3. Misexpressed genes in hindlimbs that are mutant for *Bcor* in the *Isl1*-expressing cell lineage.

17 genes were significantly ($p \leq 0.05$) up- or down-regulated by 1.3-fold in the $Bcor^{Fl/Y}$; *Isl1-Cre* mutant hindlimbs compared to $Bcor^{Fl/Y}$ wild type controls. Genes that are upregulated in mutants are shaded; downregulated genes are white.

Gene ID	Fold Change (Mutant/WT)	P-Value
Hoxc6	1.7	0.02
Hoxa5	1.6	0.02
Hoxa2	1.6	0.03
Hoxc9	1.4	0.03
Twist2	1.4	0.05
Hoxc10	1.4	0.02
4930455C21Rik	1.4	0.05
Pcbd2	1.4	0.04
Ethe1	1.4	0.04
Blvrb	1.3	0.03
Bcl2a1d	1.3	0.04
Lbh	0.75	0.04
Smarcal1	0.74	0.03
9030612M13Rik	0.73	0.02
Hoxd12	0.68	0.03
Arl5a	0.66	0.03
Smarcb1	0.64	0.03

Chapter 6:

Final Discussion.

The focus of this thesis is understanding the molecular function of the transcriptional corepressor BCOR and its role in mammalian development. In particular, the experiments described herein promote our understanding of the role of BCOR in the human multisystemic developmental disorder Oculofaciocardiodental syndrome (OFCD), focusing on the role of BCOR in OFCD relevant tissues. BCOR interacts with proteins that are capable of repressive chromatin modifications, as well as several transcription factors, suggesting a mechanism by which BCOR may impact development. The embryonic lethality of mice that overexpress BCOR ubiquitously and the tight control of *Bcor* transcript levels in B cells suggest that proper maintenance of *Bcor* expression is integral to development. In fact, *Bcor* is required in mouse neural crest cells for proper craniofacial development, in hindlimb progenitors for hindlimb formation, and in several cardiovascular precursor cell types for appropriate cardiovascular system development and function. This chapter will describe and integrate these significant results, identify currently unanswered questions, and explain potential future directions.

BCOR interacts with chromatin modifying proteins and transcription factors.

Tandem affinity purification and mass spectrometric identification of BCOR interacting proteins from human embryonic kidney cells confirmed its interaction with chromatin modifying proteins. Specifically, BCOR associates with SKP1 and FBXL10, two out of three core components of a SCF E3 ubiquitin ligase. However, it is currently unknown whether SKP1 and FBXL10 can function as an ubiquitin ligase in this context. FBXL10, via its JmjC domain is also capable of demethylation of H3K36me2, a methyl mark that may need to be removed to get full repression by PcG complexes (Yuan et al., 2011). In addition, BCOR interacts with a Polycomb-like complex containing NSPC1, RING1, RNF2, and RYBP. PcG complexes are classically known for their key role in regulating development through appropriate repression of target genes. Thus, association of BCOR with a histone demethylase and a Polycomb-like complex provides a possible molecular mechanism for its repressive function. Furthermore, since the specific protein composition of Polycomb complexes differs according to cell type and developmental stage, it is likely that preferential combinatorial assembly of BCOR complex components

under differing cellular conditions plays an important role in development and homeostasis (Kerppola, 2009; Schuettengruber et al., 2007). Future studies may focus on determining the role of BCOR in modulating the enzyme activity of its interacting proteins, as well as defining the unique protein combinations that are capable of BCOR interaction at various developmental time points and tissues.

Purification and identification of BCOR interacting proteins also yielded several transcription factors. While the role of most of these transcription factors remains relatively unknown, the BCOR-interacting transcription factor FOXC1 has a known role in development. Mice with mutations in *Foxc1* develop defects in the developing cardiovascular, dental, craniofacial, and ocular systems, and these defects partially overlap with the phenotypes observed in OFCD patients. Thus, the role of BCOR in development may be mediated, at least in part, by its interaction with FOXC1. Future studies involving our conditional mouse null allele of *Bcor* will further investigate the relevance of BCOR interaction with FOXC1 *in vivo*.

BCOR expression is tightly controlled in B cells, and ubiquitous misexpression results in embryonic lethality.

To ascertain the potential role of BCOR in mouse B cell lymphomagenesis, we attempted to specifically overexpress *Bcor* in the mouse mature B cell lineage. However, *Bcor* could not be overexpressed in mouse B cells due to strict control of *Bcor* transcript levels. Future experiments could potentially overcome this obstacle by using a stronger promoter to induce *Bcor* expression or by using an inducible *Cre* recombinase to induce *Bcor* expression in B cells at specific time points.

Although this unexpected result did not allow us to determine the effect of *Bcor* overexpression on lymphomagenesis, it lends important insight into the mechanism of *Bcor* regulation in B cells. Specifically, downregulation of endogenous *Bcor* expression upon exogenous *Bcor* expression suggests that BCOR is able to regulate its own transcription. This is further supported by chromatin immunoprecipitation showing that BCOR binds its own promoters in human lymphoma cell lines (Bardwell and Melnick,

unpublished). Although *Bcor* overexpression did not occur in B cells, ubiquitous expression of *Bcor* in mice resulted in embryonic lethality by E14.5. Thus, proper maintenance of *Bcor* expression levels is clearly required for embryogenesis. However, the upstream factors involved in regulating *Bcor* levels remain to be elucidated.

BCOR is required for proper embryonic skeletogenesis.

Bcor deletion in the whole mouse embryo results in early embryonic lethality prior to E10.5 (Wamstad, Corcoran, Hamline, Bardwell, in preparation). To circumvent this early requirement and analyze the role of *Bcor* in the development of multiple tissue lineages, we generated a mouse conditional null allele of *Bcor* to be used in combination with various tissue-specific *Cre recombinase* alleles.

Removal of *Bcor* from the neural crest cell lineage using *Pax3-Cre* revealed a requirement for *Bcor* in palatogenesis. *Bcor* mutants in the neural crest cell lineage had normal palatal shelf morphology until E13.5, when the tongue failed to depress in the oral cavity and the mutant palatal shelves failed to elevate to their horizontal position overlying the tongue. This resulted in cleft palate defect in 100% of mutants examined. In addition, E18.5 mutants had shortened tympanic bones and mandibles. Interestingly, since the proper elevation of palatal shelves requires depression of the tongue within the oral cavity, mandibular development is closely tied to proper palate formation. This prompted a closer examination of mandibular precursors in development. Meckel's cartilage, an embryonic cartilaginous scaffold for mandibular skeletogenesis, was found to be malformed in mutant E14.5 embryos. Therefore, the malformation of Meckel's cartilage provides a likely explanation for the failed palatogenesis observed in *Bcor* neural crest cell mutants, resulting in perinatal lethality.

Removal of *Bcor* from the *Isl1*-expressing cell lineage lent further insight into the requirement for *Bcor* in skeletogenesis. Specifically, removal of *Bcor* from *Isl1*-expressing cells resulted in delayed embryonic hindlimb development and misexpression of the mesenchymal condensation marker *Sox9*. Microarray gene expression analysis of *Bcor* mutant hindlimbs revealed the upregulation of several genes from the *Hox* family,

suggesting that *Bcor* plays a key role in regulating *Hox* gene expression. Thus, BCOR affects skeletogenesis in the developing hindlimb by modulating the expression of various *Hox* family members.

The failure of *Bcor* mutant hindlimbs to undergo proper mesenchymal condensation is of particular relevance to the role of *Bcor* in skeletogenesis. Mesenchymal condensation, a process that is essential to the correct development of both the mandible and hindlimbs, refers to the aggregation of cells allowing selective gene regulation to promote appropriate chondrogenesis or osteogenesis (Hall & Miyake, 2000). This process occurs in several stages, including initiation of condensation, establishing the condensation boundary, proliferation, cell adherence, growth, and finally differentiation. Each of these steps requires the expression of a specific gene subset. *Hoxa2,* which is upregulated in *Bcor* mutant hindlimbs, has multiple roles in hindlimb mesenchymal condensation, including establishment of the condensation boundary, induction of condensation growth, and the prevention of cell differentiation that terminates condensation (Hall & Miyake, 2000). Meanwhile, *Hoxd12* is downregulated in *Bcor* mutant hindlimbs and is involved in the transition from condensation to differentiation. Therefore, through its regulation of *Hox* genes, *Bcor* mutation appears to prevent proper mesenchymal condensation in developing hindlimbs.

Many questions regarding the role of *Bcor* in skeletogenesis remain unanswered. First, it is not currently known whether the *Hox* genes that were misexpressed in *Bcor* mutant hindlimbs are direct or indirect BCOR targets. The interaction of BCOR with several Polycomb group proteins, which have a known role in regulating *Hox* gene expression, supports a direct effect on at least some of these genes. In the future, chromatin immunoprecipitation will determine which *Hox* genes are direct BCOR targets. In addition, the defect in mesenchymal condensation in Bcor mutant hindlimbs presents the possibility that *Bcor* similarly affects mesenchymal condensation in the forming mandible. Future gene expression studies will assess *Hox* gene expression patterns in *Bcor* mutant mandibles, and several molecular markers for mesenchymal condensation in the palate will be assessed for defects. Finally, it is also unknown which transcription factors work with BCOR to mediate its effects on development. A thorough

understanding of BCOR targets in development will help elucidate which developmental pathways utilize BCOR and will provide candidate transcription factors that can be tested further for BCOR interaction.

BCOR may play a role in the initiation or maintenance of progenitor cell populations.

In our examination of *Bcor* neural crest cell mutants, we also unexpectedly observed the growth of ectopic salivary glands in the submandibular region. Salivary glands are formed when interactions between oral epithelium and mesenchyme specify a salivary gland progenitor cell subpopulation (Lombaert et al., 2011; Tucker, 2007). These cells then proliferate and differentiate to form the many salivary gland cell types. Given their key role in oral health, conditions resulting in the loss of salivary gland function (such as tumor removal, therapeutic irradiation, Sjogren's syndrome, and other genetic disorders) drastically affect quality of life. Therefore, recent work has focused on identifying and defining the progenitor cell pool that gives rise to the diverse cell types found within salivary glandular tissue (Arany et al., 2011; Hai et al., 2010). The sufficiency of *Bcor* mutation in inducing ectopic salivary gland formation suggests that it may play a key repressive role in salivary gland progenitors, providing a potential basis for regenerative therapy. Future studies could explore this possibility by inducing *Bcor* loss specifically in adult salivary gland tissue and assessing the effects on salivary gland regenerative potential.

BCOR is required in cardiovascular progenitor cells for proper cardiovascular development.

In addition to studying skeletogenesis, we also utilized the conditional null allele of *Bcor* to further understand the role of *Bcor* in cardiovascular development. *Bcor* mutants in the *Isl1*-expressing cell lineage died prenatally with cardiac outflow tract and ventricular septal defects, suggesting that *Bcor* is required in *Isl1*-expressing cells for proper ventricular and outflow tract septation. To confirm these results, we also analyzed

the cardiac phenotype of *Bcor* mutants in the *Nkx2.5-IRES-Cre* expressing cell lineage, which reportedly overlaps *Isl1-Cre* expression (Ma, Zhou, & Pu, 2008; Stanley, 2002; Yang et al., 2006). Surprisingly, *Bcor* mutants in the *Nkx2.5*-expressing cell lineage had a less severe phenotype of aortic insufficiency, bilateral ventricular hypertrophy, and thickening of the aortic valve leaflets. Thus, while *Bcor* is required in the *Nkx2.5* expressing lineage for efficient cardiovascular function, it is not required in this lineage for cardiac septation and embryonic survival.

There are several potential explanations for this striking difference in phenotype. First, the most likely possibility is that *Bcor* is most strongly required within a highly specific subset of cardiovascular progenitor cells, in which *Isl1* but not *Nkx2.5* is expressed. Future studies will address this by crossing a *Cre* responsive reporter into the *Isl1-Cre* and *Nkx2.5-IRES-Cre* backgrounds in order to compare the cardiovascular cell types in which *Cre* is expressed. *Bcor* expression within the cardiovascular system will also be analyzed throughout development in each of these conditional mutants. Another possibility is that the effect of *Bcor* mutation on cardiovascular development is accentuated by heterozygosity for *Isl1* in the *Isl1-Cre* animals. While it is possible that simultaneous mutation of *Bcor* and *Isl1* has a synergistic effect on cardiovascular development, *Isl1* haploinsufficiency has not been previously reported, and cardiovascular development is reportedly normal in *Isl1-Cre* mice (Yang et al., 2006). Furthermore, since it is unlikely that the 85 percent of OFCD patients with cardiovascular phenotypes are all haploinsufficient for *Isl1*, it seems rather unlikely that the more severe cardiovascular defects in *Isl1-Cre* mutants is due to *Isl1* haploinsufficiency. Finally, the difference in phenotype between the two conditional mutants could reflect an underlying difference in strain background. In this case, genetic modifiers specific to each individual strain could impact the effect of *Bcor* mutation on cardiovascular development. However, because both the *Isl1-Cre* and *Nkx2.5-IRES-Cre* were on mixed backgrounds, this is a highly unlikely cause for the discrepancy in mutant phenotypes.

Another open and important question regarding BCOR function in cardiovascular development involves the cardiovascular pathways that are regulated by the BCOR complex. We attempted to answer this question by performing microarray gene

expression analysis on hearts that were null for *Bcor* in the *Isl1*-expressing cell population. However, the resulting list of potential target genes appeared unreliable due to the high number of misregulated cardiac stress response genes. This suggested that the observed changes in gene expression may have been secondary to a physiological response to cardiovascular damage, rather than direct effects of *Bcor* loss. Therefore, future studies will attempt to more conclusively identify BCOR targets by performing gene expression analysis on hearts earlier in development, at the first sign of cardiovascular developmental defects. Such an analysis will enable a determination of the earliest cardiovascular gene expression changes associated with *Bcor* loss and will hopefully elucidate the cardiovascular molecular pathways that require *Bcor* function.

The role of BCOR in Polycomb mediated gene repression during mammalian development.

The results described herein have important implications for the role of not only BCOR itself, but also Polycomb complexes in general, in mammalian development. While Polycomb proteins have a well-defined role in maintaining embryonic stem cell pluripotency and regulating their transition to differentiation, relatively little is known regarding the role of Polycomb proteins in regulating later stages of mammalian development (Sawarkar & Paro, 2010; Surface, Thornton, & Boyer, 2010). In fact, the vital role of Polycomb proteins in embryonic stem cells complicates the study of Polycomb proteins in later development, due to the early embryonic lethality of many Polycomb knockouts. Therefore, our *Bcor* conditional null allele provides a prime opportunity to study the role of a Polycomb complex in specific lineages, bypassing the early embryonic requirement for *Bcor*.

One area of investigation emphasizes the exact make-up of Polycomb complexes and their variability between different developmental timepoints and cell types. Tandem affinity purifications have shown that BCOR interacts with a PRC1-like complex including RING1, RNF2, RYBP, and NSPC1 in human embryonic kidney cells. However, the composition of Polycomb complexes does vary according to developmental

stage and cell type (Kerppola, 2009; Schuettengruber et al., 2007). Thus, defining the BCOR complex components in varying developmental cell types will help to clarify BCOR function in craniofacial, hindlimb, and cardiovascular development. Future purifications from these and other developmental cell types will lend further insight into cell type-specific BCOR interactors and how variability in complex composition modulates Polycomb function throughout development.

In order for embryonic development to progress properly, cells must dynamically modulate specific gene expression in response to multiple extracellular patterning stimuli. In the current model, modulation of Polycomb group expression, modification, and localization is one of several means by which cells integrate these stimuli for time- and tissue-specific activation or repression of gene expression (Sawarkar & Paro, 2010). Embryonic stem cells provide one interesting model for studying Polycomb function in developmental progression. In embryonic stem cells, Polycomb target genes are "bivalent," meaning they are marked by both repressive H3K27me3 and activating H3K4me3 modifications (Bernstein et al., 2006). These bivalent domains colocalize with Polycomb-mediated H2A ubiquitination, which supports pausing of RNA polymerase in a poised configuration, waiting to enter the elongation phase (Stock et al., 2007). This bivalency is resolved upon the cell's differentiation, when each gene takes on either the repressive H3K27me3 mark or the activating H3K4me3 mark as appropriate to its intended expression pattern. Thus, it is possible that Polycomb proteins take on a similar role in later development, modulating the timing and tissue specificity of gene expression as cell fates undergo transition. Future studies may address this potential role by analyzing the methylation status and RNA polymerase configuration at BCOR target genes in relevant developmental cell types.

Concluding remarks.

Prior to the studies described within this thesis, relatively little was known regarding how and why mutations in *BCOR* cause the human developmental disorder OFCD. The experiments described herein have significantly expanded our understanding

of the role of BCOR in this disorder by elucidating some of the cell type specific requirements for *Bcor* and also addressing the molecular basis of BCOR repression within these cell types. BCOR is one of only a few proteins that is known to incorporate into a chromatin modifying complex and is also associated with a human developmental disorder (Ausió et al., 2003). Therefore, these findings play a key role in "bridging the gap" between chromatin modification and human development. Thus, our continued emphasis on BCOR function in development provides a necessary link between molecular biology and human disease, which may provide an important basis for patient diagnosis and therapy in the future.

Bibliography

Akasaka, T., Lohuizen, M van, Lugt, N. van der, Mizutani-Koseki, Y., Kanno, M., Taniguchi, M., et al. (2001). Mice doubly deficient for the Polycomb Group genes Mel18 and Bmi1 reveal synergy and requirement for maintenance but not initiation of Hox gene expression. *Development (Cambridge, England)*, *128*(9), 1587-97.

Albagli, O., Dhordain, P., Bernardin, F., Quief, S., Kerkaert, J. P., & Leprince, D. (1996). Multiple domains participate in distance-independent LAZ3/BCL6-mediated transcriptional repression. *Biochemical and biophysical research communications*, *220*(3), 911-5.

Albagli-Curiel, O. (2003). Ambivalent role of BCL6 in cell survival and transformation. *Oncogene*, *22*(4), 507-16. doi: 10.1038/sj.onc.1206152.

Arany, S., Catalán, M. a, Roztocil, E., & Ovitt, C. E. (2011). Ascl3 knockout and cell ablation models reveal complexity of salivary gland maintenance and regeneration. *Developmental biology*. doi: 10.1016/j.ydbio.2011.02.025.

Ausió, J, Levin, D., De Amorim, G., Bakker, S., & Macleod, P. (2003). Syndromes of disordered chromatin remodeling. *Clinical Genetics*, *64*(2), 83-95. doi: 10.1034/j.1399-0004.2003.00124.x.

Bajolle, F., Zaffran, Stéphane, Kelly, R. G., Hadchouel, J., Bonnet, D., Brown, N. a, et al. (2006). Rotation of the myocardial wall of the outflow tract is implicated in the normal positioning of the great arteries. *Circulation research*, *98*(3), 421-8. doi: 10.1161/01.RES.0000202800.85341.6e.

Bamford, R. N., Roessler, E., Burdine, R. D., Saplakoğlu, U., Cruz, J. dela, Splitt, M., et al. (2000). Loss-of-function mutations in the EGF-CFC gene CFC1 are associated with human left-right laterality defects. *Nature genetics*, *26*(3), 365-9. doi: 10.1038/81695.

Baron, B. W., Anastasi, J., Thirman, M. J., Furukawa, Y., Fears, S., Kim, D. C., et al. (2002). The human programmed cell death-2 (PDCD2) gene is a target of BCL6 repression: implications for a role of BCL6 in the down-regulation of apoptosis. *Proceedings of the National Academy of Sciences of the United States of America*, *99*(5), 2860-5. doi: 10.1073/pnas.042702599.

Baskind, H. a, Na, L., Ma, Quanhong, Patel, M. P., Geenen, D. L., & Wang, Q. T. (2009). Functional conservation of asxl2, a murine homolog for the Drosophila enhancer of trithorax and polycomb group gene asx. *PloS one*, *4*(3), e4750. doi: 10.1371/journal.pone.0004750.

Basso, K., & Dalla-favera, R. (2010). BCL6: Master Regulator of the Germinal Center Reaction and Key Oncogene in B Cell Lymphomagenesis. *Advances*, *105*(10), 193-210. doi: 10.1016/S0065-2776(10)05007-8.

Basso, K., Saito, M., Sumazin, P., Margolin, A. a, Wang, K., Lim, W.-K., et al. (2010). Integrated biochemical and computational approach identifies BCL6 direct target genes controlling multiple pathways in normal germinal center B cells. *Blood*, *115*(5), 975-84. doi: 10.1182/blood-2009-06-227017.

Bernstein, B. E., Mikkelsen, T. S., Xie, X., Kamal, M., Huebert, D. J., Cuff, J., et al. (2006). A bivalent chromatin structure marks key developmental genes in embryonic stem cells. *Cell*, *125*(2), 315-26. doi: 10.1016/j.cell.2006.02.041.

Bi, W., Drake, C. J., & Schwarz, J. J. (1999). The transcription factor MEF2C-null mouse exhibits complex vascular malformations and reduced cardiac expression of angiopoietin 1 and VEGF. *Developmental biology*, *211*(2), 255-67. doi: 10.1006/dbio.1999.9307.

Birke, M. (2002). The MT domain of the proto-oncoprotein MLL binds to CpG-containing DNA and discriminates against methylation. *Nucleic Acids Research*, *30*(4), 958-965. doi: 10.1093/nar/30.4.958.

Boyer, L. a, Plath, K., Zeitlinger, J., Brambrink, T., Medeiros, L. a, Lee, T. I., et al. (2006). Polycomb complexes repress developmental regulators in murine embryonic stem cells. *Nature*, *441*(7091), 349-53. doi: 10.1038/nature04733.

Breckenridge, R., Kotecha, S., Towers, N., Bennett, M., & Mohun, T. (2007). Pan-myocardial expression of Cre recombinase throughout mouse development. *genesis*, *45*(3), 135–144. Wiley Online Library. doi: 10.1002/dvg.

Briggs, S D, Bryk, M., Strahl, B. D., Cheung, W. L., Davie, J. K., Dent, S. Y., et al. (2001). Histone H3 lysine 4 methylation is mediated by Set1 and required for cell growth and rDNA silencing in Saccharomyces cerevisiae. *Genes & development*, *15*(24), 3286-95. doi: 10.1101/gad.940201.

Brown, C., & Baldwin, H. (2006). Neural crest contribution to the cardiovascular system. *Neural Crest Induction and Differentiation*, 134–154. Springer.

Buckingham, M., Meilhac, S., & Zaffran, Stéphane. (2005). Building the mammalian heart from two sources of myocardial cells. *Nature reviews. Genetics*, *6*(11), 826-35. doi: 10.1038/nrg1710.

Burstyn-Cohen, T., Stanleigh, J., Sela-Donenfeld, D., & Kalcheim, C. (2004). Canonical Wnt activity regulates trunk neural crest delamination linking BMP/noggin signaling with G1/S transition. *Development (Cambridge, England)*, *131*(21), 5327-39. doi: 10.1242/dev.01424.

Cai, Chen-Leng, Liang, X., Shi, Y., Chu, P.-H., Pfaff, S. L., Chen, J., et al. (2003). Isl1 identifies a cardiac progenitor population that proliferates prior to differentiation and contributes a majority of cells to the heart. *Developmental cell*, *5*(6), 877-89.

Cai, J., Kwak, S., Lee, J.-M., Kim, E.-J., Lee, M.-J., Park, G.-H., et al. (2010). Function analysis of mesenchymal Bcor in tooth development by using RNA interference. *Cell and tissue research*, *341*(2), 251-8. doi: 10.1007/s00441-010-0996-2.

Caldas, C., & Aparicio, S. (1999). Cell memory and cancer--the story of the trithorax and Polycomb group genes. *Cancer metastasis reviews*, *18*(2), 313-29.

Campos, E. I., & Reinberg, D. (2009). Histones: annotating chromatin. *Annual review of genetics*, *43*, 559-99. doi: 10.1146/annurev.genet.032608.103928.

Cao, R., Tsukada, Y.-I., & Zhang, Yi. (2005). Role of Bmi-1 and Ring1A in H2A ubiquitylation and Hox gene silencing. *Molecular cell*, *20*(6), 845-54. doi: 10.1016/j.molcel.2005.12.002.

Cao, R., Wang, Liangjun, Wang, Hengbin, Xia, L., Erdjument-Bromage, Hediye, Tempst, Paul, et al. (2002). Role of histone H3 lysine 27 methylation in Polycomb-group silencing. *Science (New York, N.Y.)*, *298*(5595), 1039-43. doi: 10.1126/science.1076997.

Cattoretti, Giorgio, Pasqualucci, L., Ballon, G., Tam, W., Nandula, S. V., Shen, Q., et al. (2005). Deregulated BCL6 expression recapitulates the pathogenesis of human diffuse large B cell lymphomas in mice. *Cancer cell*, *7*(5), 445-55. doi: 10.1016/j.ccr.2005.03.037.

Cerchietti, L. C., Ghetu, A. F., Zhu, X., Da Silva, G. F., Zhong, S., Matthews, M., et al. (2010). A small-molecule inhibitor of BCL6 kills DLBCL cells in vitro and in vivo. *Cancer cell*, *17*(4), 400-11. doi: 10.1016/j.ccr.2009.12.050.

Cerchietti, L. C., Yang, S. N., Shaknovich, R., Hatzi, K., Polo, J. M., Chadburn, A., et al. (2009). A peptomimetic inhibitor of BCL6 with potent antilymphoma effects in vitro and in vivo. *Blood*, *113*(15), 3397-405. doi: 10.1182/blood-2008-07-168773.

Chai, Y, Jiang, X., Ito, Y., Bringas, P., Han, J., Rowitch, D. H., et al. (2000). Fate of the mammalian cranial neural crest during tooth and mandibular morphogenesis. *Development (Cambridge, England)*, *127*(8), 1671-9.

Chai, Yang, & Maxson, R. E. (2006). Recent advances in craniofacial morphogenesis. *Developmental dynamics : an official publication of the American Association of Anatomists*, *235*(9), 2353-75. doi: 10.1002/dvdy.20833.

Chang, C., Ye, Bh, Chaganti, Rs, & Dalla-Favera, R. (1996). BCL-6, a POZ/zinc-finger protein, is a sequence-specific transcriptional repressor. *Proc Natl Acad Sci U S A.*, *93*(July), 6947-6952.

Chen, W., Iida, S., Louie, D. C., Dalla-Favera, R, & Chaganti, R. S. (1998). Heterologous promoters fused to BCL6 by chromosomal translocations affecting band 3q27 cause its deregulated expression during B-cell differentiation. *Blood*, *91*(2), 603-7.

Chen, Y, Bei, M., Woo, I., Satokata, I., & Maas, R. (1996). Msx1 controls inductive signaling in mammalian tooth morphogenesis. *Development (Cambridge, England)*, *122*(10), 3035-44.

Ci, W., Polo, J. M., Cerchietti, L., Shaknovich, R., Wang, Ling, Yang, S. N., et al. (2009). The BCL6 transcriptional program features repression of multiple oncogenes in primary B cells and is deregulated in DLBCL. *Blood*, *113*(22), 5536-48. doi: 10.1182/blood-2008-12-193037.

Clouthier, D. E., Hosoda, K., Richardson, J. a, Williams, S. C., Yanagisawa, H., Kuwaki, T., et al. (1998). Cranial and cardiac neural crest defects in endothelin-A receptor-deficient mice. *Development (Cambridge, England)*, *125*(5), 813-24.

Conen, K. L., Nishimori, S., Provot, S., & Kronenberg, H. M. (2009). The transcriptional cofactor Lbh regulates angiogenesis and endochondral bone formation during fetal bone development. *Developmental biology*, *333*(2), 348-58. doi: 10.1016/j.ydbio.2009.07.003.

Coré, N., Bel, S., Gaunt, S. J., Aurrand-Lions, M., Pearce, J., Fisher, a, et al. (1997). Altered cellular proliferation and mesoderm patterning in Polycomb-M33-deficient mice. *Development (Cambridge, England)*, *124*(3), 721-9.

Couly, G. F., Coltey, P. M., & Le Douarin, N M. (1992). The developmental fate of the cephalic mesoderm in quail-chick chimeras. *Development (Cambridge, England)*, *114*(1), 1-15.

Couly, G., Creuzet, S., Bennaceur, S., Vincent, C., & Le Douarin, Nicole M. (2002). Interactions between Hox-negative cephalic neural crest cells and the foregut endoderm in patterning the facial skeleton in the vertebrate head. *Development (Cambridge, England)*, *129*(4), 1061-73.

Czermin, B., Melfi, R., McCabe, D., Seitz, V., Imhof, A., & Pirrotta, V. (2002). Drosophila enhancer of Zeste/ESC complexes have a histone H3 methyltransferase activity that marks chromosomal Polycomb sites. *Cell*, *111*(2), 185-96.

Danielian, P. S., Muccino, D., Rowitch, D. H., Michael, S. K., & McMahon, a P. (1998a). Modification of gene activity in mouse embryos in utero by a tamoxifen-inducible form of Cre recombinase. *Current biology : CB*, *8*(24), 1323-6.

Danielian, P. S., Muccino, D., Rowitch, D. H., Michael, S. K., & McMahon, a P. (1998b). Modification of gene activity in mouse embryos in utero by a tamoxifen-inducible form of Cre recombinase. *Current biology : CB*, *8*(24), 1323-6.

Davis-Smyth, T., Duncan, R. C., Zheng, T., Michelotti, G., & Levens, D. (1996). The far upstream element-binding proteins comprise an ancient family of single-strand DNA-binding transactivators. *The Journal of biological chemistry*, *271*(49), 31679-87.

Devoy, A., Soane, T., Welchman, R., & Mayer, R. J. (2005). The ubiquitin-proteasome system and cancer. *Essays in biochemistry*, *41*, 187-203. doi: 10.1042/EB0410187.

Dhananjayan, S. C., Ismail, A., & Nawaz, Z. (2005). Ubiquitin and control of transcription. *Essays in biochemistry*, *41*, 69-80. doi: 10.1042/EB0410069.

Eberharter, A., Vetter, I., Ferreira, R., & Becker, P. B. (2004). ACF1 improves the effectiveness of nucleosome mobilization by ISWI through PHD-histone contacts. *The EMBO journal*, *23*(20), 4029-39. doi: 10.1038/sj.emboj.7600382.

Endoh, M, Endo, T. a, Endoh, T., Fujimura, Y.-ichi, Ohara, O., Toyoda, T., et al. (2008). Polycomb group proteins Ring1A/B are functionally linked to the core transcriptional regulatory circuitry to maintain ES cell identity. *Development (Cambridge, England)*, *135*(8), 1513-24. doi: 10.1242/dev.014340.

Engleka, K. a, Gitler, A. D., Zhang, M., Zhou, D. D., High, F. a, & Epstein, J. a. (2005). Insertion of Cre into the Pax3 locus creates a new allele of Splotch and identifies unexpected Pax3 derivatives. *Developmental biology*, *280*(2), 396-406. doi: 10.1016/j.ydbio.2005.02.002.

Fan, Z., Yamaza, T., Lee, J. S., Yu, J., Wang, S., Fan, G., et al. (2009). BCOR regulates mesenchymal stem cell function by epigenetic mechanisms. *nature cell biology*, *11*(8), 1002–1009. Nature Publishing Group. doi: 10.1038/ncb1913.BCOR.

Fang, J., Chen, T., Chadwick, B., Li, E., & Zhang, Yi. (2004). Ring1b-mediated H2A ubiquitination associates with inactive X chromosomes and is involved in initiation of X inactivation. *The Journal of biological chemistry*, *279*(51), 52812-5. doi: 10.1074/jbc.C400493200.

Faust, C., Lawson, K. a, Schork, N. J., Thiel, B., & Magnuson, T. (1998). The Polycomb-group gene eed is required for normal morphogenetic movements during gastrulation in the mouse embryo. *Development (Cambridge, England)*, *125*(22), 4495-506.

Faust, C., Schumacher, a, Holdener, B., & Magnuson, T. (1995). The eed mutation disrupts anterior mesoderm production in mice. *Development (Cambridge, England)*, *121*(2), 273-85.

Feldman, R. M., Correll, C. C., Kaplan, K. B., & Deshaies, R. J. (1997). A complex of Cdc4p, Skp1p, and Cdc53p/cullin catalyzes ubiquitination of the phosphorylated CDK inhibitor Sic1p. *Cell*, *91*(2), 221-30.

Feng, W., Leach, S. M., Tipney, H., Phang, T., Geraci, M., Spritz, R. a, et al. (2009). Spatial and temporal analysis of gene expression during growth and fusion of the mouse facial prominences. *PloS one*, *4*(12), e8066. doi: 10.1371/journal.pone.0008066.

Ferguson, C. a, & Graham, A. (2004). Redefining the head-trunk interface for the neural crest. *Developmental biology*, *269*(1), 70-80. doi: 10.1016/j.ydbio.2004.01.013.

Fischle, W., Wang, Ya., Jacobs, S., Kim, Y., Allis, C David, & Khorasanizadeh, S. (2003). Molecular basis for the discrimination of repressive methyl-lysine marks in histone H3 by Polycomb and HP1 chromodomains. *Genes & development*, *17*(15), 1870-81. doi: 10.1101/gad.1110503.

Franco, D. (2003). The Role of Pitx2 during Cardiac Development Linking Left–Right Signaling and Congenital Heart Diseases. *Trends in Cardiovascular Medicine*, *13*(4), 157-163. doi: 10.1016/S1050-1738(03)00039-2.

Frommer, J., & Margolies, M. R. (1971). Contribution of Meckel's Cartilage to Ossification of the Mandible in Mice. *Journal of Dental Research*, *50*(5), 1260-1267. doi: 10.1177/00220345710500052801.

Fukuda, T., Yoshida, T., Okada, S., Hatano, M., Miki, T., Ishibashi, K., et al. (1997). Disruption of the Bcl6 Gene Results in an Impaired Germinal Center Formation. *Journal of Experimental Medicine*, *186*(3), 439-448. doi: 10.1084/jem.186.3.439.

Galli, D., Domínguez, J. N., Zaffran, Stephane, Munk, A., Brown, N. a, & Buckingham, M. E. (2008). Atrial myocardium derives from the posterior region of the second heart field, which acquires left-right identity as Pitx2c is expressed. *Development (Cambridge, England)*, *135*(6), 1157-67. doi: 10.1242/dev.014563.

Garcia, E., Marcos-Gutiérrez, C., Mar Lorente, M. del, Moreno, J. C., & Vidal, M. (1999). RYBP, a new repressor protein that interacts with components of the mammalian Polycomb complex, and with the transcription factor YY1. *The EMBO Journal*, *18*(12), 3404–3418. Nature Publishing Group. doi: 10.1093/emboj/18.12.3404.

Gearhart, M. D., Corcoran, Connie M, Wamstad, Joseph A, & Bardwell, Vivian J. (2006). Polycomb group and SCF ubiquitin ligases are found in a novel BCOR complex that is recruited to BCL6 targets. *Molecular and cellular biology*, *26*(18), 6880-9. doi: 10.1128/MCB.00630-06.

Gil, J., Bernard, D., & Peters, G. (2005). Role of polycomb group proteins in stem cell self-renewal and cancer. *DNA and cell biology*, *24*(2), 117-25. Mary Ann Liebert, Inc. 2 Madison Avenue Larchmont, NY 10538 USA. doi: 10.1089/dna.2005.24.117.

Gong, Y., Wang, Xu, Liu, J., Shi, L., Yin, B., Peng, X., et al. (2005). NSPc1, a mainly nuclear localized protein of novel PcG family members, has a transcription repression activity related to its PKC phosphorylation site at S183. *FEBS letters*, *579*(1), 115-21. doi: 10.1016/j.febslet.2004.11.056.

Gorlin, R J, Marashi, A. H., & Obwegeser, H. L. (1996). Oculo-facio-cardio-dental (OFCD) syndrome. *American journal of medical genetics*, *63*(1), 290-2. doi: 10.1002/(SICI)1096-8628(19960503)63:1<290::AID-AJMG47>3.0.CO;2-G.

Habets, P. E. M. H., Moorman, A. F. M., Clout, D. E. W., Roon, M. a van, Lingbeek, M., Lohuizen, Maarten van, et al. (2002). Cooperative action of Tbx2 and Nkx2.5 inhibits ANF expression in the atrioventricular canal: implications for cardiac chamber formation. *Genes & development*, *16*(10), 1234-46. doi: 10.1101/gad.222902.

Hai, B., Yang, Z., Millar, S. E., Choi, Y. S., Taketo, M. M., Nagy, A., et al. (2010). Wnt/β-catenin signaling regulates postnatal development and regeneration of the salivary gland. *Stem cells and development*, *19*(11), 1793-801. doi: 10.1089/scd.2009.0499.

Hall, B. K., & Miyake, T. (2000). All for one and one for all: condensations and the initiation of skeletal development. *BioEssays : news and reviews in molecular, cellular and developmental biology*, *22*(2), 138-47. doi: 10.1002/(SICI)1521-1878(200002)22:2<138::AID-BIES5>3.0.CO;2-4.

Han, P., Hang, C. T., Yang, J., & Chang, C.-P. (2011). Chromatin Remodeling in Cardiovascular Development and Physiology. *Circulation Research*, *108*(3), 378-396. doi: 10.1161/CIRCRESAHA.110.224287.

Haworth, K. E., Healy, C., Morgan, P., & Sharpe, Paul T. (2004). Regionalisation of early head ectoderm is regulated by endoderm and prepatterns the orofacial epithelium. *Development (Cambridge, England)*, *131*(19), 4797-806. doi: 10.1242/dev.01337.

Helms, J. a, Cordero, D., & Tapadia, M. D. (2005). New insights into craniofacial morphogenesis. *Development (Cambridge, England)*, *132*(5), 851-61. doi: 10.1242/dev.01705.

Hilton, E., Black, G., & Bardwell, V.J. (2007). The BCL-6 corepressor (BCOR) and oculofaciocardiodental syndrome. *Inborn Errors of Development*. Oxford University Press.

Hilton, E. N., Manson, F. D. C., Urquhart, J. E., Johnston, J. J., Slavotinek, A. M., Hedera, P., et al. (2007). Left-sided embryonic expression of the BCL-6 corepressor, BCOR, is required for vertebrate laterality determination. *Human molecular genetics*, *16*(14), 1773-82. doi: 10.1093/hmg/ddm125.

Hilton, Emma, Johnston, J., Whalen, S., Okamoto, N., Hatsukawa, Y., Nishio, J., et al. (2009). BCOR analysis in patients with OFCD and Lenz microphthalmia syndromes, mental retardation with ocular anomalies, and cardiac laterality defects. *European journal of human genetics : EJHG*, *17*(10), 1325-35. doi: 10.1038/ejhg.2009.52.

Hoffman, J. I. E., & Kaplan, S. (2002). The incidence of congenital heart disease. *Journal of the American College of Cardiology*, *39*(12), 1890-900.

Honkanen, R. (2003). A family with Axenfeld–Rieger syndrome and Peters Anomaly caused by a point mutation (Phe112Ser) in the FOXC1 gene. *American Journal of Ophthalmology*, *135*(3), 368-375. doi: 10.1016/S0002-9394(02)02061-5.

Horn, Denise, Chyrek, M., Kleier, S., Lüttgen, S., Bolz, H., Hinkel, G.-K., et al. (2005). Novel mutations in BCOR in three patients with oculo-facio-cardio-dental syndrome, but none in Lenz microphthalmia syndrome. *European journal of human genetics : EJHG*, *13*(5), 563-9. doi: 10.1038/sj.ejhg.5201391.

Hutson, M. R., & Kirby, M. L. (2007). Model systems for the study of heart development and disease. Cardiac neural crest and conotruncal malformations. *Seminars in cell & developmental biology*, *18*(1), 101-10. doi: 10.1016/j.semcdb.2006.12.004.

Huynh, K. D., & Bardwell, V.J. (1998). The BCL-6 POZ domain and other POZ domains interact with the co-repressors N-CoR and SMRT. *Oncogene*, *17*(19), 2473.

Huynh, K. D., Fischle, Wolfgang, Verdin, E., & Bardwell, V.J. (2000). BCoR, a novel corepressor involved in BCL-6 repression. *Genes & development*, *14*(14), 1810. Cold Spring Harbor Lab. doi: 10.1101/gad.14.14.1810.

Ieda, M., Fu, J.-D., Delgado-Olguin, P., Vedantham, V., Hayashi, Y., Bruneau, B. G., et al. (2010). Direct Reprogramming of Fibroblasts into Functional Cardiomyocytes by Defined Factors. *Cell*, *142*(3), 375-386. doi: 10.1016/j.cell.2010.07.002.

Jacobs, J. J. L., & Lohuizen, Maarten van. (2002). Polycomb repression: from cellular memory to cellular proliferation and cancer. *Biochimica et biophysica acta*, *1602*(2), 151-61.

Jason, L. J. M., Finn, R. M., Lindsey, G., & Ausió, Juan. (2005). Histone H2A ubiquitination does not preclude histone H1 binding, but it facilitates its association with the nucleosome. *The Journal of biological chemistry*, *280*(6), 4975-82. doi: 10.1074/jbc.M410203200.

Jegalian, B. G., Miller, R. W., Wright, C. V., Blum, M., & De Robertis, E. M. (1992). A Hox 3.3-lacZ transgene expressed in developing limbs. *Mechanisms of development*, *39*(3), 171-80.

Jin, B., Tao, Q., Peng, J., Soo, H. M., Wu, W., Ying, J., et al. (2008). DNA methyltransferase 3B (DNMT3B) mutations in ICF syndrome lead to altered epigenetic modifications and aberrant expression of genes regulating development, neurogenesis and immune function. *Human molecular genetics*, *17*(5), 690-709. doi: 10.1093/hmg/ddm341.

Jin, J., Cardozo, T., Lovering, R. C., Elledge, Stephen J, Pagano, M., & Harper, J Wade. (2004). Systematic analysis and nomenclature of mammalian F-box proteins. *Genes & development*, *18*(21), 2573-80. doi: 10.1101/gad.1255304.

Joh, T., Kagami, Y., Yamamoto, K., Segawa, T., Takizawa, J., Takahashi, T., et al. (1996). Identification of MLL and chimeric MLL gene products involved in 11q23 translocation and possible mechanisms of leukemogenesis by MLL truncation. *Oncogene*, *13*(9), 1945-53.

Jones, P. A., & Baylin, S. B. (2007). The epigenomics of cancer. *Cell*, *128*(4), 683-92. doi: 10.1016/j.cell.2007.01.029.

Jorgensen, H. F., Ben-Porath, I., & Bird, A. P. (2004). Mbd1 is recruited to both methylated and nonmethylated CpGs via distinct DNA binding domains. *Molecular and cellular biology*, *24*(8), 3387. Am Soc Microbiol. doi: 10.1128/MCB.24.8.3387.

Kerppola, T. (2009). POLYCOMB GROUP COMPLEXES – MANY COMBINATIONS, MANY FUNCTIONS. *Trends in cell biology*, *19*(12), 692–704. Elsevier. doi: 10.1016/j.tcb.2009.10.001.POLYCOMB.

Kim, T., & Buratowski, S. (2007). Two Saccharomyces cerevisiae JmjC domain proteins demethylate histone H3 Lys36 in transcribed regions to promote elongation. *The Journal of biological chemistry*, *282*(29), 20827-35. doi: 10.1074/jbc.M703034200.

Kisanuki, Y. Y., Hammer, R. E., Miyazaki, J., Williams, S. C., Richardson, J. a, & Yanagisawa, M. (2001). Tie2-Cre transgenic mice: a new model for endothelial cell-lineage analysis in vivo. *Developmental biology*, *230*(2), 230-42. doi: 10.1006/dbio.2000.0106.

Klymenko, T., & Müller, J. (2004). The histone methyltransferases Trithorax and Ash1 prevent transcriptional silencing by Polycomb group proteins. *EMBO reports*, *5*(4), 373-7. doi: 10.1038/sj.embor.7400111.

Kraus, M., Alimzhanov, M. B., Rajewsky, N., Rajewsky, K., East, W. S., & York, N. (2004). Survival of resting mature B lymphocytes depends on BCR signaling via the Igalpha/beta heterodimer. *Cell*, *117*(6), 787-800.

Lagarou, A., Mohd-Sarip, A., Moshkin, Y. M., Chalkley, G. E., Bezstarosti, K., Demmers, J. a a, et al. (2008). dKDM2 couples histone H2A ubiquitylation to histone H3 demethylation during Polycomb group silencing. *Genes & development*, *22*(20), 2799-810. doi: 10.1101/gad.484208.

Lang, D., Lu, M. M., Huang, L., Engleka, K. a, Zhang, M., Chu, E. Y., et al. (2005). Pax3 functions at a nodal point in melanocyte stem cell differentiation. *Nature*, *433*(7028), 884-7. doi: 10.1038/nature03292.

Lange, M., Kaynak, B., Forster, U. B., Tönjes, M., Fischer, J. J., Grimm, C., et al. (2008). Regulation of muscle development by DPF3, a novel histone acetylation and methylation reader of the BAF chromatin remodeling complex. *Genes & development*, *22*(17), 2370-84. doi: 10.1101/gad.471408.

Law, D. J., Du, M., Law, G. L., & Merchant, J. L. (1999). ZBP-99 defines a conserved family of transcription factors and regulates ornithine decarboxylase gene expression. *Biochemical and biophysical research communications*, *262*(1), 113-20. doi: 10.1006/bbrc.1999.1180.

Lawson, K. a, Meneses, J. J., & Pedersen, R. a. (1991). Clonal analysis of epiblast fate during germ layer formation in the mouse embryo. *Development (Cambridge, England)*, *113*(3), 891-911.

Le Douarin, Nicole M, Creuzet, S., Couly, G., & Dupin, E. (2004). Neural crest cell plasticity and its limits. *Development (Cambridge, England)*, *131*(19), 4637-50. doi: 10.1242/dev.01350.

Lee, T. I., Jenner, R. G., Boyer, L. a, Guenther, M. G., Levine, Stuart S, Kumar, R. M., et al. (2006). Control of developmental regulators by Polycomb in human embryonic stem cells. *Cell*, *125*(2), 301-13. doi: 10.1016/j.cell.2006.02.043.

Lessard, J., Schumacher, a, Thorsteinsdottir, U., Lohuizen, M van, Magnuson, T., & Sauvageau, G. (1999). Functional antagonism of the Polycomb-Group genes eed and Bmi1 in hemopoietic cell proliferation. *Genes & development*, *13*(20), 2691-703.

Levine, S.S., Weiss, A., Erdjument-Bromage, H., Shao, Z., Tempst, Paul, & Kingston, R.E. (2002). The core of the polycomb repressive complex is compositionally and functionally conserved in flies and humans. *Molecular and cellular biology*, *22*(17), 6070. Am Soc Microbiol. doi: 10.1128/MCB.22.17.6070.

Levine, Stuart S, King, I. F. G., & Kingston, Robert E. (2004). Division of labor in polycomb group repression. *Trends in biochemical sciences*, *29*(9), 478-85. doi: 10.1016/j.tibs.2004.07.007.

Lewis, E. B. (1978). A gene complex controlling segmentation in Drosophila. *Nature*, *276*(5688), 565–570.

Lin, Q., Schwarz, J., Bucana, C., & Olson, E. (1997). Control of Mouse Cardiac Morphogenesis and Myogenesis by Transcription Factor MEF2C. *Science*, *276*(5317), 1404-1407. doi: 10.1126/science.276.5317.1404.

Lisowsky, T. (1999). Identification of human GC-box-binding zinc finger protein, a new Krüppel-like zinc finger protein, by the yeast one-hybrid screening with a GC-rich target sequence. *FEBS Letters*, *453*(3), 369-374. doi: 10.1016/S0014-5793(99)00754-1.

Lo Coco, F., Ye, Bh, Lista, F., Corradini, Paolo, Offit, K., Knowles, D., et al. (1994). Rearrangements of the BCL6 gene in diffuse large cell non-Hodgkin's lymphoma. *Blood*, *83*(7), 1757. Am Soc Hematology.

Logan, M., & Tabin, C. J. (1999). Role of Pitx1 Upstream of Tbx4 in Specification of Hindlimb Identity. *Science*, *283*(5408), 1736-1739. doi: 10.1126/science.283.5408.1736.

Lombaert, I., Knox, S., & Hoffman, M. (2011). Salivary gland progenitor cell biology provides a rationale for therapeutic salivary gland regeneration. *Oral diseases*, (November 2010). doi: 10.1111/j.1601-0825.2010.01783.x.

Lugt, N. M. van der, Alkema, M., Berns, a, & Deschamps, J. (1996). The Polycomb-group homolog Bmi-1 is a regulator of murine Hox gene expression. *Mechanisms of development*, *58*(1-2), 153-64.

Lyons, I., Parsons, L. M., Hartley, L., Li, R., Andrews, J. E., Robb, L., et al. (1995). Myogenic and morphogenetic defects in the heart tubes of murine embryos lacking the homeo box gene Nkx2-5. *Genes & Development*, *9*(13), 1654-1666. doi: 10.1101/gad.9.13.1654.

Ma, Qing, Zhou, B., & Pu, W. T. (2008). Reassessment of Isl1 and Nkx2-5 cardiac fate maps using a Gata4-based reporter of Cre activity. *Developmental biology*, *323*(1), 98-104. Elsevier Inc. doi: 10.1016/j.ydbio.2008.08.013.

Mar Lorente, M. del, Marcos-Gutiérrez, C., Pérez, C., Schoorlemmer, J., Ramírez, a, Magin, T., et al. (2000). Loss- and gain-of-function mutations show a polycomb group function for Ring1A in mice. *Development (Cambridge, England)*, *127*(23), 5093-100.

Mears, a J., Jordan, T., Mirzayans, F., Dubois, S., Kume, T., Parlee, M., et al. (1998). Mutations of the forkhead/winged-helix gene, FKHL7, in patients with Axenfeld-Rieger anomaly. *American journal of human genetics*, *63*(5), 1316-28. doi: 10.1086/302109.

Miletich, I., & Sharpe, Paul T. (2004). Neural crest contribution to mammalian tooth formation. *Birth defects research. Part C, Embryo today : reviews*, *72*(2), 200-12. doi: 10.1002/bdrc.20012.

Miller, S. a, Huang, A. C., Miazgowicz, M. M., Brassil, M. M., & Weinmann, A. S. (2008). Coordinated but physically separable interaction with H3K27-demethylase and H3K4-methyltransferase activities are required for T-box protein-mediated activation of developmental gene expression. *Genes & development*, *22*(21), 2980-93. doi: 10.1101/gad.1689708.

Miller, S. a, Mohn, S. E., & Weinmann, A. S. (2010). Jmjd3 and UTX Play a Demethylase-Independent Role in Chromatin Remodeling to Regulate T-Box Family Member-Dependent Gene Expression. *Molecular cell*, *40*(4), 594-605. doi: 10.1016/j.molcel.2010.10.028.

Miller, S. a, & Weinmann, A. S. (2009). An essential interaction between T-box proteins and histone-modifying enzymes. *Epigenetics : official journal of the DNA Methylation Society*, *4*(2), 85-8.

Mills, A. a. (2010). Throwing the cancer switch: reciprocal roles of polycomb and trithorax proteins. *Nature reviews. Cancer*, *10*(10), 669-82. doi: 10.1038/nrc2931.

Min, J., Zhang, Y., & Xu, R. (2003). Structural basis for specific binding of Polycomb chromodomain to histone H3 methylated at Lys 27. *Genes & development*, *17*(15), 1823-8. doi: 10.1101/gad.269603.

Mohan, M., Lin, C., Guest, E., & Shilatifard, A. (2010). Licensed to elongate: a molecular mechanism for MLL-based leukaemogenesis. *Nature reviews. Cancer*, *10*(10), 721-8. doi: 10.1038/nrc2915.

Mootoosamy, R. C., & Dietrich, S. (2002). Distinct regulatory cascades for head and trunk myogenesis. *Development (Cambridge, England)*, *129*(3), 573-83.

Moretti, A., Caron, L., Nakano, A., Lam, J. T., Bernshausen, A., Chen, Yinhong, et al. (2006). Multipotent embryonic isl1+ progenitor cells lead to cardiac, smooth muscle, and endothelial cell diversification. *Cell*, *127*(6), 1151-65. doi: 10.1016/j.cell.2006.10.029.

Moses, K. A., DeMayo, F., Braun, R. M., Reecy, J. L., & Schwartz, R.J. (2001). Embryonic expression of an Nkx2-5/Cre gene using ROSA26 reporter mice. *genesis*, *31*(4), 176–180. Wiley Online Library. doi: 10.1002/gene.10022.

Mueller, D., Bach, C., Zeisig, D., Garcia-Cuellar, M.-P., Monroe, S., Sreekumar, A., et al. (2007). A role for the MLL fusion partner ENL in transcriptional elongation and chromatin modification. *Blood*, *110*(13), 4445-54. doi: 10.1182/blood-2007-05-090514.

Muratani, M., & Tansey, W. P. (2003). How the ubiquitin-proteasome system controls transcription. *Nature reviews. Molecular cell biology*, *4*(3), 192-201. doi: 10.1038/nrm1049.

Männer, J., Pérez-Pomares, J. M., Macías, D., & Muñoz-Chápuli, R. (2001). The origin, formation and developmental significance of the epicardium: a review. *Cells, tissues, organs*, *169*(2), 89-103.

Müller, J., Hart, C. M., Francis, N. J., Vargas, M. L., Sengupta, A., Wild, B., et al. (2002). Histone methyltransferase activity of a Drosophila Polycomb group repressor complex. *Cell*, *111*(2), 197-208.

Napoles, M. de, Mermoud, J. E., Wakao, R., Tang, Y. A., Endoh, Mitusuhiro, Appanah, R., et al. (2004). Polycomb group proteins Ring1A/B link ubiquitylation of histone H2A to heritable gene silencing and X inactivation. *Developmental cell*, *7*(5), 663-76. doi: 10.1016/j.devcel.2004.10.005.

Ng, D., Thakker, N., Corcoran, Connie M, Donnai, D., Perveen, R., Schneider, A., et al. (2004). Oculofaciocardiodental and Lenz microphthalmia syndromes result from distinct classes of mutations in BCOR. *Nature genetics*, *36*(4), 411-6. doi: 10.1038/ng1321.

Ng, R. K., & Gurdon, J. B. (2008). Epigenetic inheritance of cell differentiation status ND ES RIB ND ES SC RIB Inheritance of Epigenetic Memory. *Cell Cycle*, (May), 1173-1177.

Nimura, K., Ura, K., Shiratori, H., Ikawa, M., Okabe, M., Schwartz, Robert J, et al. (2009). A histone H3 lysine 36 trimethyltransferase links Nkx2-5 to Wolf-Hirschhorn syndrome. *Nature*, *460*(7252), 287-91. doi: 10.1038/nature08086.

Niu, H., Cattoretti, G, & Dalla-Favera, R. (2003). BCL6 controls the expression of the B7-1/CD80 costimulatory receptor in germinal center B cells. *The Journal of experimental medicine*, *198*(2), 211-21. doi: 10.1084/jem.20021395.

Nunes, M., Blanc, I., Maes, J., Fellous, M., Robert, B., & McElreavey, K. (2001). NSPc1, a novel mammalian Polycomb gene, is expressed in neural crest-derived structures of the peripheral nervous system. *Mechanisms of development*, *102*(1-2), 219-22.

Ogawa, H., Ishiguro, K.-I., Gaubatz, S., Livingston, D. M., & Nakatani, Y. (2002). A complex with chromatin modifiers that occupies E2F- and Myc-responsive genes in G0 cells. *Science (New York, N.Y.)*, *296*(5570), 1132-6. doi: 10.1126/science.1069861.

others. (2004). Nkx2-5 mutation causes anatomic hypoplasia of the cardiac conduction system. *Journal of Clinical Investigation*, *113*(8), 1130–1137. Am Soc Clin Investig. doi: 10.1172/JCI200419846.1130.

others. (2007). An Nkx2-5/Bmp2/Smad1 negative feedback loop controls second heart field progenitor specification and proliferation. *Cell*, *128*(5), 947–959. Elsevier.

Ozcelik, C., Bit-Avragim, N., Panek, A., Gaio, U., Geier, C., Lange, P. E., et al. (2006). Mutations in the EGF-CFC gene cryptic are an infrequent cause of congenital heart disease. *Pediatric cardiology*, *27*(6), 695-8. doi: 10.1007/s00246-006-1082-0.

O'Carroll, N. A. L., Erhardt, S., Pagani, M., & Barton, S. C. (2001). The Polycomb-Group Gene Ezh2 Is Required for Early Mouse Development. *Society*, *21*(13), 4330-4336. doi: 10.1128/MCB.21.13.4330.

Pagan, J. K., Arnold, J., Hanchard, K. J., Kumar, R., Bruno, T., Jones, M. J. K., et al. (2007). A novel corepressor, BCoR-L1, represses transcription through an interaction with CtBP. *The Journal of biological chemistry*, *282*(20), 15248-57. doi: 10.1074/jbc.M700246200.

Park, I.-kyung, Qian, D., Kiel, M., Becker, M. W., Pihalja, M., Weissman, I. L., et al. (2003). Bmi-1 is required for maintenance of adult self-renewing haematopoietic stem cells. *Nature*, *423*(6937), 302-5. doi: 10.1038/nature01587.

Pashmforoush, M., Lu, J. T., Chen, H., Amand, T. S., Kondo, R., Pradervand, S., et al. (2004). Nkx2-5 pathways and congenital heart disease; loss of ventricular myocyte lineage specification leads to progressive cardiomyopathy and complete heart block. *Cell*, *117*(3), 373-86.

Pasini, D., Bracken, A. P., Jensen, M. R., Lazzerini Denchi, E., & Helin, K. (2004). Suz12 is essential for mouse development and for EZH2 histone methyltransferase activity. *The EMBO journal*, *23*(20), 4061-71. doi: 10.1038/sj.emboj.7600402.

Pasqualucci, L., Migliazza, A., Basso, K., Houldsworth, J., Chaganti, Rsk, & Dalla-Favera, R. (2003). Mutations of the BCL6 proto-oncogene disrupt its negative autoregulation in diffuse large B-cell lymphoma. *Blood*, *101*(8), 2914. Am Soc Hematology. doi: 10.1182/blood-2002-11-3387.Supported.

Patton, E. (1998). Combinatorial control in ubiquitin-dependent proteolysis: don't Skp the F-box hypothesis. *Trends in Genetics*, *14*(6), 236-243. doi: 10.1016/S0168-9525(98)01473-5.

Phan, R. T., & Dalla-favera, R. (2004). The BCL6 proto-oncogene suppresses p53 expression in germinal-centre B cells. *Nature*, *432*(December), 635-639. doi: 10.1038/nature03148.

Raaphorst, F. M. (2005). Deregulated expression of Polycomb-group oncogenes in human malignant lymphomas and epithelial tumors. *Human molecular genetics*, *14 Spec No*(1), R93-R100. doi: 10.1093/hmg/ddi111.

Rajasekhar, V. K., & Begemann, M. (2007). Concise review: roles of polycomb group proteins in development and disease: a stem cell perspective. *Stem cells (Dayton, Ohio)*, *25*(10), 2498-510. doi: 10.1634/stemcells.2006-0608.

Ramsdell, A. F. (2005). Left-right asymmetry and congenital cardiac defects: getting to the heart of the matter in vertebrate left-right axis determination. *Developmental biology*, *288*(1), 1-20. doi: 10.1016/j.ydbio.2005.07.038.

Ramsdell, A. F., Bernanke, J. M., & Trusk, T. C. (2006). Left-right lineage analysis of the embryonic Xenopus heart reveals a novel framework linking congenital cardiac defects and laterality disease. *Development (Cambridge, England)*, *133*(7), 1399-410. doi: 10.1242/dev.02292.

Ringrose, L., & Paro, R. (2007). Polycomb/Trithorax response elements and epigenetic memory of cell identity. *Development (Cambridge, England)*, *134*(2), 223-32. doi: 10.1242/dev.02723.

Rodriguez-Esteban, C., Tsukui, T., Yonei, S., Magallon, J., Tamura, K., & Belmonte, J. C. I. (1999). The T-box genes Tbx4 and Tbx5 regulate limb outgrowth and identity. *Nature*, *398*(6730), 814–818. Nature Publishing Group.

Roguev, a, Schaft, D., Shevchenko, a, Pijnappel, W. W., Wilm, M., Aasland, R., et al. (2001). The Saccharomyces cerevisiae Set1 complex includes an Ash2 homologue and methylates histone 3 lysine 4. *The EMBO journal*, *20*(24), 7137-48. doi: 10.1093/emboj/20.24.7137.

Rouleau, M., Saxena, V., Rodrigue, A., Paquet, E. R., Gagnon, A., Hendzel, M. J., et al. (2011). A key role for poly(ADP-ribose) polymerase 3 in ectodermal specification and neural crest development. *PloS one*, *6*(1), e15834. doi: 10.1371/journal.pone.0015834.

Rubnitz, J. E., Morrissey, J., Savage, P. a, & Cleary, M. L. (1994). ENL, the gene fused with HRX in t(11;19) leukemias, encodes a nuclear protein with transcriptional activation potential in lymphoid and myeloid cells. *Blood*, *84*(6), 1747-52.

Sakano, D., Kato, A., Parikh, N., McKnight, K., Terry, D., Stefanovic, B., et al. (2010). BCL6 canalizes Notch-dependent transcription, excluding Mastermind-like1 from selected target genes during left-right patterning. *Developmental cell*, *18*(3), 450-62. doi: 10.1016/j.devcel.2009.12.023.

Sauvageau, M., & Sauvageau, G. (2010). Polycomb Group Proteins: Multi-Faceted Regulators of Somatic Stem Cells and Cancer. *Cell stem cell*, *7*(3), 299-313. doi: 10.1016/j.stem.2010.08.002.

Savard, P., Gates, P. B., & Brockes, J. P. (1988). Position dependent expression of a homeobox gene transcript in relation to amphibian limb regeneration. *The EMBO Journal*, *7*(13), 4275. Nature Publishing Group.

Sawarkar, R., & Paro, R. (2010). Interpretation of developmental signaling at chromatin: the polycomb perspective. *Developmental cell*, *19*(5), 651-61. doi: 10.1016/j.devcel.2010.10.012.

Schuettengruber, B., Chourrout, D., Vervoort, M., Leblanc, B., & Cavalli, G. (2007). Genome regulation by polycomb and trithorax proteins. *Cell*, *128*(4), 735-45. doi: 10.1016/j.cell.2007.02.009.

Schulze, B. R., Horn, D, Kobelt, A., Tariverdian, G., & Stellzig, A. (1999). Rare dental abnormalities seen in oculo-facio-cardio-dental (OFCD) syndrome: three new cases and review of nine patients. *American journal of medical genetics*, *82*(5), 429-35.

Seyfert, V. L., Allman, D., He, Y., & Staudt, L M. (1996). Transcriptional repression by the proto-oncogene BCL-6. *Oncogene*, *12*(11), 2331-42.

Shaffer, A L, Yu, X, He, Y., Boldrick, J., Chan, E. P., & Staudt, L M. (2000). BCL-6 represses genes that function in lymphocyte differentiation, inflammation, and cell cycle control. *Immunity*, *13*(2), 199-212.

Sheth, R., Bastida, M. F., & Ros, M. (2007). Hoxd and Gli3 interactions modulate digit number in the amniote limb. *Developmental biology*, *310*(2), 430-41. doi: 10.1016/j.ydbio.2007.07.023.

Shi, X., Kachirskaia, I., Walter, K. L., Kuo, J.-H. a, Lake, A., Davrazou, F., et al. (2007). Proteome-wide analysis in Saccharomyces cerevisiae identifies several PHD fingers as novel direct and selective binding modules of histone H3 methylated at either lysine 4 or lysine 36. *The Journal of biological chemistry*, *282*(4), 2450-5. doi: 10.1074/jbc.C600286200.

Shirai, Manabu, Osugi, T., Koga, H., Kaji, Y., Takimoto, E., Komuro, I., et al. (2002). The Polycomb-group gene Rae28 sustains Nkx2 . 5 / Csx expression and is essential for cardiac morphogenesis. *In Situ*, *110*(2), 177-184. doi: 10.1172/JCI200214839.Introduction.

Skowyra, D., Craig, K. L., Tyers, M, Elledge, S J, & Harper, J W. (1997). F-box proteins are receptors that recruit phosphorylated substrates to the SCF ubiquitin-ligase complex. *Cell*, *91*(2), 209-19.

Slepak, T. I., Webster, K. a, Zang, J., Prentice, H., O'Dowd, a, Hicks, M. N., et al. (2001). Control of cardiac-specific transcription by p300 through myocyte enhancer factor-2D. *The Journal of biological chemistry*, *276*(10), 7575-85. doi: 10.1074/jbc.M004625200.

Smith, E., & Shilatifard, A. (2010). The Chromatin Signaling Pathway: Diverse Mechanisms of Recruitment of Histone-Modifying Enzymes and Varied Biological Outcomes. *Molecular Cell*, *40*(5), 689-701. doi: 10.1016/j.molcel.2010.11.031.

Sparmann, A., & Lohuizen, Maarten van. (2006). Polycomb silencers control cell fate, development and cancer. *Nature reviews. Cancer*, *6*(11), 846-56. Nature Publishing Group. doi: 10.1038/nrc1991.

Srinivasan, R. S., Erkenez, A. C. de, & Hemenway, C. S. (2003). The mixed lineage leukemia fusion partner AF9 binds specific isoforms of the BCL-6 corepressor. *Oncogene*, *22*(22), 3395–3406. Nature Publishing Group. doi: 10.1038/sj.onc.1206361.

Srivastava, D. (2006). Making or breaking the heart: from lineage determination to morphogenesis. *Cell*, *126*(6), 1037-48. doi: 10.1016/j.cell.2006.09.003.

Stanley, E. G., Biben, C., Elefanty, A., & Barnett, L. (2002). Efficient cre-mediated deletion in cardiac progenitor cells con-ferred by a 3'UTR-ires-Cre allele of the homeobox gene Nkx2-5. *Int. J. Dev. Biol*, *46*(2002), 431–439.

Stock, J. K., Giadrossi, S., Casanova, M., Brookes, E., Vidal, Miguel, Koseki, Haruhiko, et al. (2007). Ring1-mediated ubiquitination of H2A restrains poised RNA polymerase II at bivalent genes in mouse ES cells. *Nature cell biology*, *9*(12), 1428-35. doi: 10.1038/ncb1663.

Su, I.-H., Basavaraj, A., Krutchinsky, A. N., Hobert, O., Ullrich, A., Chait, B. T., et al. (2003). Ezh2 controls B cell development through histone H3 methylation and Igh rearrangement. *Nature immunology*, *4*(2), 124-31. doi: 10.1038/ni876.

Sun, Y., Liang, X., Najafi, N., Cass, M., Lin, L., Cai, Cheng-Leng, et al. (2007). Islet 1 is expressed in distinct cardiovascular lineages, including pacemaker and coronary vascular cells. *Developmental biology*, *304*(1), 286-96. doi: 10.1016/j.ydbio.2006.12.048.

Surface, L. E., Thornton, S. R., & Boyer, L. a. (2010). Polycomb Group Proteins Set the Stage for Early Lineage Commitment. *Cell stem cell*, *7*(3), 288-298. doi: 10.1016/j.stem.2010.08.004.

Suzuki, Takeshi, Minehata, K.-ichi, Akagi, K., Jenkins, N. a, & Copeland, N. G. (2006). Tumor suppressor gene identification using retroviral insertional mutagenesis in Blm-deficient mice. *The EMBO journal*, *25*(14), 3422-31. doi: 10.1038/sj.emboj.7601215.

Suzuki, Takeshi, Shen, H., Akagi, K., Morse, H. C., Malley, J. D., Naiman, D. Q., et al. (2002). New genes involved in cancer identified by retroviral tagging. *Nature Genetics*, *32*(1), 166-174.

Sánchez, C., Sánchez, I., Demmers, J. a a, Rodriguez, P., Strouboulis, J., & Vidal, Miguel. (2007a). Proteomics analysis of Ring1B/Rnf2 interactors identifies a novel complex with the Fbxl10/Jhdm1B histone demethylase and the Bcl6 interacting corepressor. *Molecular & cellular proteomics : MCP*, *6*(5), 820-34. doi: 10.1074/mcp.M600275-MCP200.

Sánchez, C., Sánchez, I., Demmers, J. a a, Rodriguez, P., Strouboulis, J., & Vidal, Miguel. (2007b). Proteomics analysis of Ring1B/Rnf2 interactors identifies a novel complex with the Fbxl10/Jhdm1B histone demethylase and the Bcl6 interacting corepressor. *Molecular & cellular proteomics : MCP*, *6*(5), 820-34. doi: 10.1074/mcp.M600275-MCP200.

Takeuchi, J. K., Koshiba-Takeuchi, K., Matsumoto, K., Vogel-Hopker, A., Naitoh-Matsuo, M., Ogura, K., et al. (1999). Tbx5 and Tbx4 genes determine the wing/leg identity of limb buds. *Nature*, *398*(6730), 810–813. [London: Macmillan Journals], 1869-.

Takihara, Y, Tomotsune, D., Shirai, M, Katoh-Fukui, Y., Nishii, K., Motaleb, M. a, et al. (1997). Targeted disruption of the mouse homologue of the Drosophila polyhomeotic gene leads to altered anteroposterior patterning and neural crest defects. *Development (Cambridge, England)*, *124*(19), 3673-82.

Takihara, Y, Tomotsune, D., Shirai, M, Katoh-Fukui, Y., Nishii, K., Motaleb, M. a, et al. (1997). Targeted disruption of the mouse homologue of the Drosophila polyhomeotic gene leads to altered anteroposterior patterning and neural crest defects. *Development (Cambridge, England)*, *124*(19), 3673-82.

Takihara, Yoshihiro. (2008). Role of Polycomb-group genes in sustaining activities of normal and malignant stem cells. *International journal of hematology*, *87*(1), 25-34. doi: 10.1007/s12185-007-0006-y.

Tam, P. P., Parameswaran, M., Kinder, S. J., & Weinberger, R. P. (1997). The allocation of epiblast cells to the embryonic heart and other mesodermal lineages: the role of ingression and tissue movement during gastrulation. *Development (Cambridge, England)*, *124*(9), 1631-42.

Tanaka, M, Chen, Z., Bartunkova, S., Yamasaki, N., & Izumo, S. (1999). The cardiac homeobox gene Csx/Nkx2.5 lies genetically upstream of multiple genes essential for heart development. *Development (Cambridge, England)*, *126*(6), 1269-80.

Tanaka, Mikiko, Hale, L. a, Amores, A., Yan, Y.-L., Cresko, W. a, Suzuki, Tohru, et al. (2005). Developmental genetic basis for the evolution of pelvic fin loss in the pufferfish Takifugu rubripes. *Developmental biology*, *281*(2), 227-39. doi: 10.1016/j.ydbio.2005.02.016.

Tessari, A., Pietrobon, M., Notte, A., Cifelli, G., Gage, P. J., Schneider, M. D., et al. (2008). Myocardial Pitx2 differentially regulates the left atrial identity and ventricular asymmetric remodeling programs. *Circulation research*, *102*(7), 813-22. doi: 10.1161/CIRCRESAHA.107.163188.

Trinkle-Mulcahy, L., Boulon, S., Lam, Y. W., Urcia, R., Boisvert, F.-M., Vandermoere, F., et al. (2008). Identifying specific protein interaction partners using quantitative mass spectrometry and bead proteomes. *The Journal of Cell Biology*, *183*(2), 223-239. doi: 10.1083/jcb.200805092.

Trokovic, N., Trokovic, R., Mai, P., & Partanen, J. (2003). Fgfr1 regulates patterning of the pharyngeal region. *Genes & development*, *17*(1), 141-53. doi: 10.1101/gad.250703.

Trokovic, N., Trokovic, R., & Partanen, J. (2005). Fibroblast growth factor signalling and regional specification of the pharyngeal ectoderm. *The International journal of developmental biology*, *49*(7), 797-805. doi: 10.1387/ijdb.051976nt.

Tsukada, Y.-ichi, Fang, J., Erdjument-Bromage, Hediye, Warren, M. E., Borchers, C. H., Tempst, Paul, et al. (2006). Histone demethylation by a family of JmjC domain-containing proteins. *Nature*, *439*(7078), 811-6. doi: 10.1038/nature04433.

Tucker, A. S. (2007). Salivary gland development. *Seminars in cell & developmental biology*, *18*(2), 237-44. doi: 10.1016/j.semcdb.2007.01.006.

Tucker, a S., & Sharpe, P.T. (1999). Molecular Genetics of Tooth Morphogenesis and Patterning: The Right Shape in the Right Place. *Journal of Dental Research*, *78*(4), 826-834. doi: 10.1177/00220345990780040201.

Tunyaplin, C., Shaffer, A. L., Angelin-Duclos, C. D., Yu, Xin, Staudt, L.M., & Calame, K. L. (2004). Direct Repression of prdm1 by Bcl-6 Inhibits Plasmacytic Differentiation. *Immunogenetics*, *173*, 1158-1165. doi: 10.1007/s00251-010-0505-5.

Vandamme, J., Volkel, P., Rosnoblet, C., Le Faou, P., & Angrand, P.-O. (2011). Interaction proteomics analysis of Polycomb proteins defines distinct PRC1 complexes in mammalian cells. *Molecular & cellular proteomics : MCP*. doi: 10.1074/mcp.M110.002642.

Vincent, S. D., & Buckingham, M. E. (2010). *Organogenesis in Development* (Vol. 90). Elsevier. doi: 10.1016/S0070-2153(10)90001-X.

Voncken, J. W., Roelen, B. a J., Roefs, M., Vries, S. de, Verhoeven, E., Marino, S., et al. (2003). Rnf2 (Ring1b) deficiency causes gastrulation arrest and cell cycle inhibition. *Proceedings of the National Academy of Sciences of the United States of America*, *100*(5), 2468-73. doi: 10.1073/pnas.0434312100.

Voo, K. S., Carlone, D. L., Jacobsen, B. M., Flodin, a, & Skalnik, D. G. (2000). Cloning of a mammalian transcriptional activator that binds unmethylated CpG motifs and shares a CXXC domain with DNA methyltransferase, human trithorax, and methyl-CpG binding domain protein 1. *Molecular and cellular biology*, *20*(6), 2108-21.

Waldo, K. L., Hutson, M. R., Stadt, H. a, Zdanowicz, M., Zdanowicz, J., & Kirby, M. L. (2005). Cardiac neural crest is necessary for normal addition of the myocardium to the arterial pole from the secondary heart field. *Developmental biology*, *281*(1), 66-77. doi: 10.1016/j.ydbio.2005.02.011.

Wamstad, Joseph A, & Bardwell, Vivian J. (2007). Characterization of Bcor expression in mouse development. *Gene expression patterns : GEP*, *7*(5), 550-7. doi: 10.1016/j.modgep.2007.01.006.

Wamstad, Joseph Alan, Corcoran, Connie Marie, Keating, A. M., & Bardwell, Vivian J. (2008). Role of the transcriptional corepressor Bcor in embryonic stem cell differentiation and early embryonic development. *PloS one*, *3*(7), e2814. doi: 10.1371/journal.pone.0002814.

Wang, H., Wang, L., Erdjument-Bromage, H., Vidal, M., Tempst, P., Jones, R., et al. (2004). Role of histone H2A ubiquitination in Polycomb silencing. *Nature*, *431*(7010), 873-8. doi: 10.1038/nature02926.

Wang, Hengbin, Wang, Liangjun, Erdjument-Bromage, Hediye, Vidal, Miguel, Tempst, Paul, Jones, R. S., et al. (2004). Role of histone H2A ubiquitination in Polycomb silencing. *Nature*, *431*(7010), 873-8. doi: 10.1038/nature02985.

Wang, X., Li, Z., Naganuma, A., & Ye, B. (2002). Negative autoregulation of BCL-6 is bypassed by genetic alterations in diffuse large B cell lymphomas. *Proceedings of the National Academy of Sciences of the United States of America*, *99*(23), 15018-23. doi: 10.1073/pnas.232581199.

Wang, Y, Kobori, J. a, & Hood, L. (1993). The ht beta gene encodes a novel CACCC box-binding protein that regulates T-cell receptor gene expression. *Molecular and cellular biology*, *13*(9), 5691-701.

Willems, A. R., Schwab, M., & Tyers, Mike. (2004). A hitchhiker's guide to the cullin ubiquitin ligases: SCF and its kin. *Biochimica et biophysica acta*, *1695*(1-3), 133-70. doi: 10.1016/j.bbamcr.2004.09.027.

Winnier, G. E., Kume, T., Deng, K., Rogers, R., Bundy, J., Raines, C., et al. (1999). Roles for the winged helix transcription factors MF1 and MFH1 in cardiovascular development revealed by nonallelic noncomplementation of null alleles. *Developmental biology*, *213*(2), 418-31. doi: 10.1006/dbio.1999.9382.

Wysocka, J., Swigut, T., Xiao, H., Milne, T. A., Kwon, S. Y., Landry, J., et al. (2006). A PHD finger of NURF couples histone H3 lysine 4 trimethylation with chromatin remodelling. *Nature*, *442*(7098), 86-90. Nature Publishing Group. doi: 10.1038/nature04815.

Yamamoto, Y., Tsuzuki, S., Tsuzuki, M., Handa, K., Inaguma, Y., & Emi, N. (2010). BCOR as a novel fusion partner of retinoic acid receptor alpha in a t(X;17)(p11;q12) variant of acute promyelocytic leukemia. *Blood*, 4274-4283. doi: 10.1182/blood-2010-01-264432.

Yang, L., Cai, Chen-Leng, Lin, L., Qyang, Y., Chung, C., Monteiro, R. M., et al. (2006). Isl1Cre reveals a common Bmp pathway in heart and limb development. *Development (Cambridge, England)*, *133*(8), 1575-85. doi: 10.1242/dev.02322.

Yashiro, K., Shiratori, H., & Hamada, H. (2007). Haemodynamics determined by a genetic programme govern asymmetric development of the aortic arch. *Nature*, *450*(7167), 285-8. Nature Publishing Group. doi: 10.1038/nature06254.

Ye, B. H., Chaganti, S., Chang, C. C., Niu, H., Corradini, P, Chaganti, R. S., et al. (1995). Chromosomal translocations cause deregulated BCL6 expression by promoter substitution in B cell lymphoma. *The EMBO journal*, *14*(24), 6209-17.

Yuan, W., Xu, M., Huang, C., Liu, N., Chen, S., & Zhu, B. (2011). H3K36 methylation antagonizes PRC2 mediated H3K27 methylation. *The Journal of biological chemistry*, *286*(10), 7983-7989. doi: 10.1074/jbc.M110.194027.

Zhang, X. (2003). ZBP-89 represses vimentin gene transcription by interacting with the transcriptional activator, Sp1. *Nucleic Acids Research*, *31*(11), 2900-2914. doi: 10.1093/nar/gkg380.

Zhao, Q., Eberspaecher, H., Lefebvre, V., & Crombrugghe, B. de. (1997). Parallel Expression of Sox9 and Col2a1 in Cells Undergoing Chondrogenesis. *Developmental dynamics*, *209*(4), 377–386. Wiley Online Library.